Pair Distribution Function analysis for the structural study of materials

Pierre BORDET
Institut Néel,
CNRS-UGA Grenoble
pierre.bordet@neel.cnrs.fr

Crystallography studies and uses crystals to investigate the structure of materials

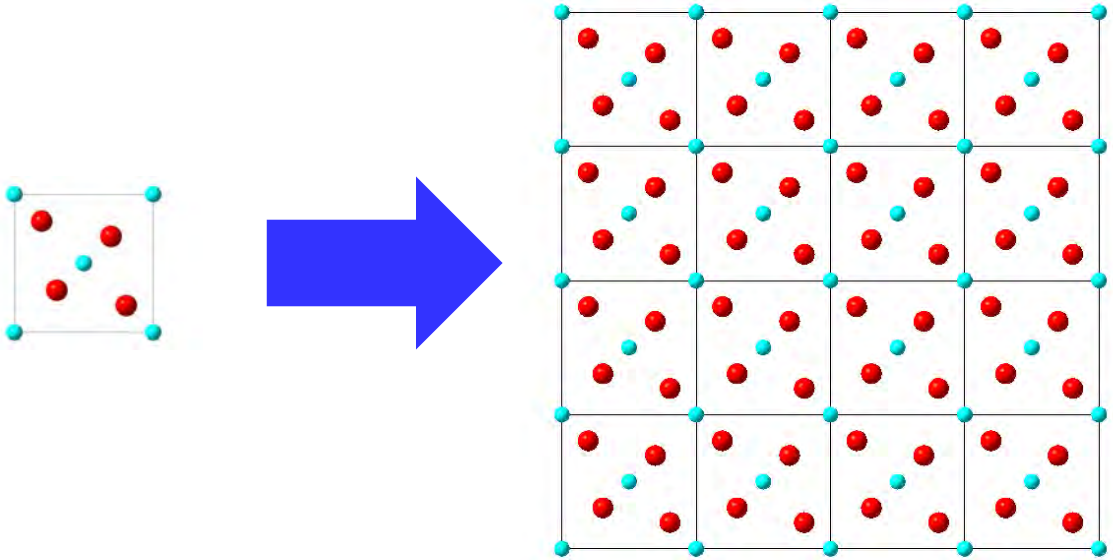

Crystal are periodic and symmetric
That's why diffraction (RX, etc…) is so powerful

In principle, we know how to determine the structure of a crystal

But all materials of interest are not in the form of single crystals

To study their strucure

=> **1** = make a single crystal (but often difficult, or not what we want to study)

=> **2** = study materials as they are
=> powders, amorphous, disordered…..

=>Diffraction, spectroscopies (IR, Raman, RMN), electron microscopy , SAXS, EXAFS…

Analysis of total scattering using the pair distribution function

Powder diffraction : the Rietveld method

$$yci = ybi + \sum_{\Phi=1}^{N} S_{\Phi} \sum_{k=k1}^{k2} j_{\Phi k}.Lp_{\Phi k}.O_{\Phi k}.M.\left|F_{\Phi k}\right|^{2}.\Omega_{i\Phi k}$$

$$F_{hkl} = \sum_{j \subset cell} f_j T_j \exp(2i\pi(hx_j + ky_j + lz_j))$$

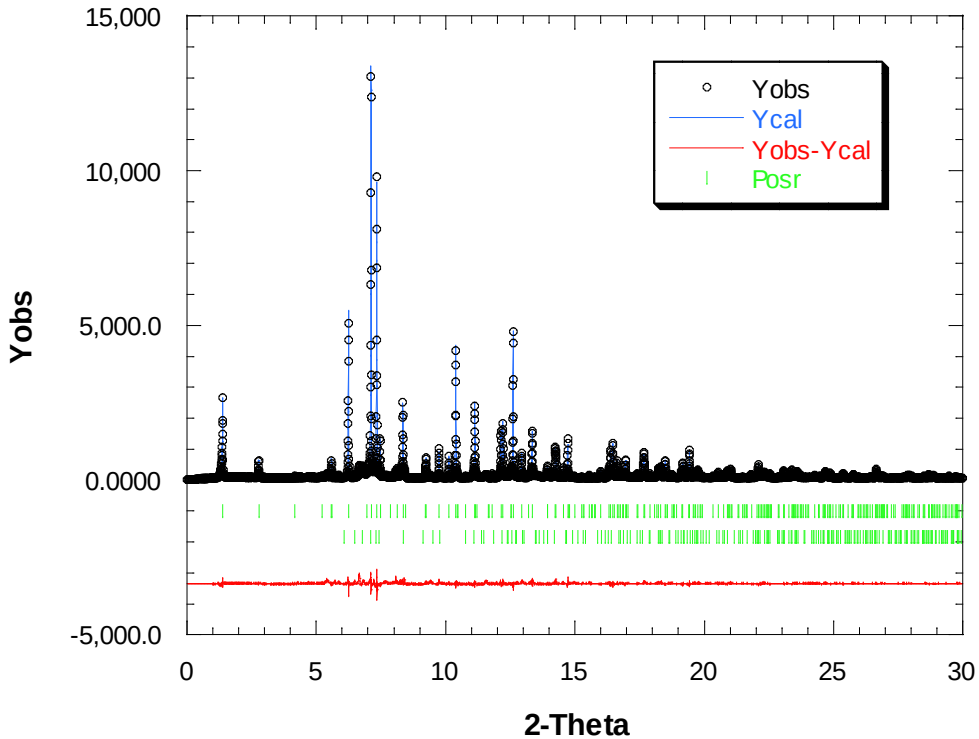

Only interested in Bragg peaks
= access to LRO structure.

Everything else:
« background »
« diffuse scttering»

For a full study of the real material:
modelization of total scattering

Deffects => diffuse scattering

Example : stacking faults in close packed structure

Interactive Tutorial about Diffraction, Neder, R.B. & Proffen, Tj. *J. Appl. Cryst.* (1996), **29**, 727-735

http://www.pa.msu.edu/cmp/billinge-group/teaching/teaching.html

ALPHA	probability of "ab" followed by "a"
1 - ALPHA	probability of "ab" followed by "c"
BETA	probability of "ba" followed by "b"
1 - BETA	probability of "ba" followed by "c"

ALPHA	BETA	resulting structure
0.0	0.0	pure cubic sequence
0.05	0.05	Sequence of cubic twins
0.5	0.5	random stacking
1.0	1.0	pure hexagonal sequence

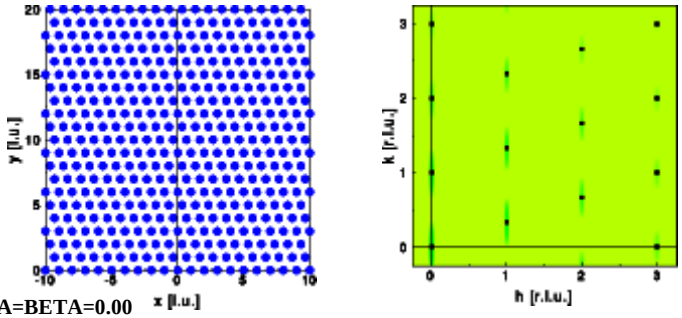

ALPHA=BETA=0.00

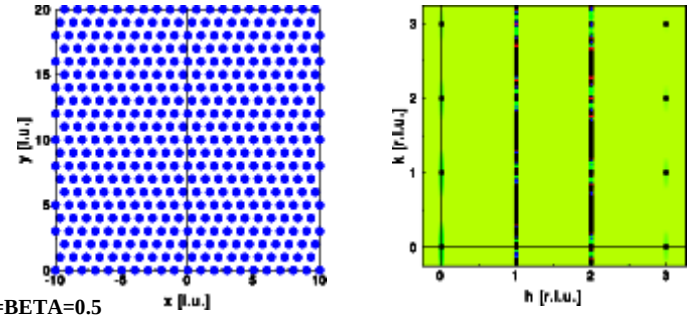

ALPHA=BETA=0.5

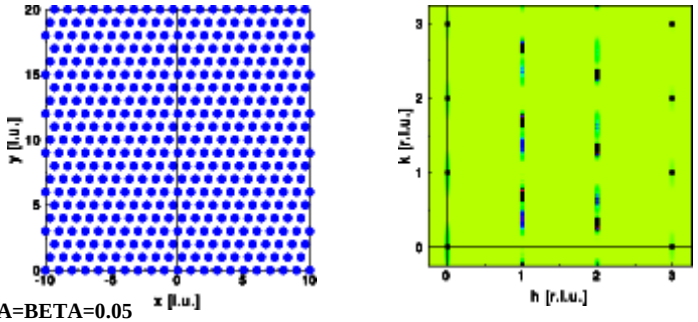

ALPHA=BETA=0.05

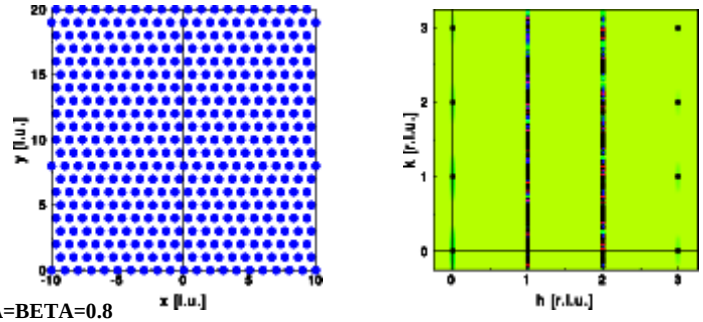

ALPHA=BETA=0.8

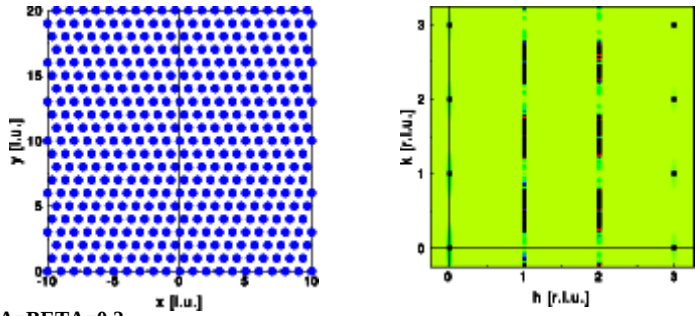

ALPHA=BETA=0.2

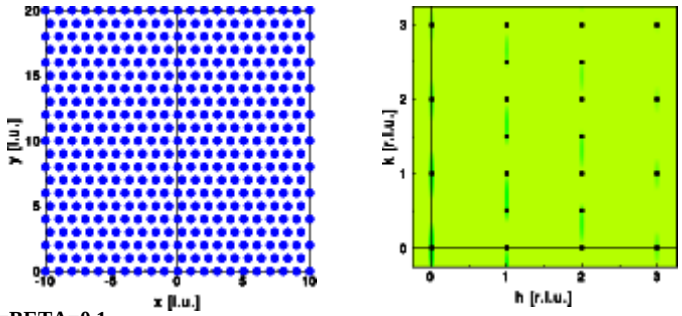

ALPHA=BETA=0.1

We want to understand the structure of “bad” crystals

powder compounds, synthesized by chemistry or nature

crystalline material + short-range order

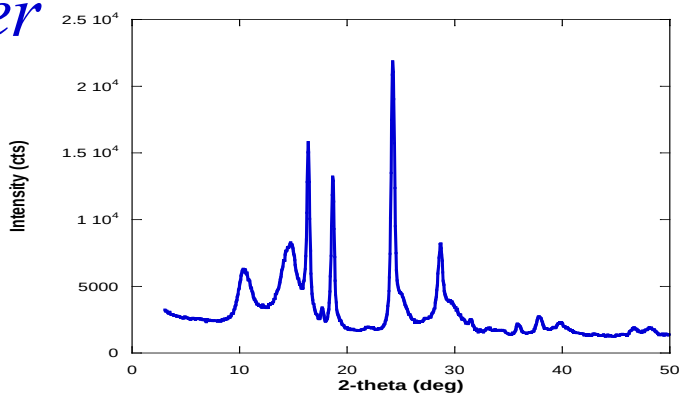

<u>direct space</u> :

average structure exists ≠ local structure

<u>reciprocal space</u> :

Bragg peaks + diffuse scattering background

nano-crystalline powders

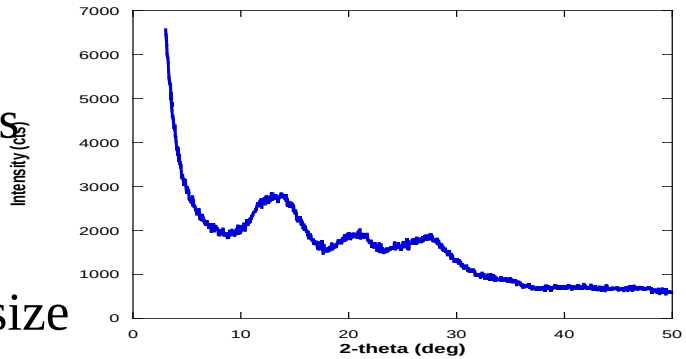

<u>direct space</u> :

well defined structure in small coherent domains

≠amorphous

<u>reciprocal space</u> :

wide or no “Bragg” peaks, depending on grain size

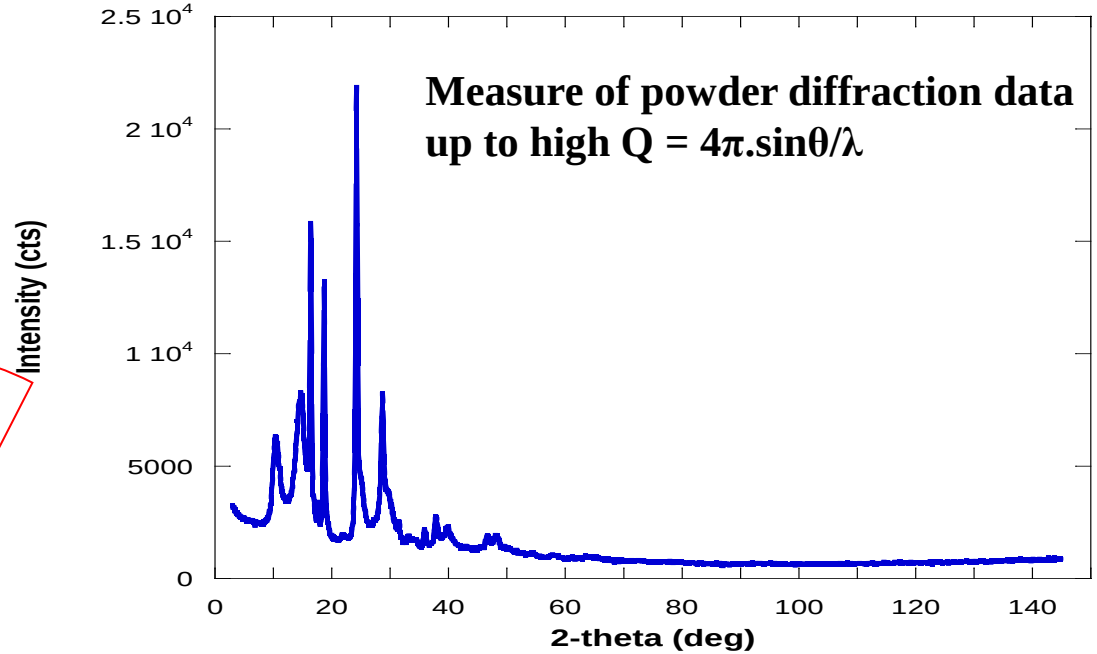

Reciprocal space

Direct space

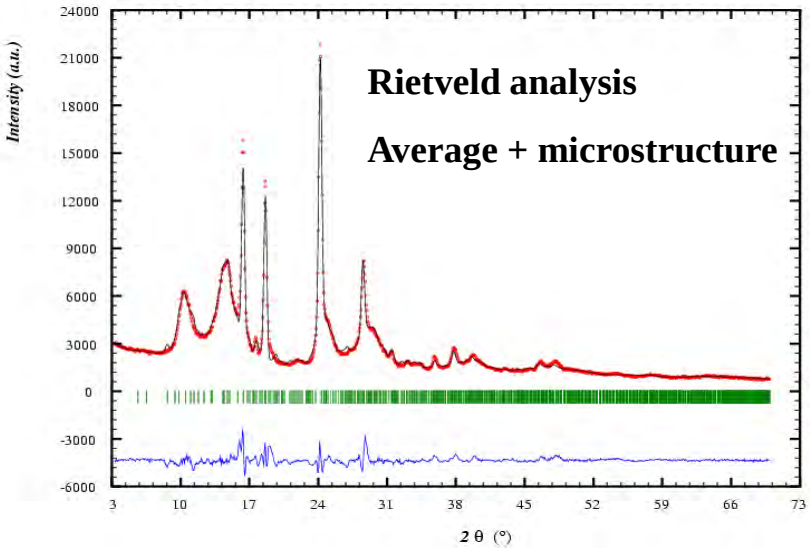

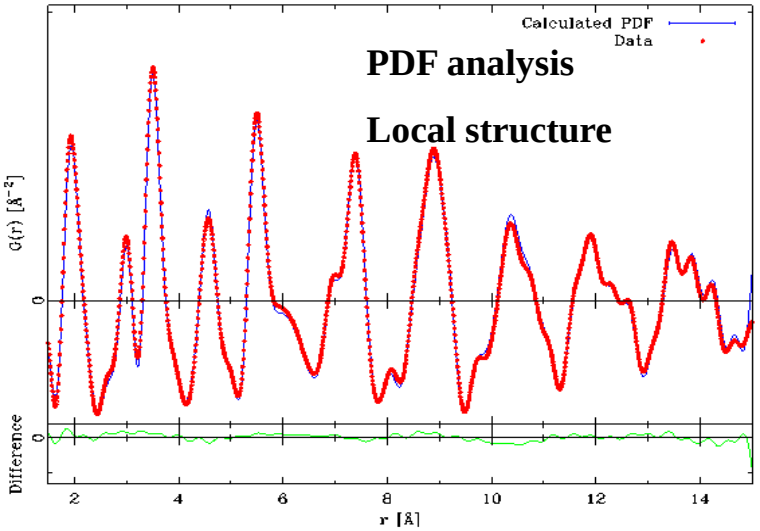

What is the PDF ??

(1) $$I_{exp}(Q) = I_C(Q) + I_I(Q) + I_{MC}(Q) + I_{BG}(Q)$$

Total measured intensity

(2) $$I_C(\mathbf{Q}) = AP\frac{d\sigma_C}{d\Omega}$$

Coherent measured intensity
+ corrections absorption, polarization

(3) $$\frac{d\sigma_C}{d\Omega} = \sum_{i,j} f_j^* f_i e^{i\mathbf{Q}\cdot(\mathbf{R}_j - \mathbf{R}_i)} = \langle f(Q)\rangle^2 |\Psi(\mathbf{Q})|^2$$

Coherent scattering cross section

(4) $$\Psi(\mathbf{Q}) = \frac{1}{\langle f(Q)\rangle}\sum_{\nu} f_\nu(Q) e^{i\mathbf{Q}\mathbf{R}_\nu} = \int \rho(r) e^{i\mathbf{Q}r} dr$$

Scattering amplitude

(5) $$\boxed{S(\mathbf{Q}) = \frac{1}{N}|\Psi(\mathbf{Q})|^2 = \frac{1}{N}\iint \rho(r)\rho(r')e^{i\mathbf{Q}(r-r')}drdr'}$$

$S(\mathbf{Q})$ = Structure function
$\rho(\boldsymbol{r})$ = atomic density

(6) $$TF(S(\mathbf{Q})) = \frac{1}{8\pi^3}\int S(\mathbf{Q})e^{i\mathbf{Q}\boldsymbol{R}}d\mathbf{Q} = \frac{1}{8\pi^3 N}\iiint \rho(\boldsymbol{r})\rho(\boldsymbol{r}')e^{i\mathbf{Q}(\boldsymbol{r}-\boldsymbol{r}'+\boldsymbol{R})}d\boldsymbol{r}d\boldsymbol{r}'d\mathbf{Q}$$
$$= \frac{1}{N}\iint \rho(\boldsymbol{r})\rho(\boldsymbol{r}')\delta(\boldsymbol{r}-\boldsymbol{r}'+\boldsymbol{R})d\boldsymbol{r}d\boldsymbol{r}' = \frac{1}{N}\int \rho(\boldsymbol{r})\rho(\boldsymbol{r}+\boldsymbol{R})\,d\boldsymbol{r} = \rho_0 g(\boldsymbol{R})$$

$g(\boldsymbol{R})$ = pair distribution function

$Q=4\pi\sin\theta/\lambda$

ρ_0 = numerical density

For an isotropic sample (powder, glass…)

integrating over angular variables

(7) $$\rho_0 g(R) = \frac{1}{8\pi^3} \iiint S(Q) e^{iQR\,cos\theta} dcos\theta\; d\varphi\; Q^2 dQ$$

(8) $$\rho_0 g(R) = \frac{1}{2\pi^2} \int_0^\infty S(Q) \frac{\sin(QR)}{QR} Q^2\, dQ$$

(9) $$\rho_0 [g(R) - 1] = \frac{1}{2\pi^2 R} \int_0^\infty [S(Q) - 1] \sin(QR)\, Q\, dQ$$

(10) $$\boxed{G(R) = 4\pi R \rho_0 [g(R) - 1] = \frac{2}{\pi} \int_0^\infty Q[S(Q) - 1] \sin(QR)\, dQ}$$

G(R) = reduced pair distribution function

From an atomic structure model, one can define:

Radial distribution function

(11) $$R(r) = \sum_{i,j} \frac{f_i f_j}{\langle f \rangle^2} \delta(r - r_{i,j})$$

Pair distribution function

(12) $$g(r) = \frac{1}{4\pi r^2 \rho_0} R(r) = \frac{1}{4\pi r^2 \rho_0} \sum_{i,j} \frac{f_i f_j}{\langle f \rangle^2} \delta(r - r_{i,j})$$

Reduced pair distribution function

(13) $$\boxed{G(r) = 4\pi r \rho_0 [g(r) - 1] = \frac{1}{r} \sum_{i,j} \frac{f_i f_j}{\langle f \rangle^2} \delta(r - r_{i,j}) - 4\pi r \rho_0}$$

Getting *S(Q)* from experimental data:

(1) $$I_{exp}(Q) = I_C(Q) + I_I(Q) + I_{MC}(Q) + I_{BG}(Q)$$

(14) $$I_C^{corr}(\mathbf{Q}) = \frac{I_C(\mathbf{Q})}{AP} = \frac{d\sigma_C}{d\Omega} = \sum_{i,j} f_j^* f_i e^{i\mathbf{Q}\cdot(\mathbf{R}_j - \mathbf{R}_i)}$$

(15) $$I_C^{corr}(\mathbf{Q}) = \sum_i f_i^* f_i + \sum_{i \neq j} f_j^* f_i e^{i\mathbf{Q}\cdot(\mathbf{R}_j - \mathbf{R}_i)}$$

$$= N\langle f^2 \rangle + \sum_{i \neq j} f_j^* f_i e^{i\mathbf{Q}\cdot(\mathbf{R}_j - \mathbf{R}_i)}$$

1st term = self scattering, 2nd term = structure

We normalize by $N\langle f \rangle^2$ and subtract self-scattering

(16) $$\frac{I_C^{corr}(\mathbf{Q})}{N\langle f \rangle^2} - \frac{\langle f^2 \rangle}{\langle f \rangle^2} = \frac{1}{N\langle f \rangle^2} \sum_{i \neq j} f_j^* f_i e^{i\mathbf{Q}\cdot(\mathbf{R}_j - \mathbf{R}_i)}$$

On définit :

(17) $$S(\mathbf{Q}) - 1 = \frac{I_C^{corr}(\mathbf{Q})}{N\langle f \rangle^2} - \frac{\langle f^2 \rangle}{\langle f \rangle^2} = \frac{1}{N\langle f \rangle^2} \sum_{i \neq j} f_j^* f_i e^{i\mathbf{Q}\cdot(\mathbf{R}_j - \mathbf{R}_i)}$$

chosing: $I(\mathbf{Q}) = I_C^{corr}(\mathbf{Q})/N = I_C(\mathbf{Q})/NAP$

(18) comes :

$$S(\mathbf{Q}) = \frac{I(\mathbf{Q}) - \langle f^2 \rangle + \langle f \rangle^2}{\langle f \rangle^2}$$

Total scattering structure function

(19) One defines:

$$F(Q) = Q(S(Q) - 1)$$

Reduced structure function

Reduced pair distribution function

$$G(R) = 4\pi R \rho_0 [g(R) - 1] = \frac{2}{\pi} \int_0^\infty Q[S(Q) - 1] \sin(QR)\, dQ$$

$$G(r) = 4\pi r \rho_0 [g(r) - 1] = \frac{1}{r} \sum_{i,j} \frac{f_i f_j}{\langle f \rangle^2} \delta(r - r_{i,j}) - 4\pi r \rho_0$$

$$g(r) = \frac{1}{4\pi r \rho_0} G(r) + 1$$

pair distribution function

$$R(r) = 4\pi r^2 \rho_0 g(r) = rG(r) + 4\pi r^2 \rho_0$$

radial distribution function

$$G(r) = 4\pi r[\rho(r) - \rho_0] = \frac{2}{\pi}\int_0^{\infty} Q[S(Q) - 1]\sin(Qr)dQ,$$

G(r) : reduced PDF= *TF {F(Q)=Q.[S(Q)-1]}*

→ *0 qd r→∞ ; amplitude indepdt of r, e.s.d.constant with r*

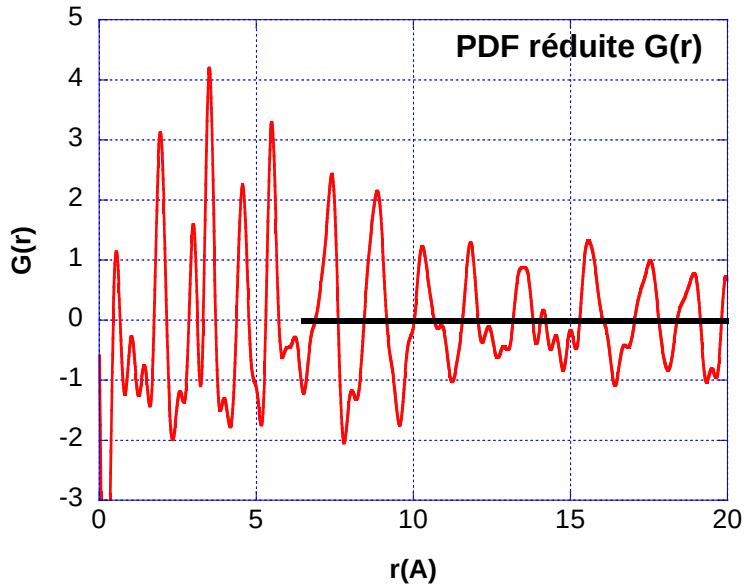

$$G(r) = 4\pi r \rho_0 (g(r) - 1) \qquad g(r) = 1 + G(r)/4\pi r \rho_0$$

g(r) : PDF= *TF {S(Q)}*

→ *1 qd r→∞ ; enhances low r, esd increases with r*

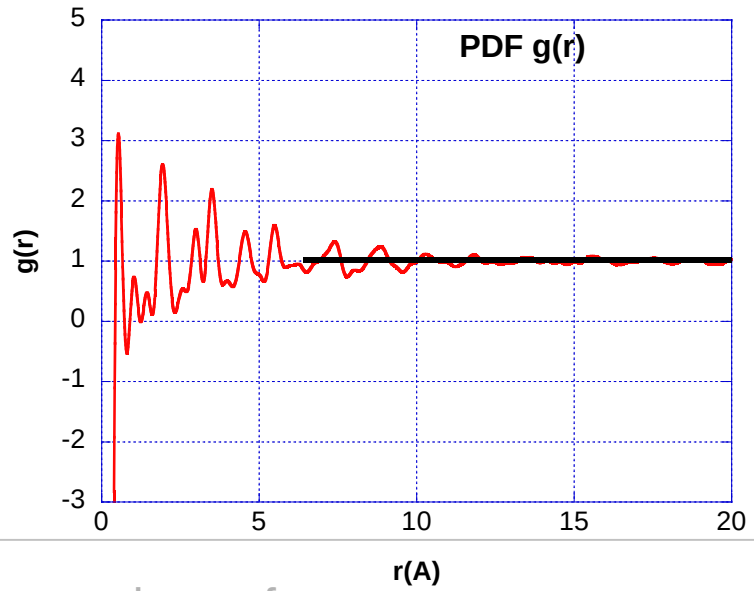

$$R(r) = 4\pi r^2 \rho_0 g(r)$$

R(r) : RDF

Increases as r^2

$$Nc = \int_{r1}^{r2} R(r)dr$$

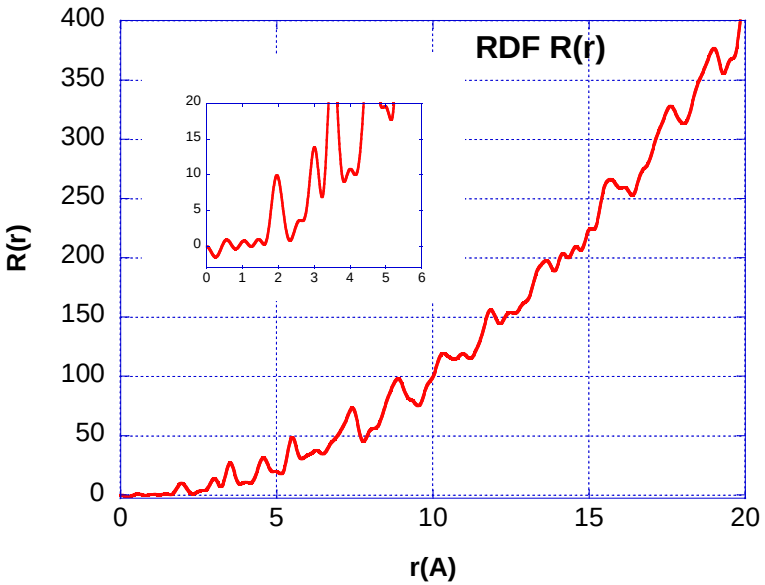

$$G(r) = 4\pi r(\rho(r) - \rho_0) = \frac{2}{\pi}\int_0^{\infty} Q.(S(Q) - 1).\sin(Qr).dQ$$

$$G(r) = \frac{1}{r}\sum_{i,j}\frac{f_i f_j}{\langle f\rangle^2}\delta(r - r_{i,j}) - 4\pi r\rho_0$$

(units: Å^{-2})

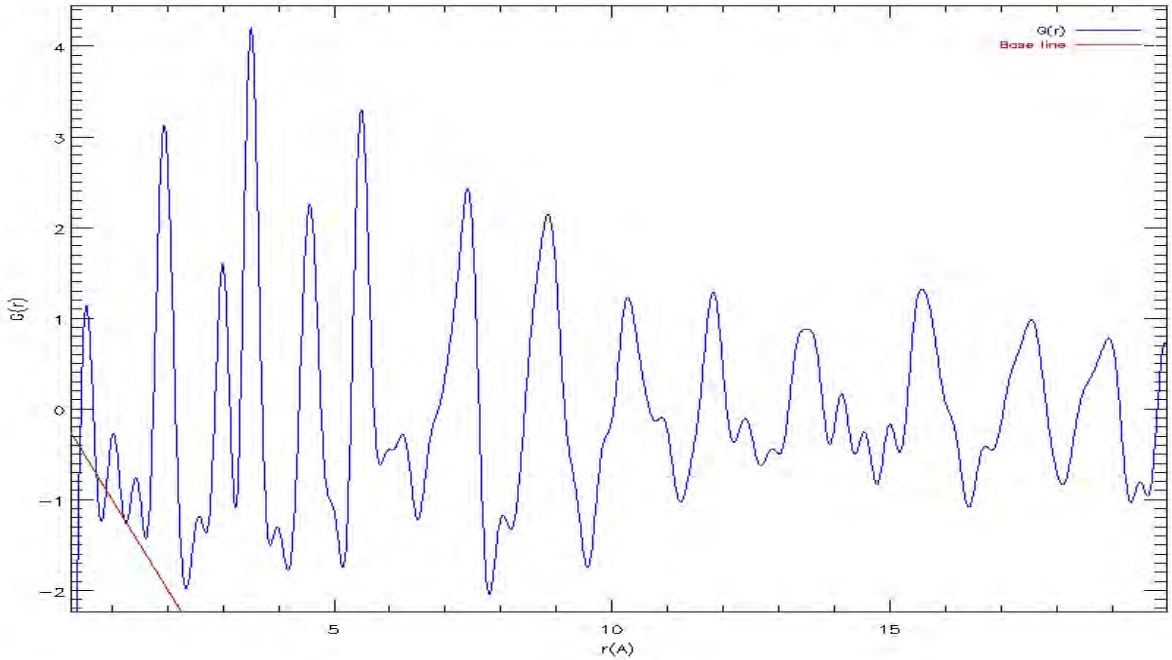

G(r) = reduced PDF: oscillations around zero because the contribution of the average pair density has been subtracted. (baseline = red line above).

PDF peak width and experimental effects

Peak width σ_{ij} related to the distribution of interatomic distances in the material, Calculated from a.d.p.'s of individual atoms. The peak shape is assumed gaussian (≠ diffraction !!) ***+ corrections :***

$$\sigma_{ij} = \sigma'_{ij}\sqrt{1 - \frac{\delta_1}{r_{ij}} - \frac{\delta_2}{r_{ij}^2} + Q_{broad}^2 r_{ij}^2}$$

δ_1, δ_2 empirical coorection of effects of displacement correlations
Q_{broad} : broadening due to Q resolution

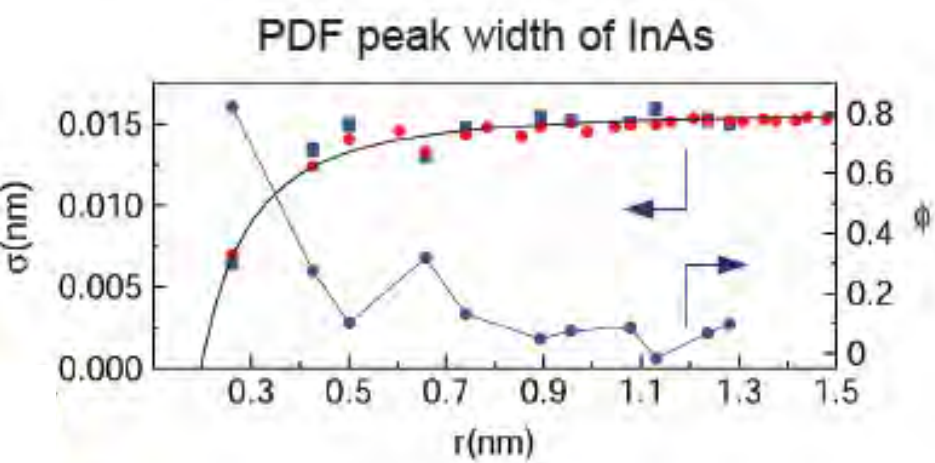

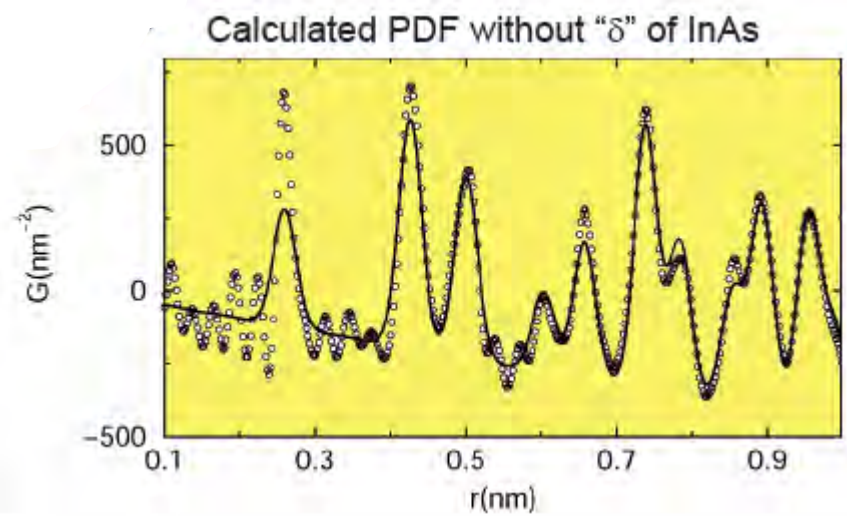

Jeong et al., *J. Phys. Chem. A* **103**, 921 (1999)

Effect of Q_{max}

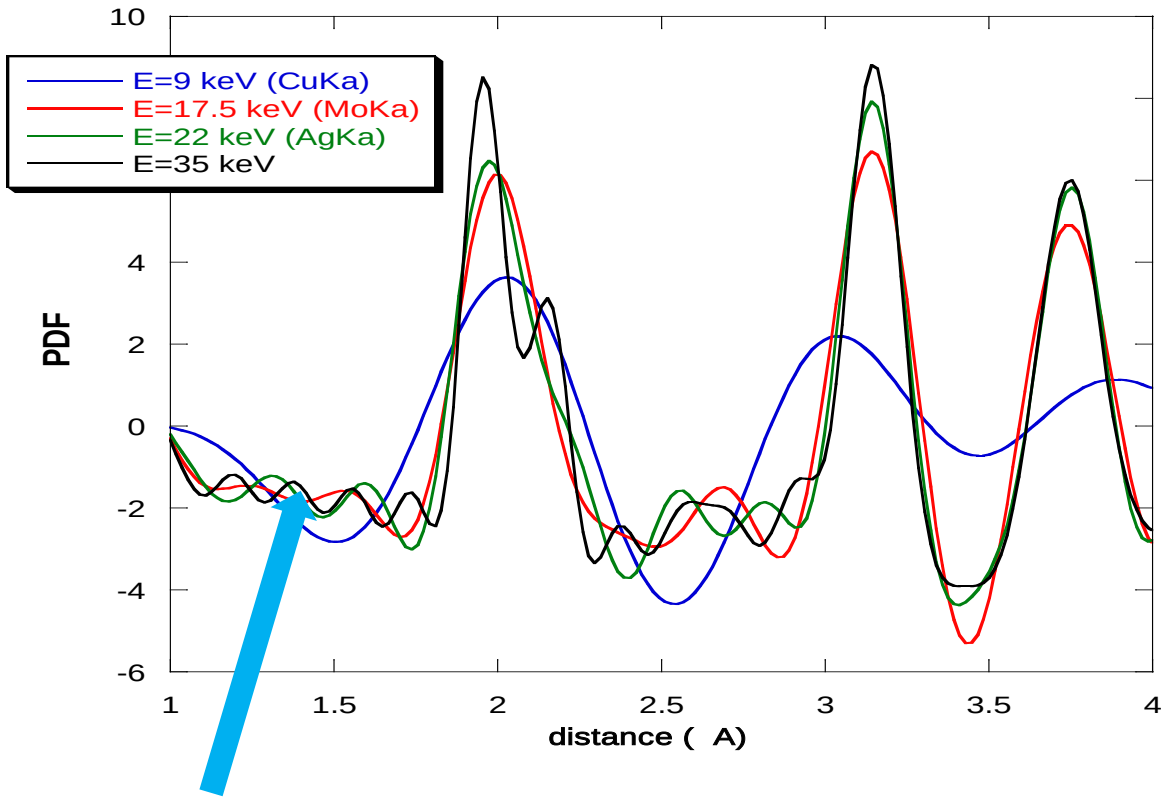

Ripples due to FT termination at Qmax

Q-position changes vs Qmax

PDF extension, instrumental resolution and size of coherent domains

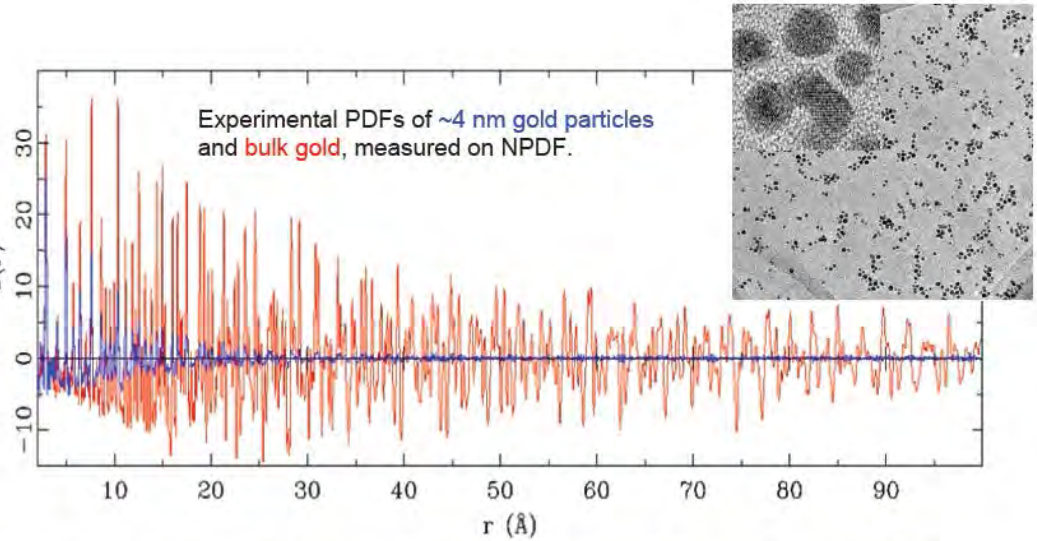

K.L. Page, Th. Proffen, H. Terrones, M. Terrones, L. Lee, Y. Yang, S. Stemmer, R. Seshadri and A.K. Cheetham, **Direct Observation of the Structure of Gold Nanoparticles by Total Scattering Powder Neutron Diffraction**, *Chem. Phys. Lett.* **393**, 385-388 (2004).

Q_{damp} : r-dependent (Gaussian) decrease in the amplitude of the PDF oscillations due to Q resolution (FWHM)

$$B(r) = e^{-\frac{(rQ_{damp})^2}{2}}$$

Particle form factor:

"Finite Size Effects of Nanoparticles to the Atomic Pair Distribution Functions"
K. Kodama, S. Iikubo, T. Taguchi and S. Shamoto, Acta Cryst. A 62 (2006) 444-453.

$$G(r) \approx f(r) G_{\infty}(r)$$

f(r) depends on particle shape (cf *SAS*)

For a sphere: $f(r) = 1 - \frac{3}{2}\frac{r}{R} + \frac{1}{2}\left(\frac{r}{R}\right)^3$

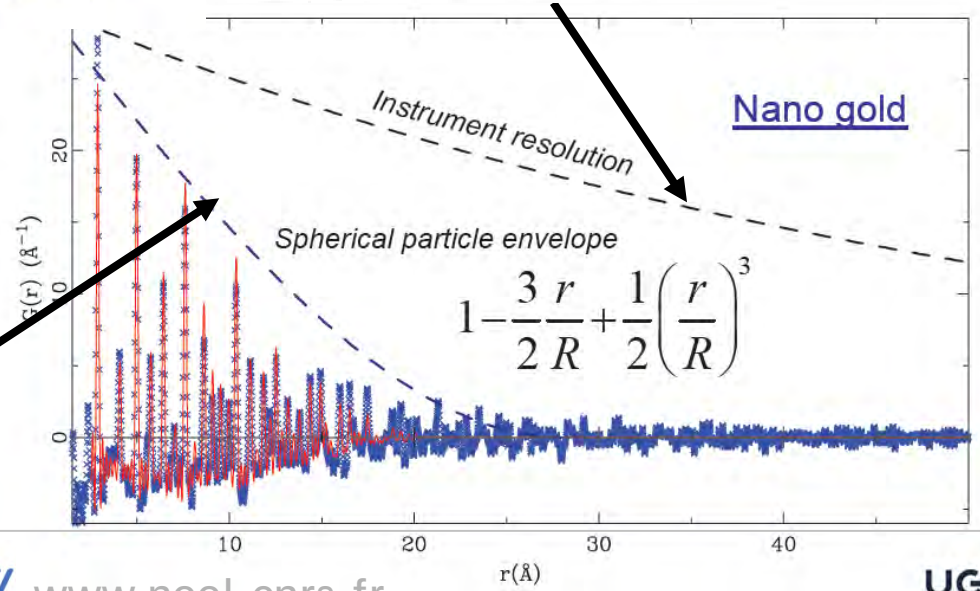

Use of the PDF: study of partly disordered crystal structures and nano-crystalline powders

Experimentally, from powder diffraction data :

$$G(r) = 4\pi r(\rho(r) - \rho_0) = \frac{2}{\pi}\int_0^{\infty} Q.(S(Q) - 1).\sin(Qr).dQ$$

r = interatomic distance

$\rho(r)$ = pair density, ρ_0 : average numerical density

$S(Q)$=normalised coherent scattered intensity,

$Q=4\pi\sin(\theta)/\lambda$

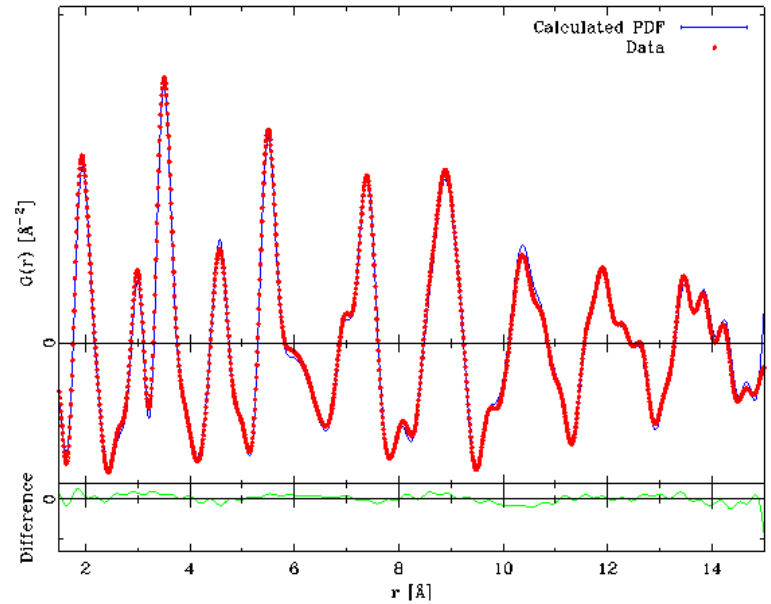

From a structural model :

$$G(r) = \frac{1}{r}\sum_{j \neq k} \frac{f_j f_k^*}{(\sum_j f_j)^2}.\delta(r - r_{jk}) - 4\pi\rho_0$$

r_{ij} = interatomic distance
b_i : scattering power

=> **Fit using « direct space Rietveld »** (PDFgui *Farrow et al.,. JPCM,2007)*

=> **RMC fit on PDF and/or S(Q)** (RMCProfile, *Keen et al., JPCM 2005)*

Why use the pdf :

Complementary to “classical crystallographic analysis:

independent from Bragg, use total coherent scattering

local structure studies (glasses, SRO, nano-grains…)

Example :

PDF of C60 (neutron powder diffraction)

results :

inter molecular C-C distances

Diameter of the bucky ball

Bucky balls move incoherently

F lattice organization

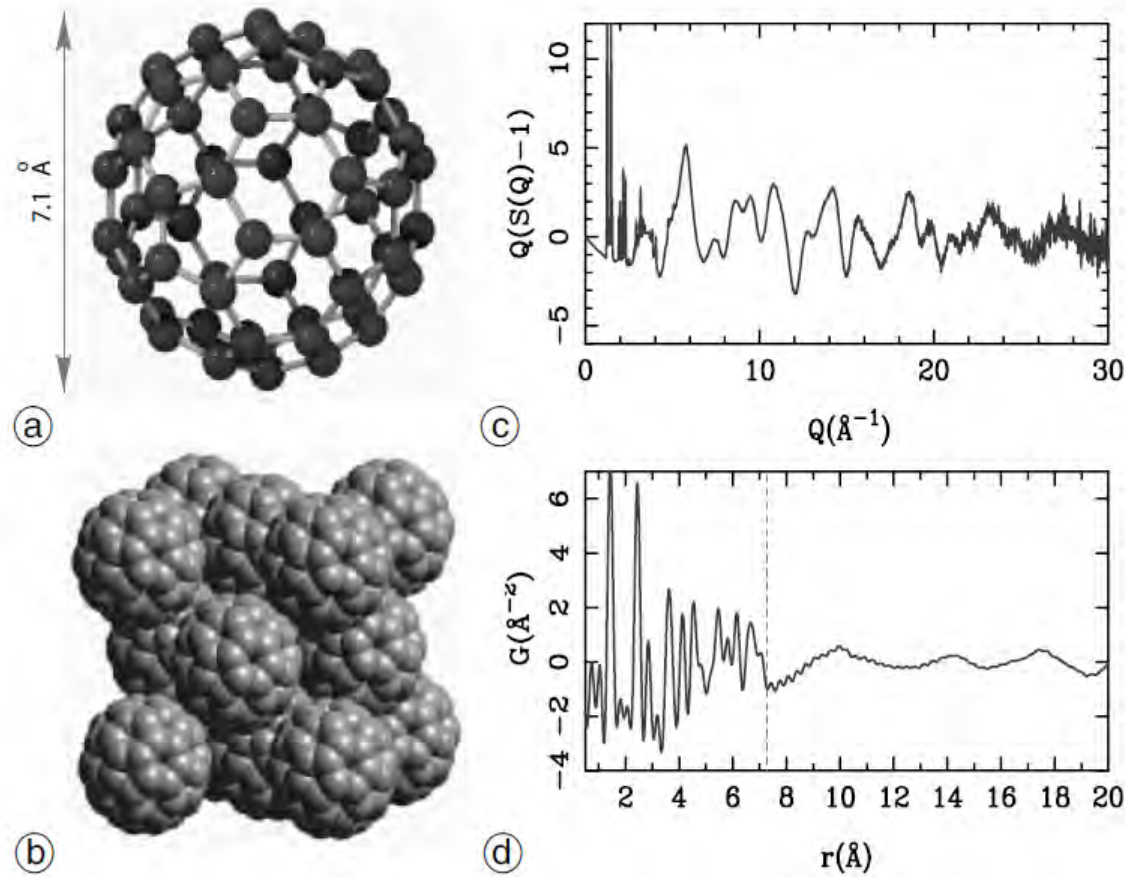

Th. Proffen, S. J. L. Billinge, T. Egami and D. Louca, Z. Kristallogr. 218 (2003) 132–143

Structural studies of nanocrystalline materials

$RuO_2.xH_2O$

Different annealing temperatures
=>different hydrations and crystallinity

DRXP

(labo)
CuKα

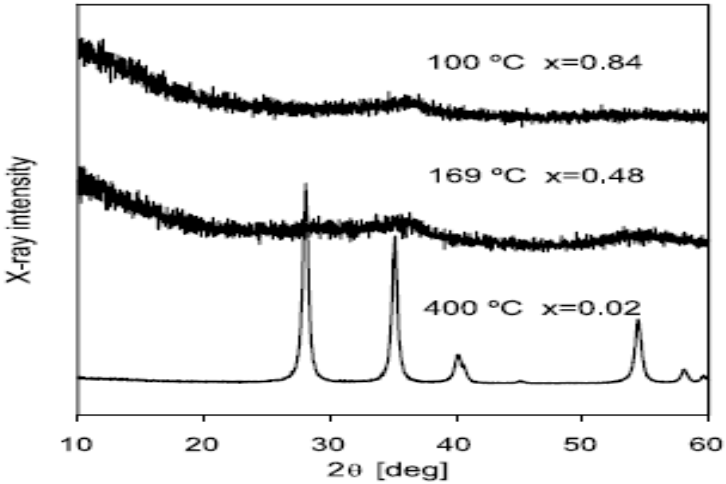

The pdf derivative indicates the size of coherent domains in anhydrous and poly/nanocrystallized RuO_2

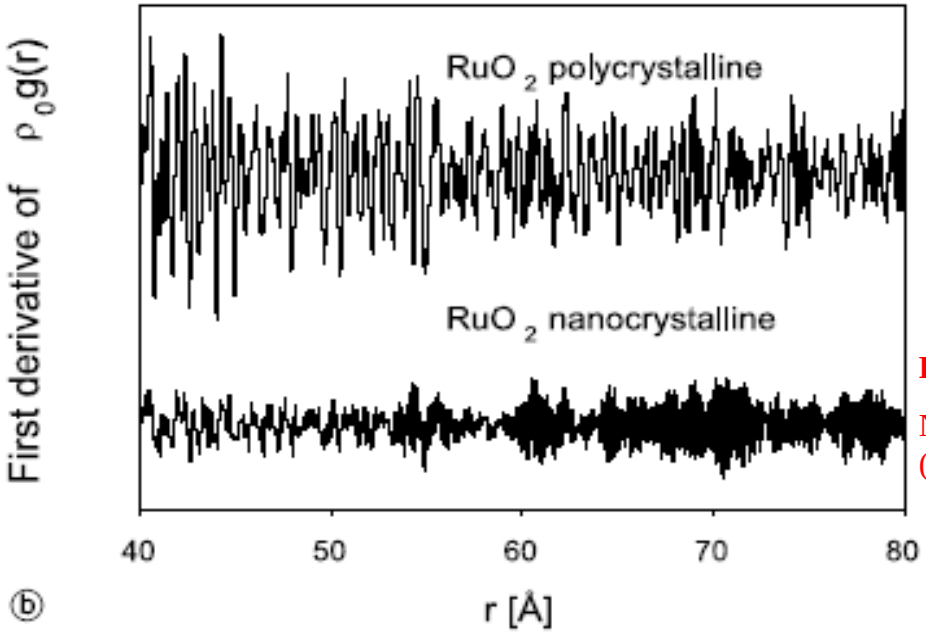

PDF

Neutron
(Argonne)

PDF

RX-(X7A)
Qmax=20 A^{-1}.

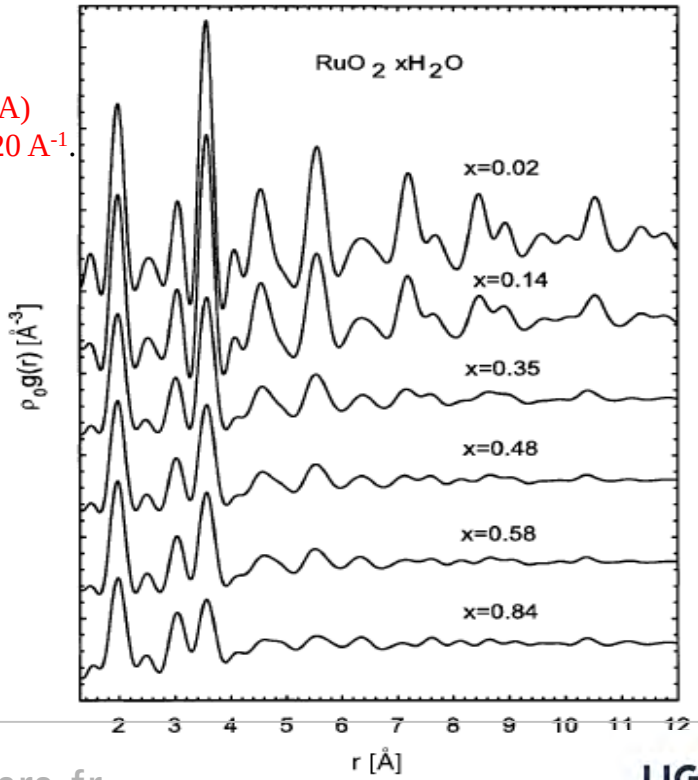

W. Dmowski and K. E. Swider-Lyons, Z. Kristallogr. 219 (2004) 136–142

PDF = The ***multi-scale*** structural analysis technique

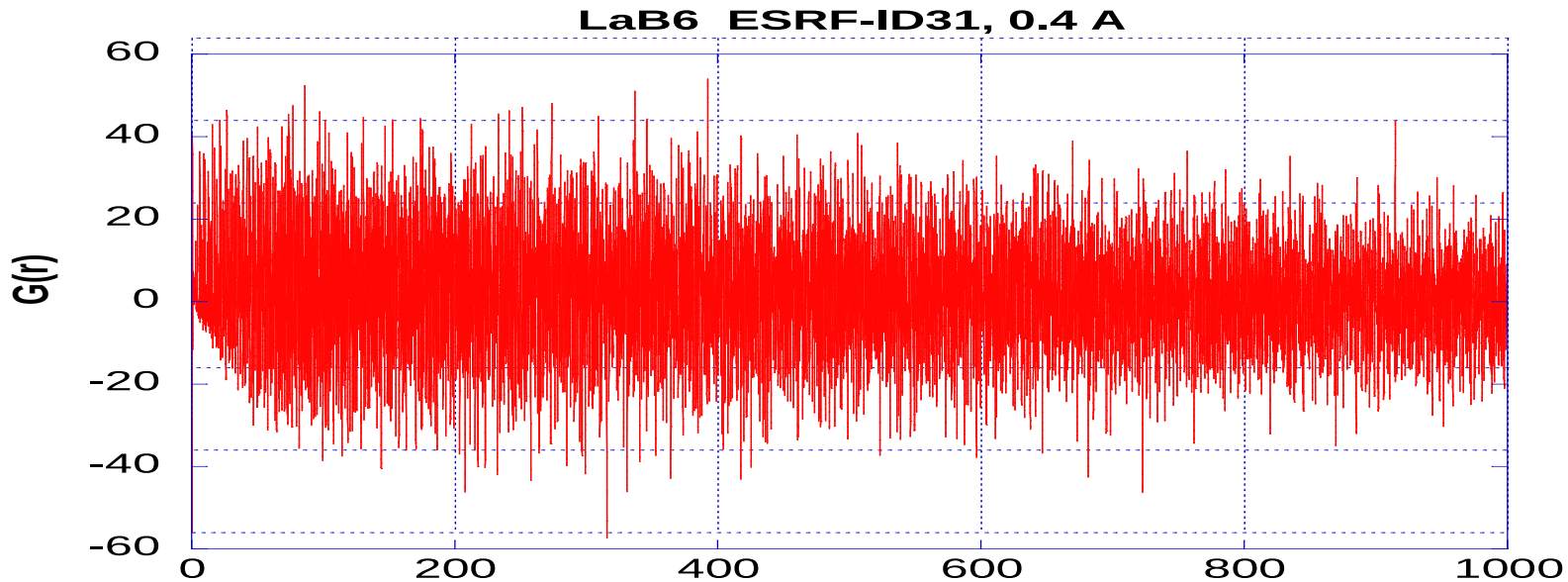

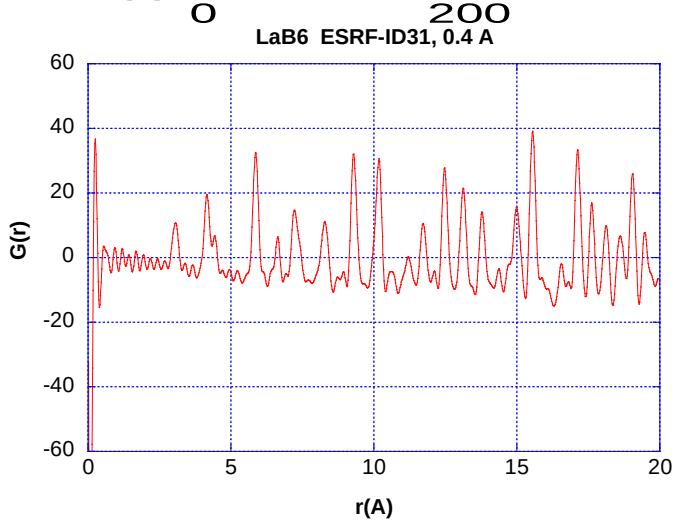

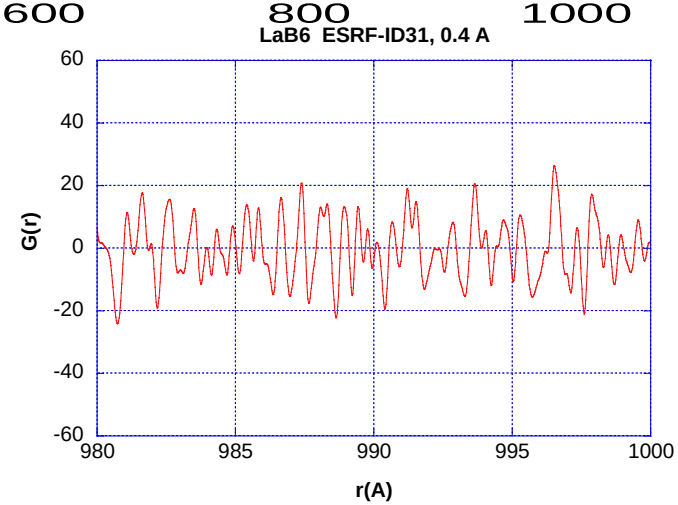

For this you need ultimate experimental spatial resolution

Specific possibilities offered by the PDF:

- Structural characterization independent of the crystalline/amorphous state...
- Identification of amorphous/crystalline phases
- Quantization of amorphous/crystalline phases
- Intrinsically multi-scale (structure according to distance...)
- Local and "average" structure
- Microstructure characterization: size of coherent domains
- and: from powder diffraction data, thus complementary to Rietveld
  (for crystalline phases)

Limitations:

- Difficult to identify phases from PDFs only (no database)
- No ab initio resolution from the PDF (for now)
- Requires access to high-Q data, i.e. high-energy sources (neutrons, X-rays)

in situ/operando experiments possible

Measuring the PDF

It is (almost) a classic powder diffraction measurement

But requires high-Q measurements and strong statistics

=>Use of instruments at large facilities

Neutrons

constant scattering factor (b) => still signal at very high Qs

scattering contrast between elements (O, close Zs , isotopes…)

high flux reactors, ex : ILL-D4, λ=0.7,0.5,0.35Å =>Qmax ≈ 33Å^{-1}

spallation sources, ex : ISIS-GEM, Qmax > 45Å^{-1}

Synchrotrons X-rays

signal falls down as *f(2θ)*

very high fluxes to very high energies (≈100keV)

Parallel Beam + Crystal Analyzer-> eliminates inelastic contributions

2D detectors: in-situ, time-resolved experiments

Neutron time of flight

GEM at ISIS

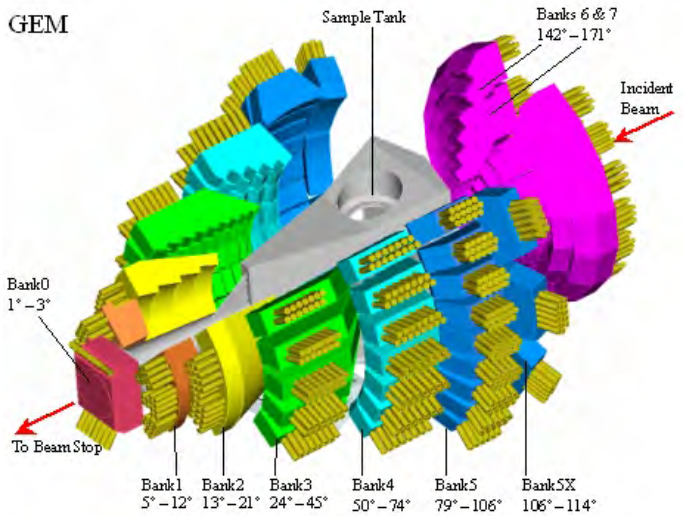

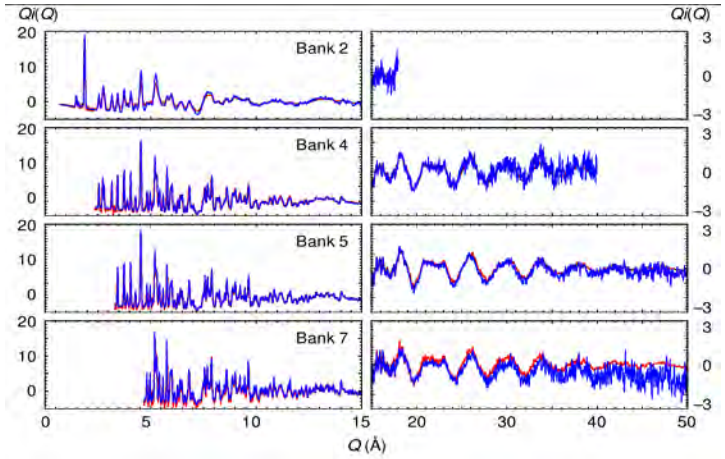

Neutron reactor

D4c at the ILL

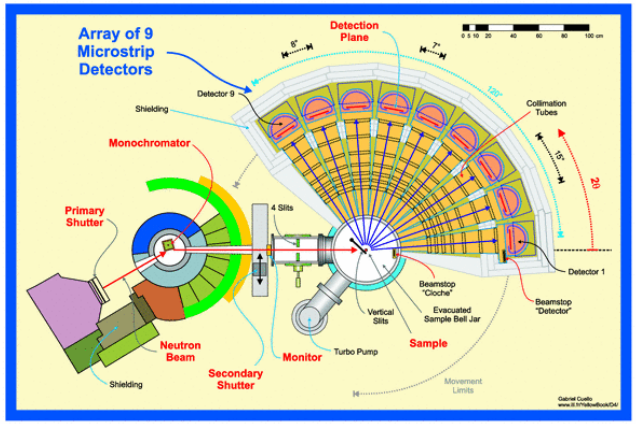

λ =0.5Å, Qmax= 23Å^{-1}

Diffractometer for
"Amorphous liquids and materials"
Moderate spatial resolution
=> Limited Q domain (few 10s Å)

Synchrotron beamlines

High resolution :

ID31-ESRF,etc…

high resolution parallel beam geometry, multi-analyzer

Qmax=*25Å*$^{-1}$

Ultimate resolution

minimal background

1 data set = several hours

High energy :

NSLSII, etc…

Use of 2D detector ; PDF in a few min

In situ, operando, complex environments…

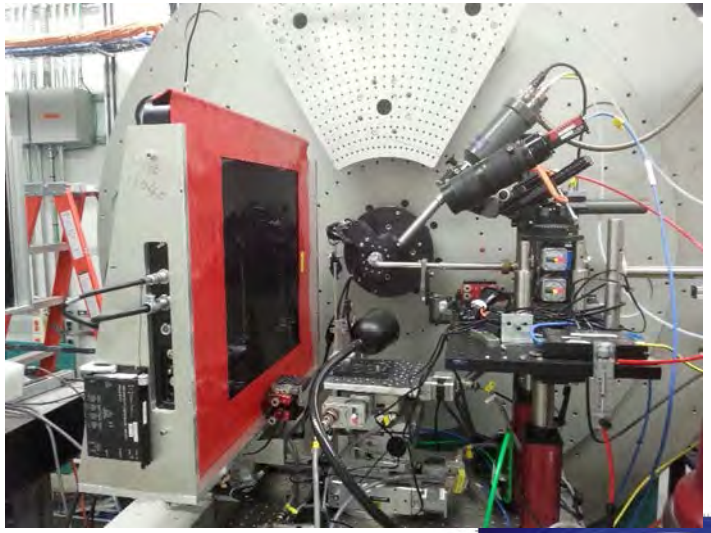

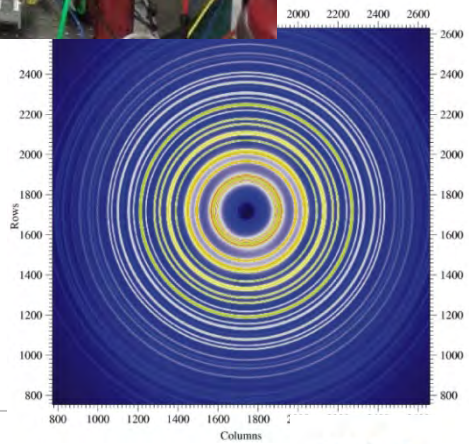

Two-dimensional contour plot from the Mar345 image-plate detector. The data are from nickel powder measured at room temperature with 97.572 keV incident X-rays. The concentric circles are where Debye–Scherrer cones intersect the area detector.

Peter J. Chupas *et al.*

J. Appl. Cryst. (2003). **36**, 1342–1347

Laboratory instrument

Lab. powder Diffractometer optimized for high Q, high flux, 2theta max > 150°

λMoKα (0.71Å) => Qmax≈ 17Å^{-1} ;
λAgKα (0.56Å) => Qmax≈ 22Å^{-1}

Capillary or Bragg-Brentano reflection geometry
Relaxed monochromatization, for higher flux (Göbel mirrors)
PSD: with high efficiency at high energy (thick Si or CdTe)
energy discrimination, for filtering of inelastic/fluorescence

For long r-range PDF, MoKα 1+2 may be a problem
⇒ Use focusing monochromator, but less flux
⇒ Use e.g. GudrunX

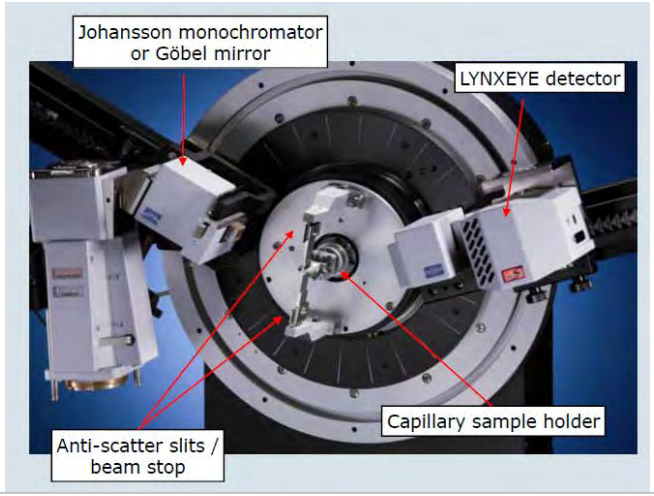

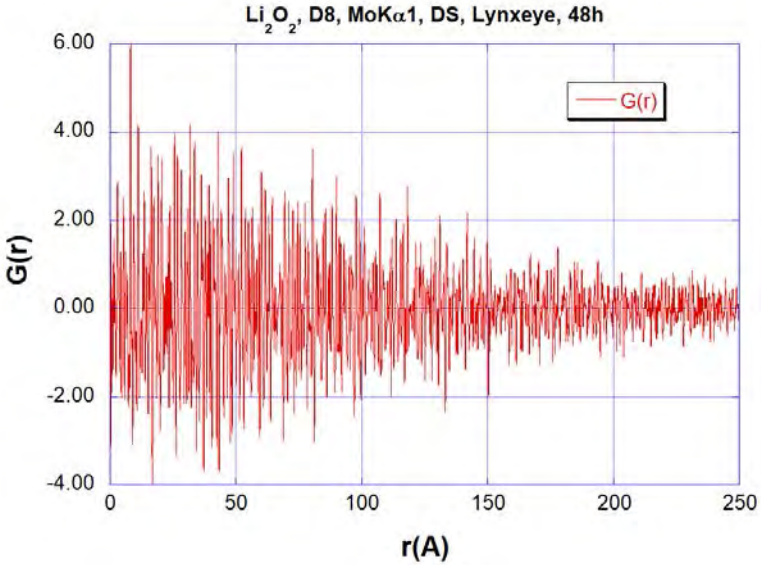

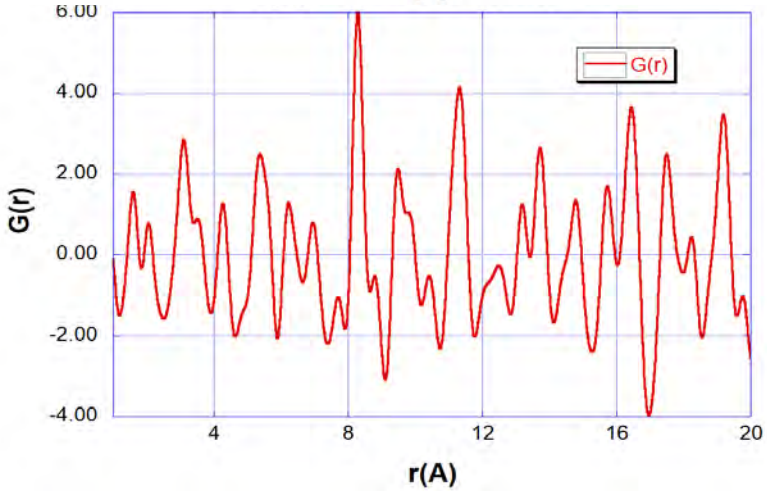

Single crystal diffractometer
CCD / pixel detector
+ microsource Ag to measure the PDF

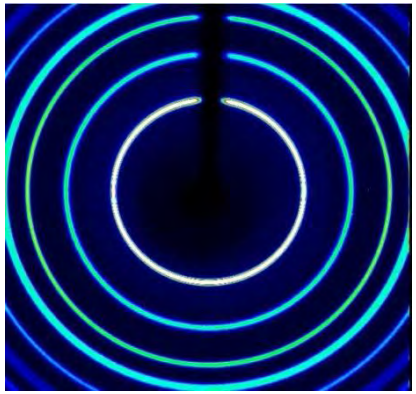

θ=0°

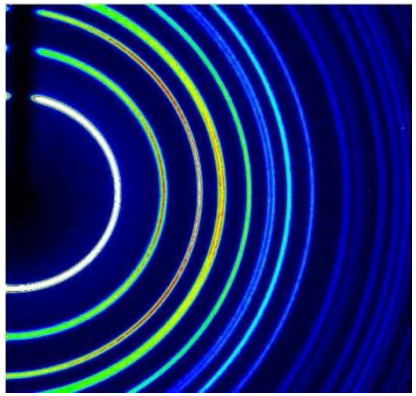

θ=9°

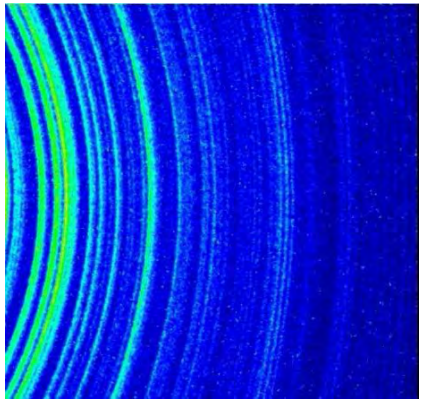

θ=25°

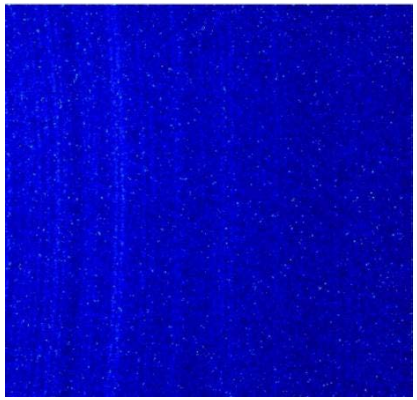

θ=41°

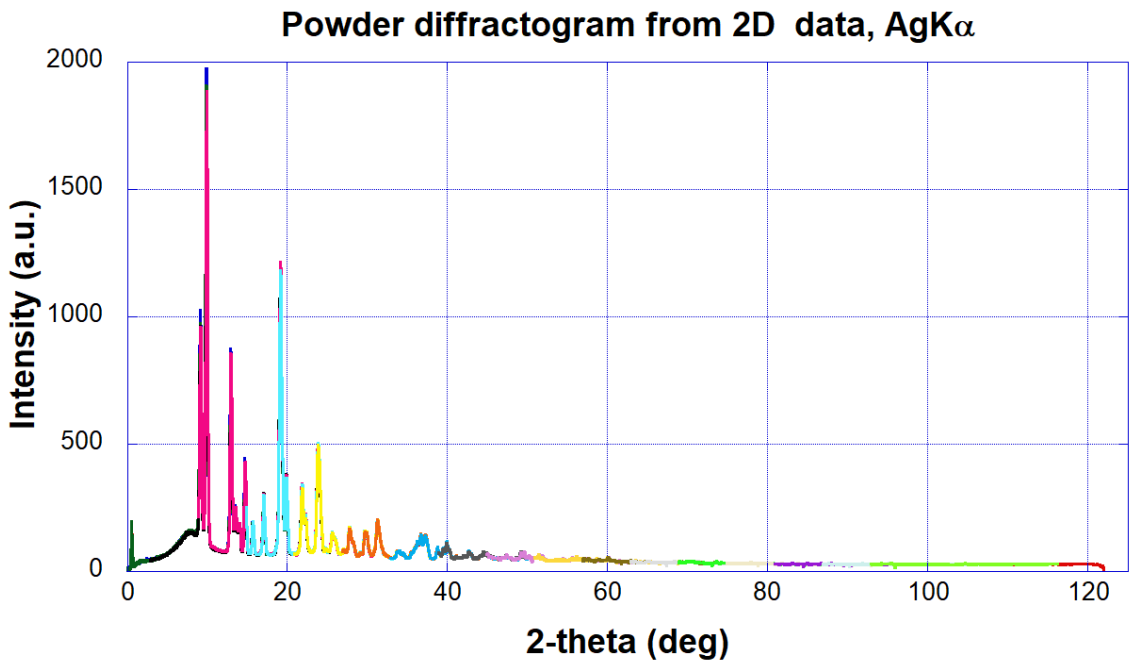

36 images every 3°, 5min/image

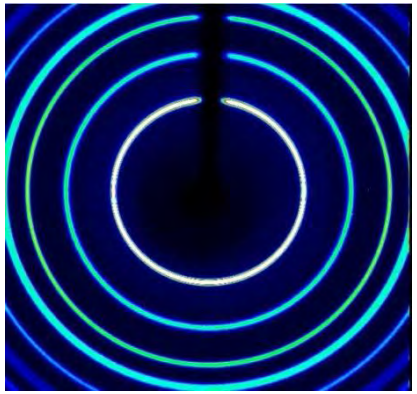

θ=0°

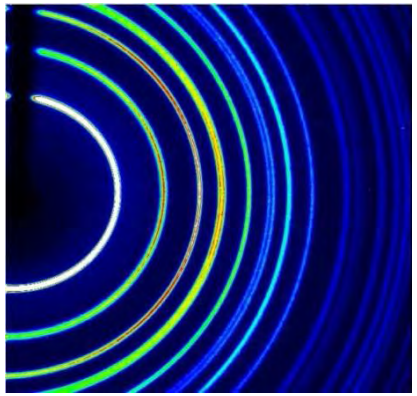

θ=9°

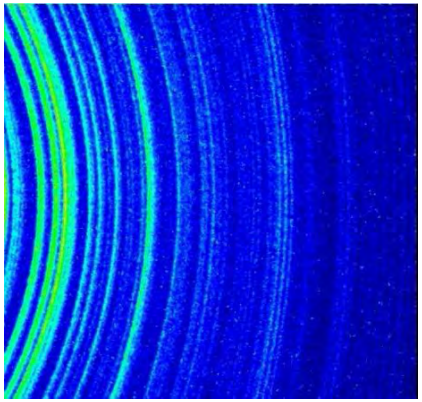

θ=25°

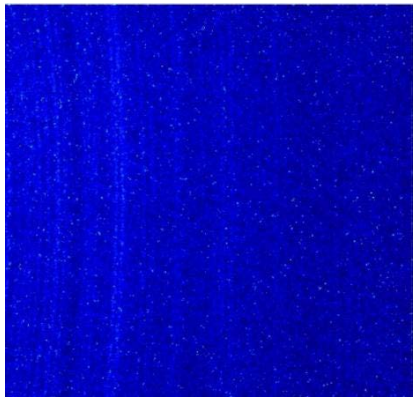

θ=41°

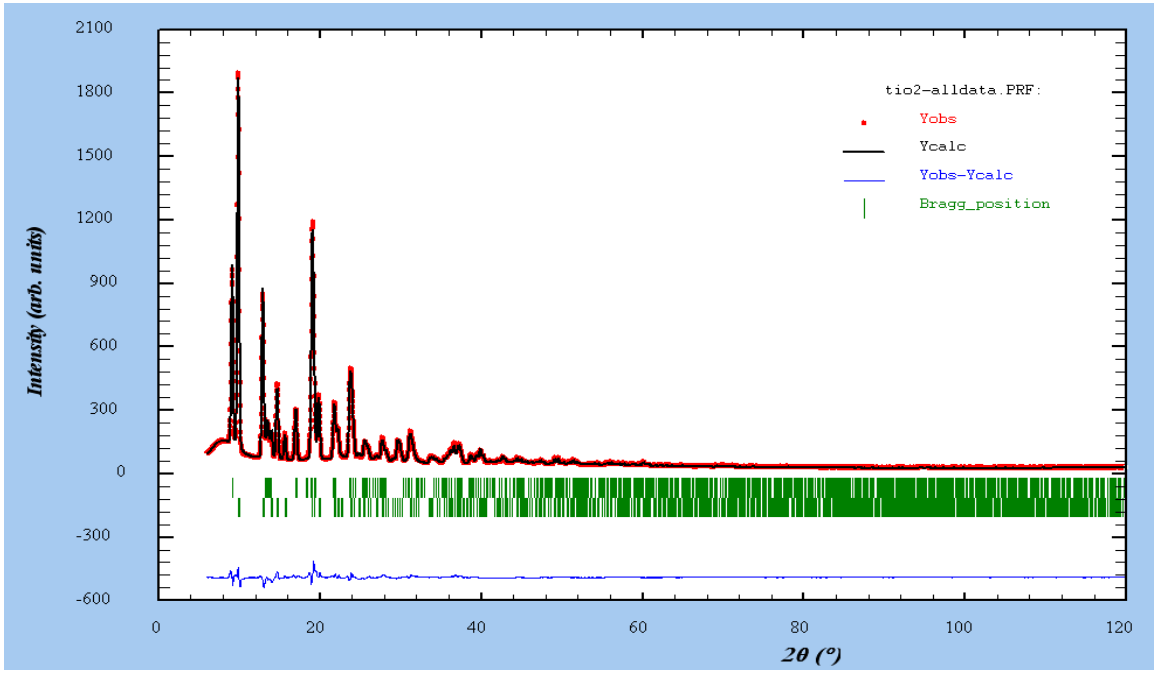
tio2-alldata.PRF:
Yobs
Ycalc
Yobs-Ycalc
Bragg_position
Intensity (arb. units)
2θ (°)
2100
1800
1500
1200
900
600
300
0
-300
-600
0
20
40
60
80
100
120

Fit of the PDF, mixture TiO_2 Rutile + Anatase

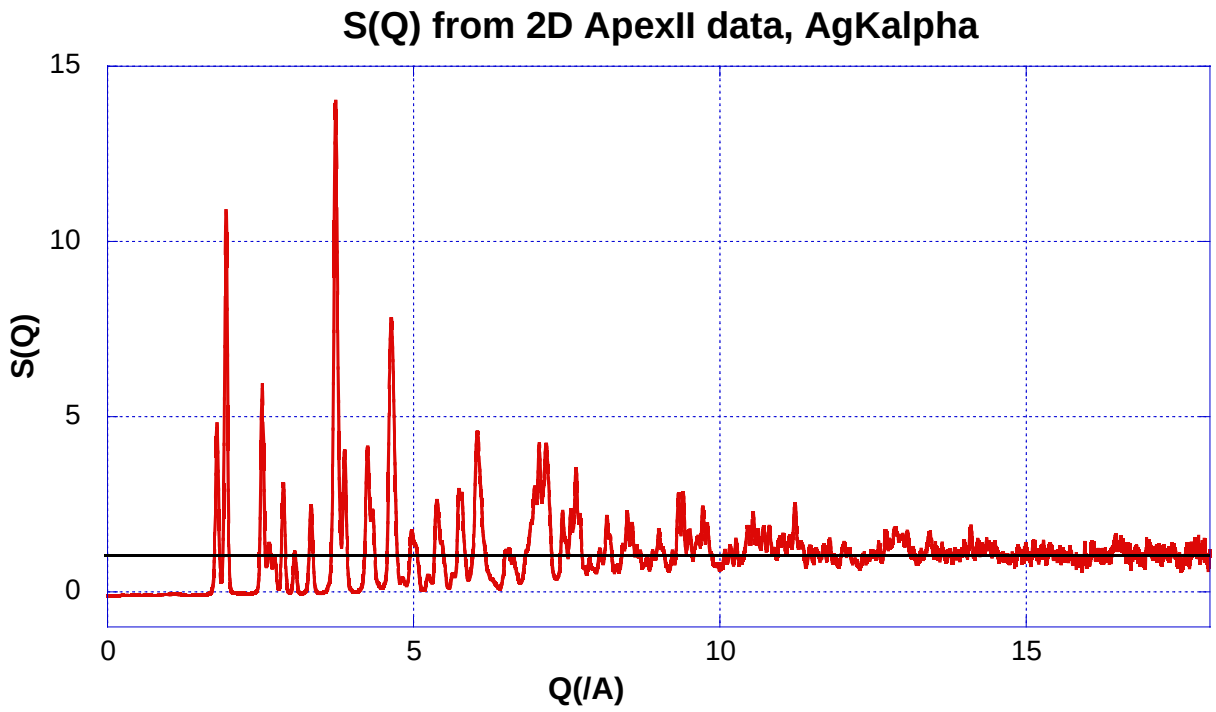

Fit of the PDF, mixture TiO_2 Rutile + Anatase

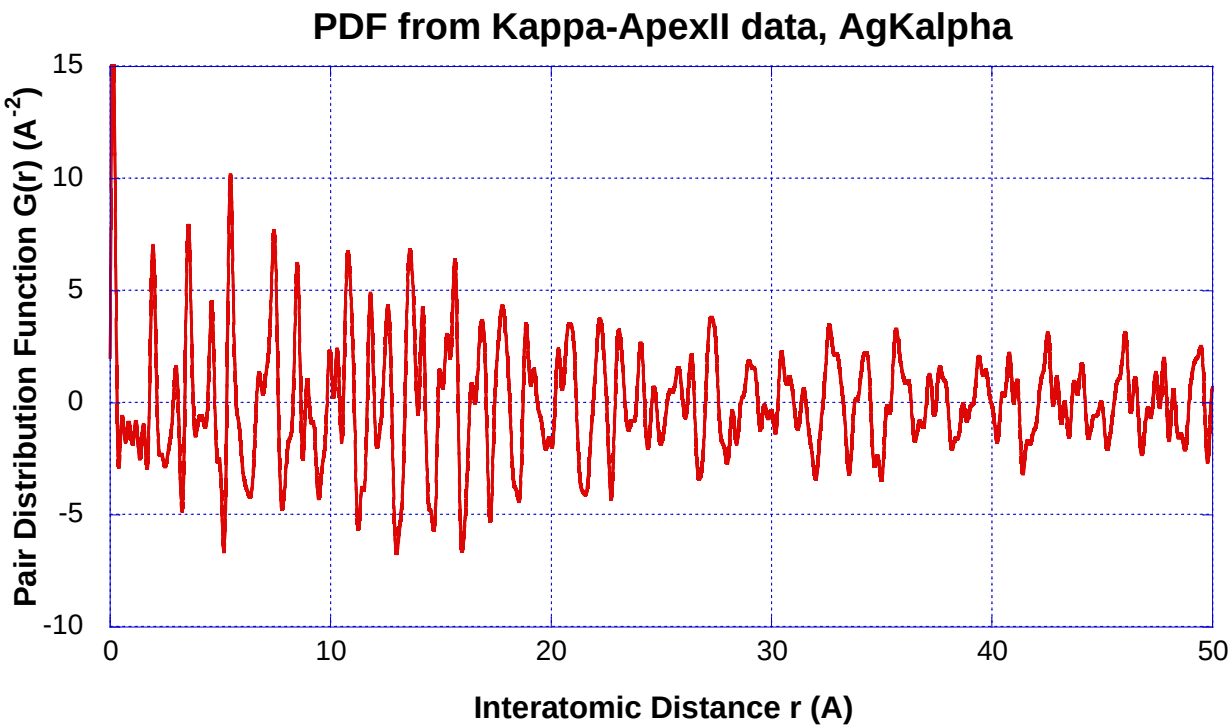

Fit of the PDF, mixture TiO_2 Rutile + Anatase

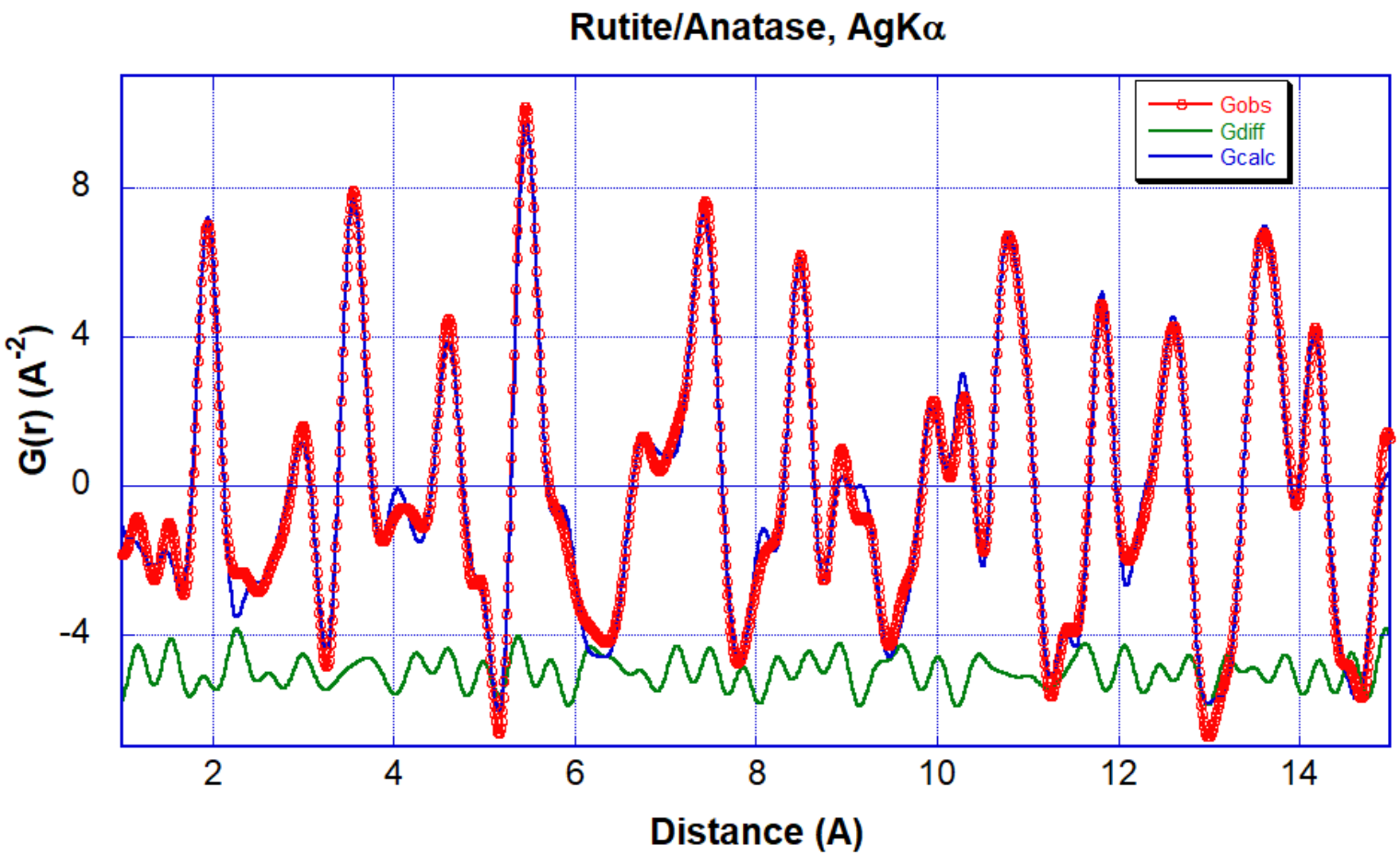

Measurement conditions for in situ/operando (synchrotron)

Method 1 = scanning of a small 2D detector, on moderate energy beamlines (≈25-30keV)

Qmax ≈20Å-1, measurement time <1h, good spatial resolution (depends on the sample/detector distance). Requires a wide angular range (120°)

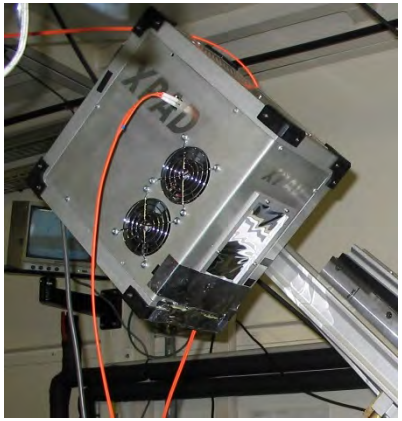

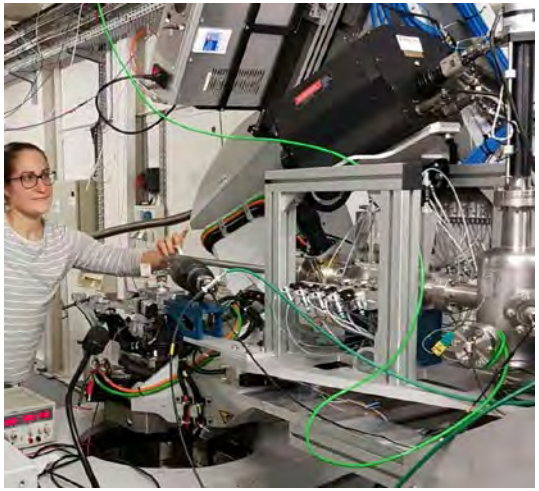

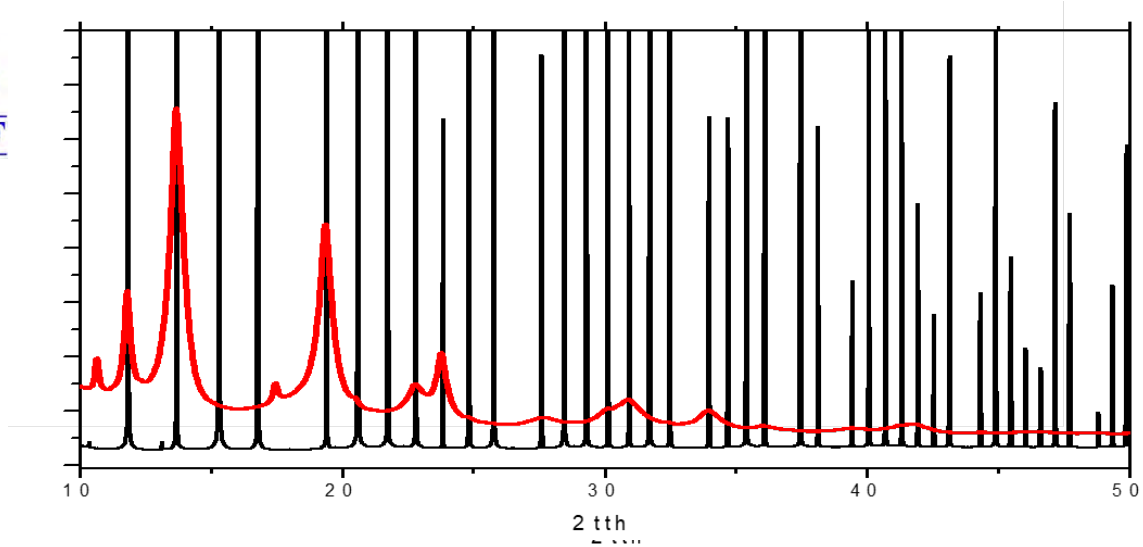

- XPAD Pixel Detector
- 120 images, every degrees in 2theta (≈<1h)
- Calibration with LaB_6
- Resolution: $\Delta Q/Q \sim 10^{-3} - 10^{-4}$ (depends on the distance to the detector
- λ = 0.5 Å, 25 keV
- Qmax = 25 $Å^{-1}$
- Fast azimuth integration with pyFAI

pyFAI *J. Kieffer et al. Journal of Applied Crystallography (2015) 48 (2), 510-519*

Method 2 = "large" 2D detector, on very high energy lines (>60keV)

Qmax ≈20Å^{-1}, measurement time ≈ qq min,
sample/detector distance set by Qmax and detector size,
Spatial resolution limited by pixel size and sample-to-detector distance

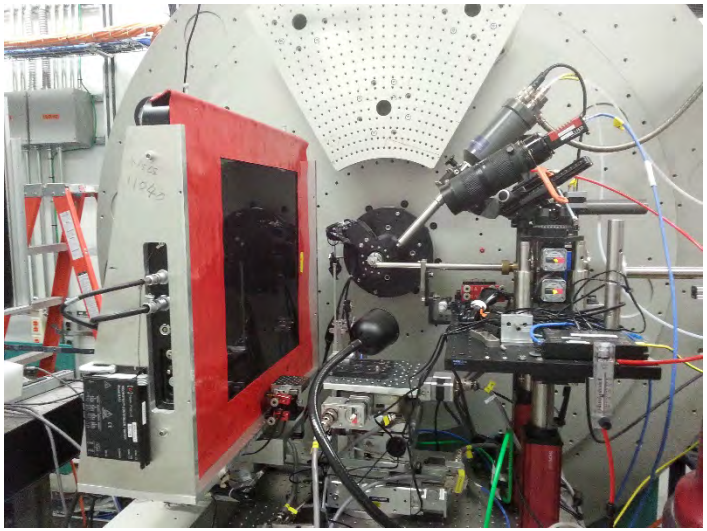

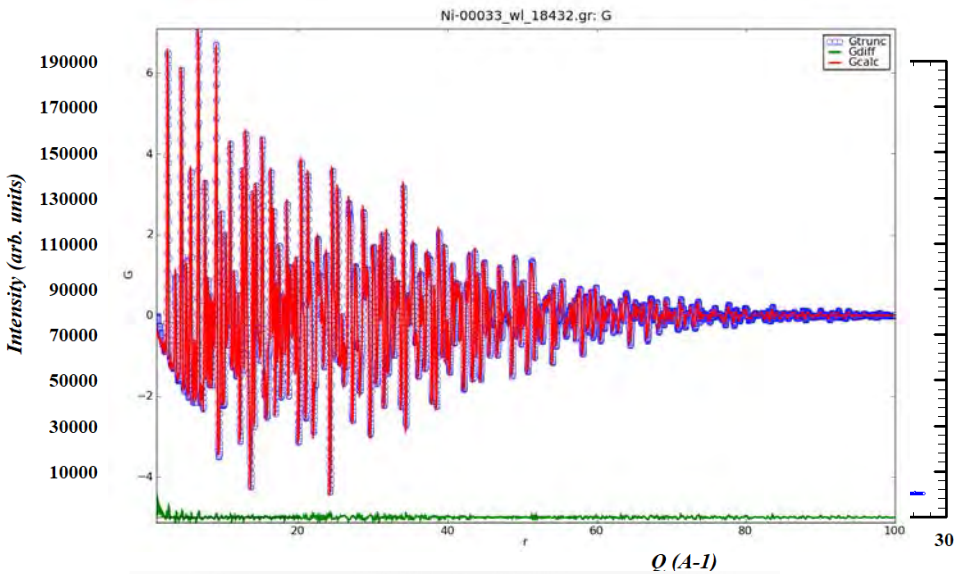

- Perkin Elmer detector: 41 × 41 cm^2 CsI scintillator bonded to an amorphous silicon substrate, 100x100µm
- 1 frame/10s (=5°/frame (DSC))
- Calibration with Ni
- Sample-to-detector distance = 240 mm (1 pixel= 0.024°)
- λ = 0.186 Å, 66.7 keV
- Qmax > 20 Å-1
- Fast azimuth integration with PDFGetX3

!! Also watch out for Qmin!!
Do not cut reflection at low angles

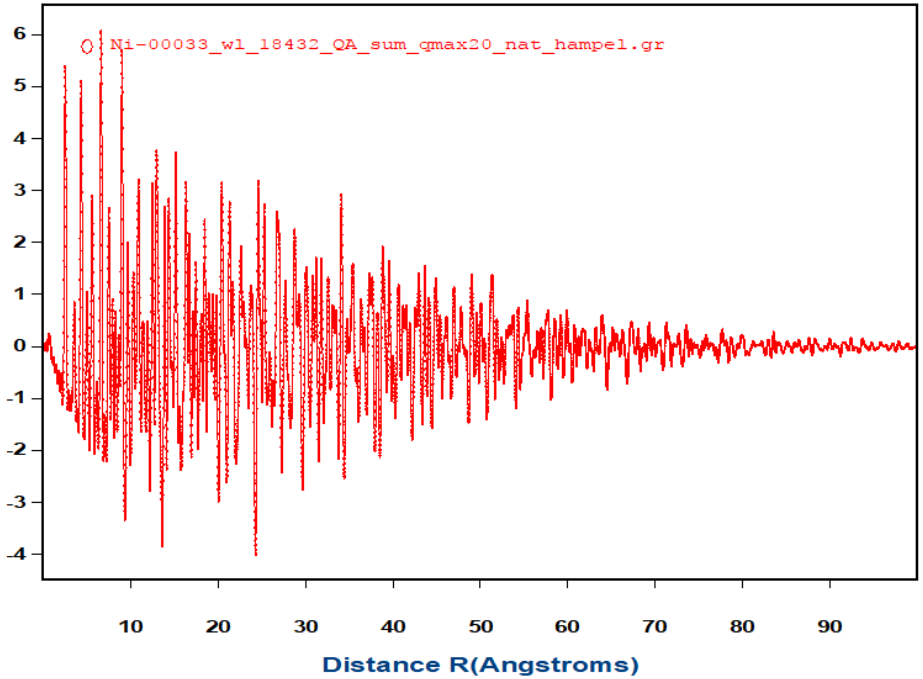

- NSLSII
- Sample-to-detector distance= **240 mm**
  (1 pixel= 0.024°)
- λ = 0.186 Å, 66.7 keV
- Qmax > 20 Å^{-1}

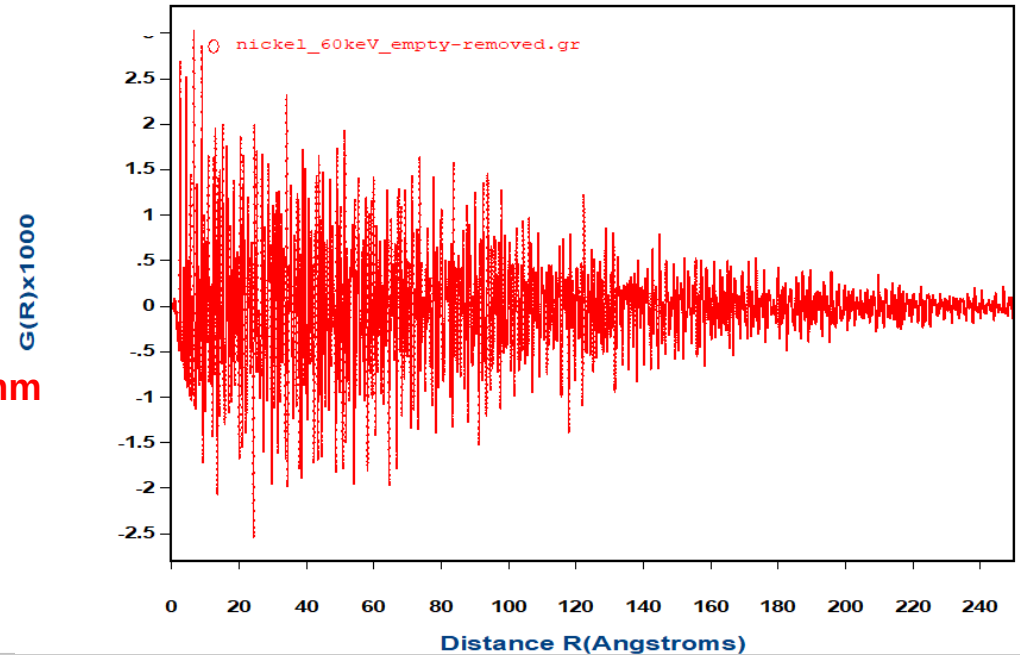

- ID22-ESRF
- Sample-to-detector distance= **385 mm**
  (1 pixel= 0.015°)
- λ = 0.207 Å, 60.0 keV
- Qmax > 20 Å^{-1}

How to process the diagram to extract the PDF ??

Obtain the experimental PDF (case of B.B. X-rays)

$$G(r) = 4\pi r[\rho(r) - \rho_0] = \frac{2}{\pi}\int_0^{\infty} Q[S(Q) - 1]\sin(Qr)dQ,$$

I(Q)
X'pert
Bragg-Brentano
X'celerator
λMoKα
Miroir Göbel

No sample holder

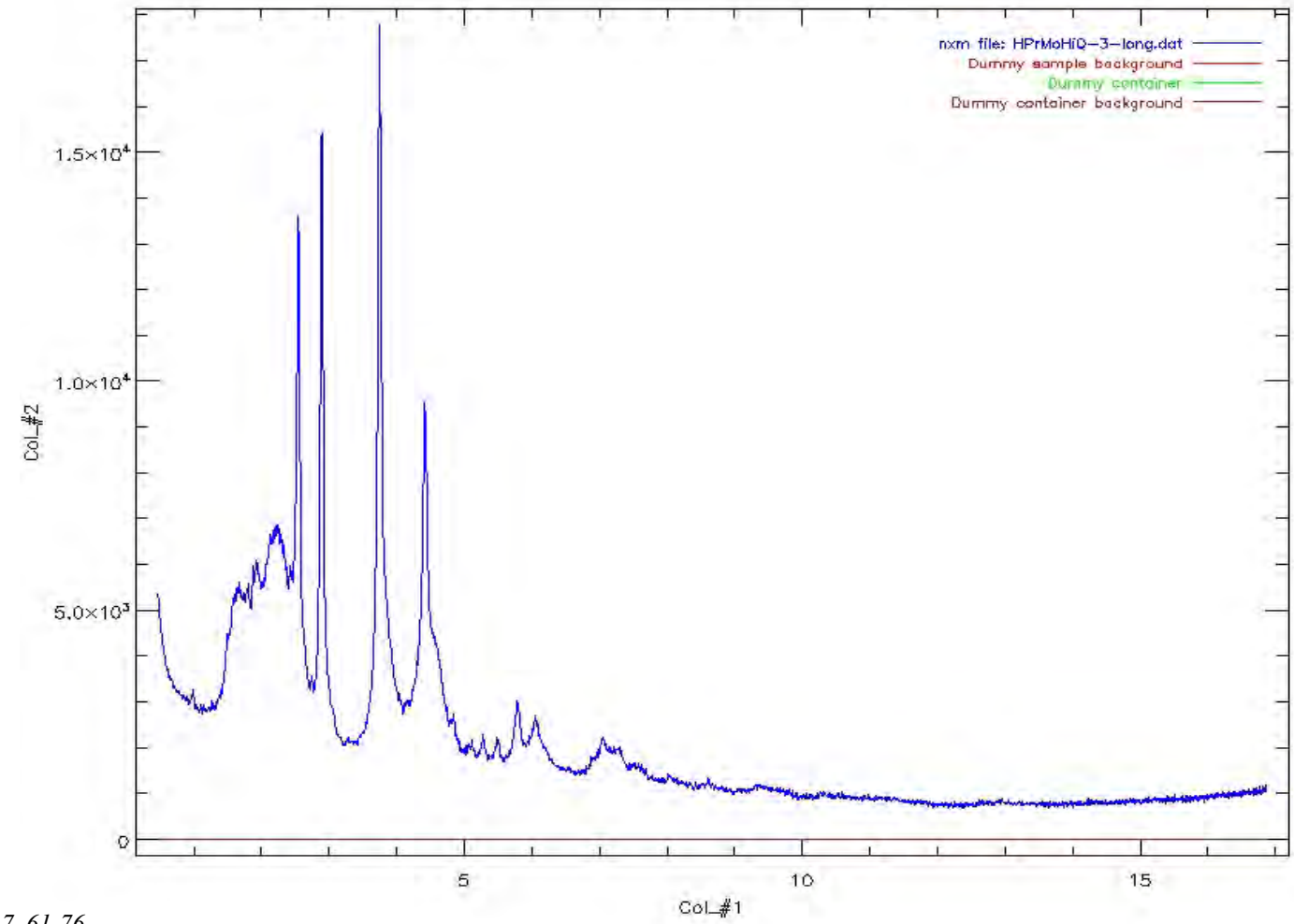

B.J. Thijsse, J. Appl. Cryst. (1984). 17, 61-76

Obtain the experimental PDF (case of B.B. X-rays)

$$P = (1 + x\,\cos^2 2\theta)/(1 + y)$$

$x = \cos^2 2\alpha_c$ ou $\cos 2\alpha_c$ Mono. mosaic ou parfait; primaire : *x=y*; diffracté, *y=1*

Polarization
(no Lorentz corr.)

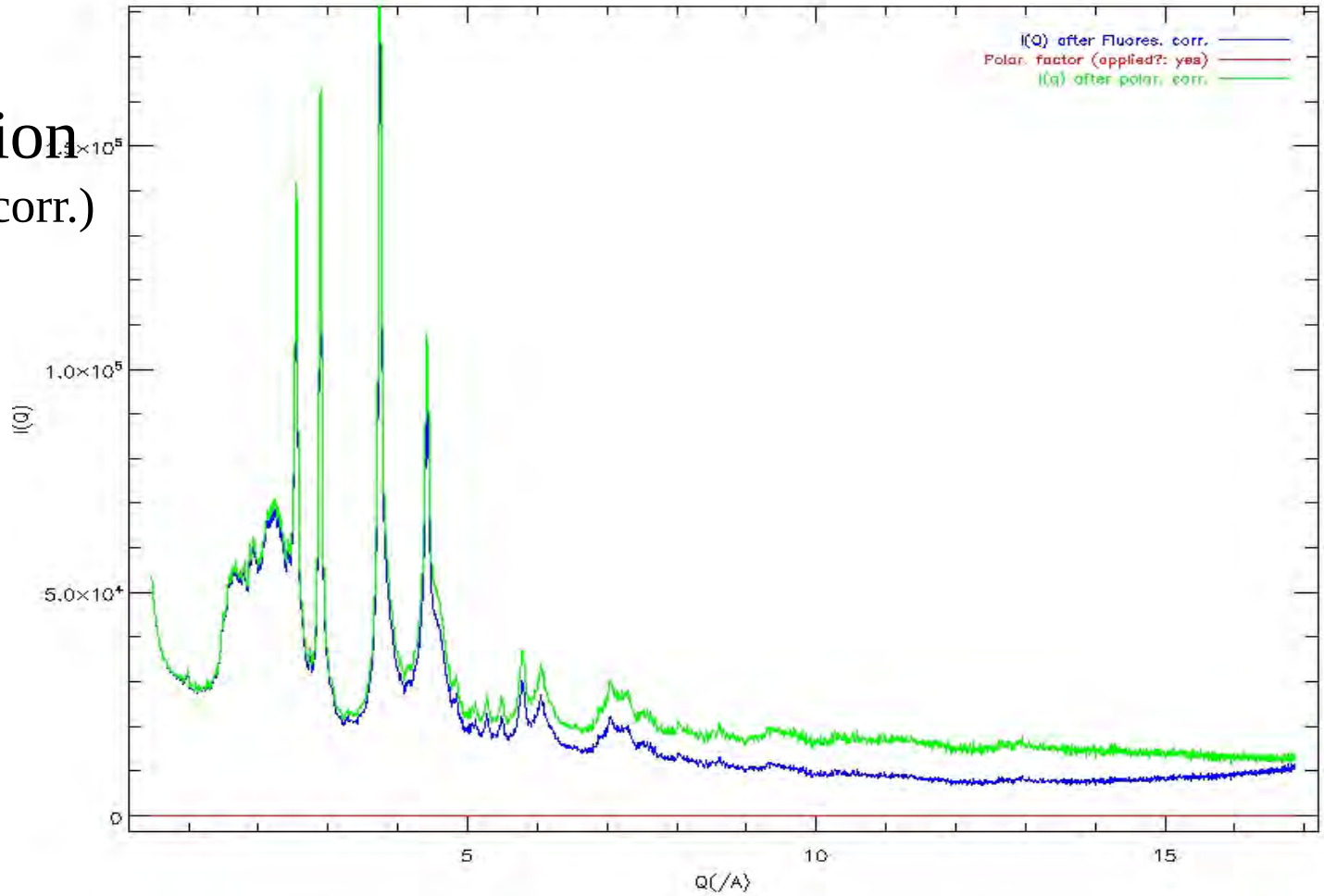

Obtain the experimental PDF (case of B.B. X-rays)

$$A_{refl} = [1 - \exp(-2\,\mu\, t/\sin\theta]/2\,\mu$$

Absorption

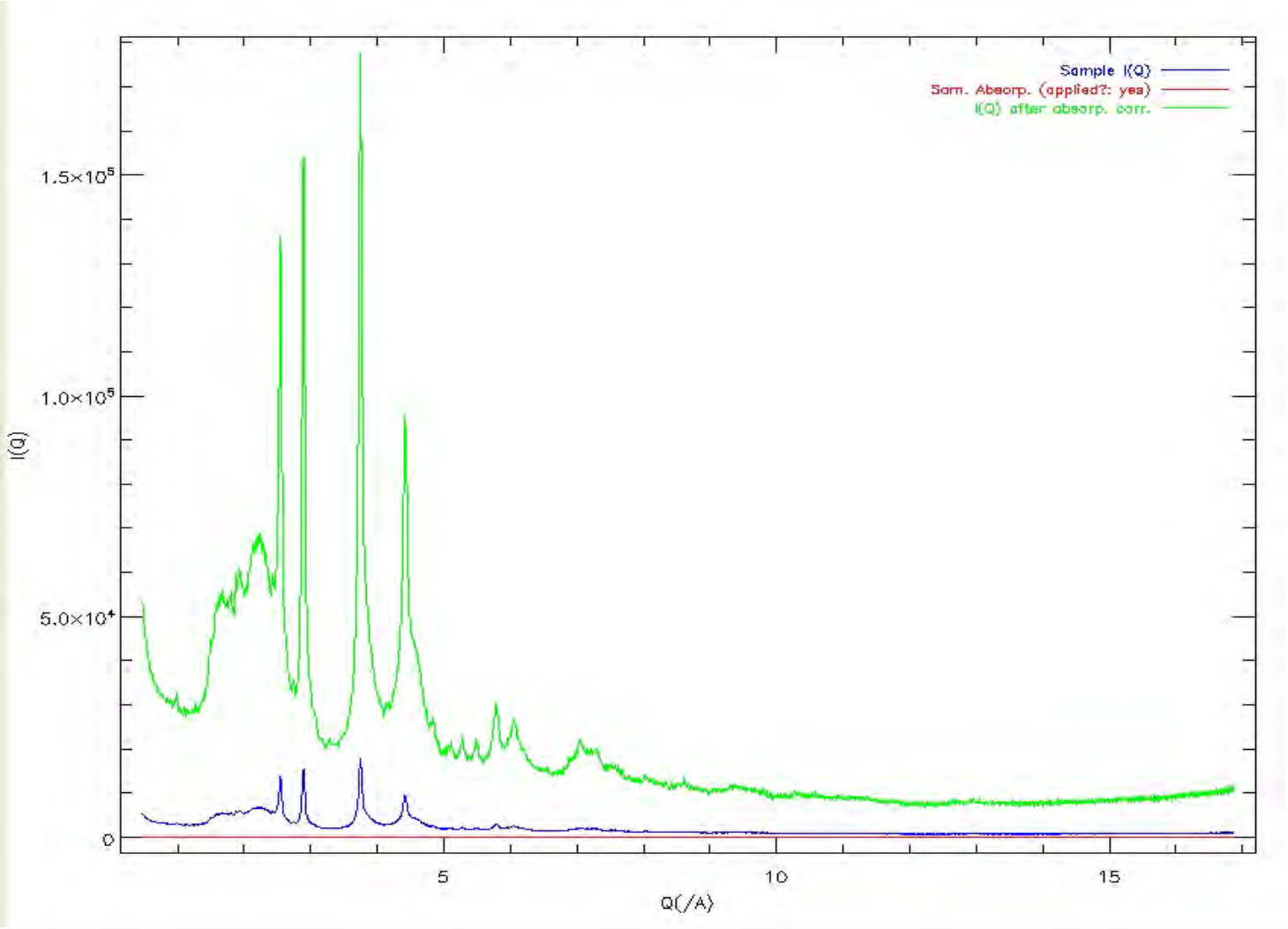

Obtain the experimental PDF (case of B.B. X-rays)

Compton

$$I_a^{\text{incoh}}(Q) = \left(\frac{\lambda}{\lambda'}\right)^2 \sum_{j=1}^{n} c_j Z_j \frac{(b_j Q)^{a_j}}{1+(b_j Q)^{a_j}} \qquad (A2)$$

with n the number of atomic species, Z_j the atomic number of species j, and a_j and b_j semi-empirical expressions given by

$$a_j = 2{\cdot}6917\, Z_j^{-1} + 1{\cdot}2450 \qquad (A3)$$

$$b_j = 1{\cdot}1870\, Z_j^{-1} + 0{\cdot}1075 + 0{\cdot}00436\, Z_j - (0{\cdot}01543\, Z_j)^2 + (0{\cdot}01422\, Z_j)^3. \qquad (A4)$$

Formulas (A2), (A3), (A4) are based on the data in Cromer & Mann (1967).

(g) *The Ruland monochromator cut-off function* $Y_R(Q)$

$$Y_R(Q) = \left\{\left(1+\frac{\Delta\lambda}{b}\right)\left[1+\frac{\pi^2(\lambda'-\lambda)^2}{(\Delta\lambda+b)^2}\right]\right\}^{-1}, \qquad (A17)$$

with $\Delta\lambda = \Delta q_{\max}\lambda^2 s^3 c^{-1}(a^2+s^2)^{-1}$, $s = Q/2\pi$, $a = 5{\cdot}3$ nm^{-1}, $b = 6{\cdot}9$ pm, $c = 137$ and $\Delta q_{\max} = 3{\cdot}05$ (Ruland, 1964).

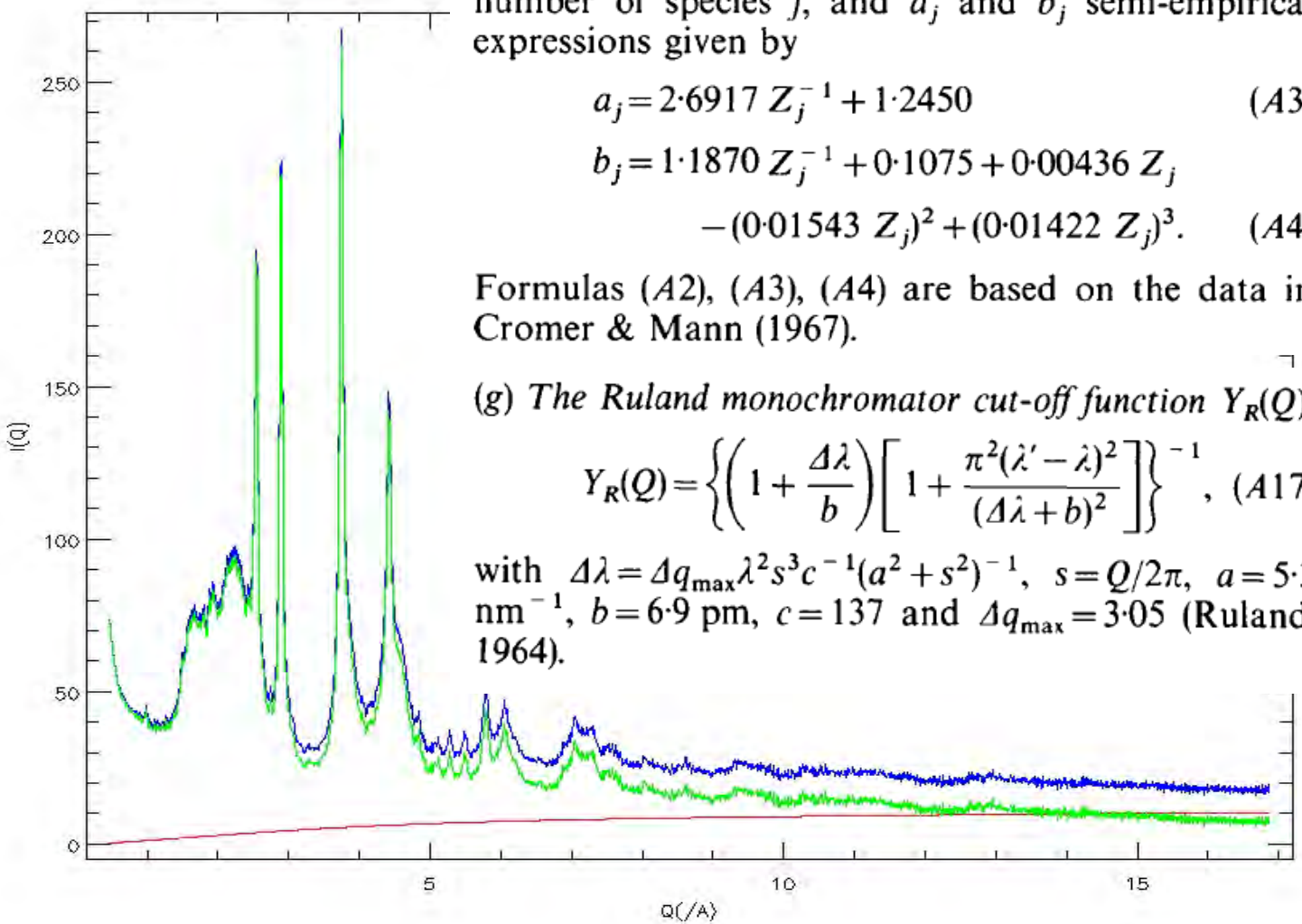

Obtain the experimental PDF (case of B.B. X-rays)

$$S(Q) = [I_{eu}^{coh} - (\langle f^2 \rangle - \langle f \rangle^2)]/\langle f \rangle^2$$

Laue diffuse scattering

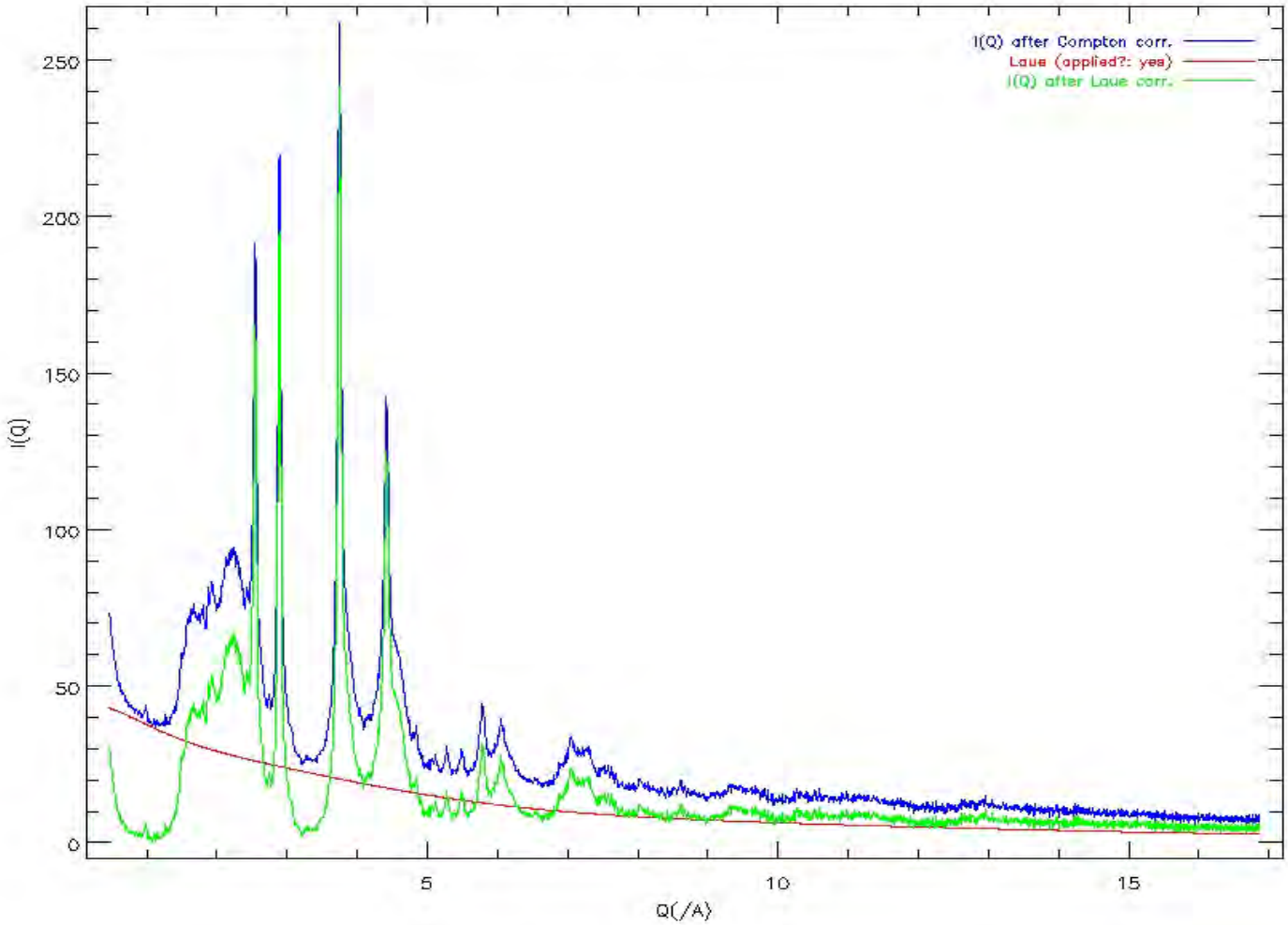

Obtain the experimental PDF (case of B.B. X-rays)

$$S(Q) = [I_{eu}^{coh} - (\langle f^2 \rangle - \langle f \rangle^2)]/\langle f \rangle^2$$

Normalization
$\langle f \rangle^2$

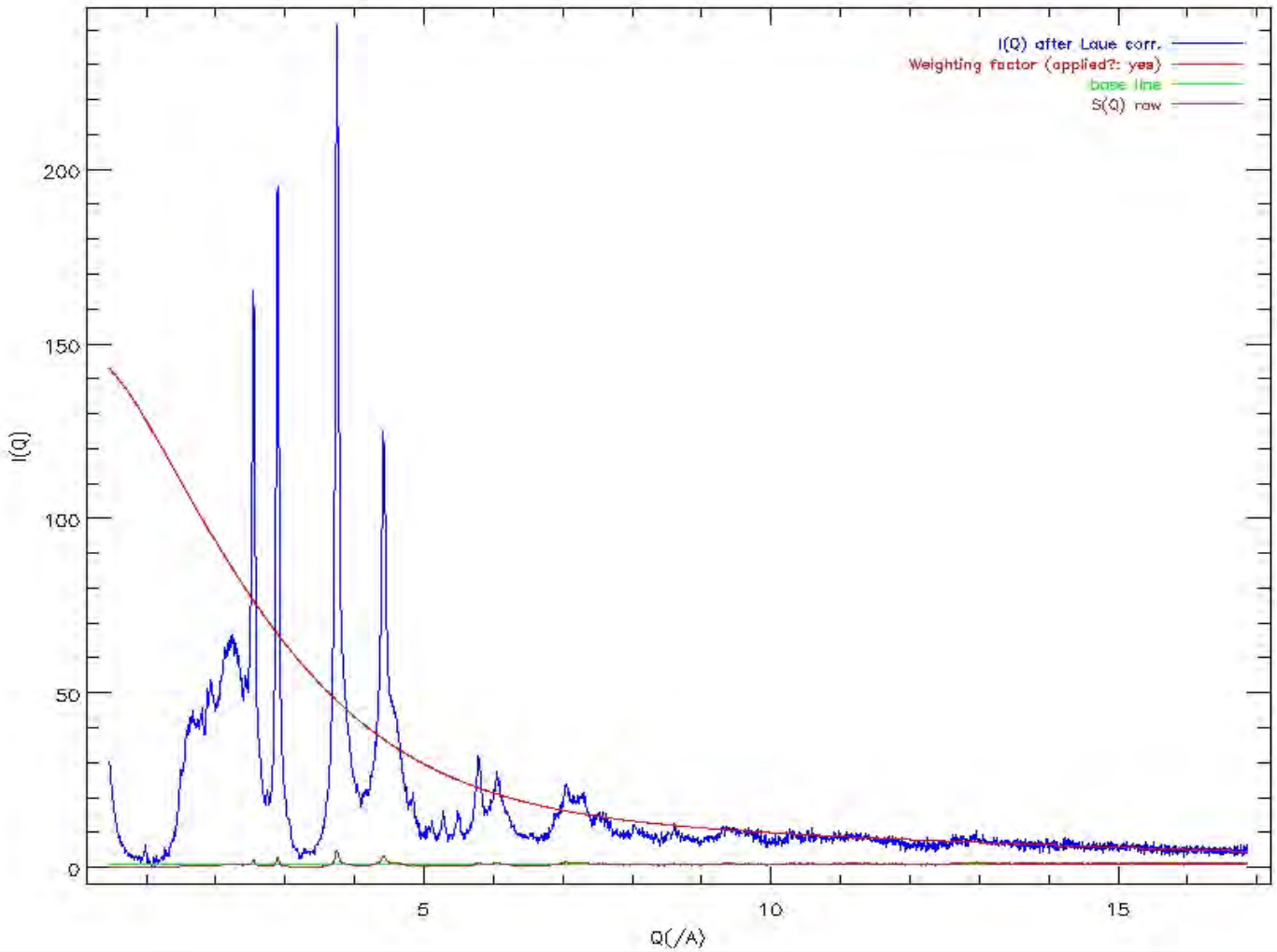

Obtain the experimental PDF (case of B.B. X-rays)

$$G(r) = 4\pi r[\rho(r) - \rho_0] = \frac{2}{\pi}\int_0^{\infty} Q[S(Q) - 1]\sin(Qr)dQ,$$

S(Q)

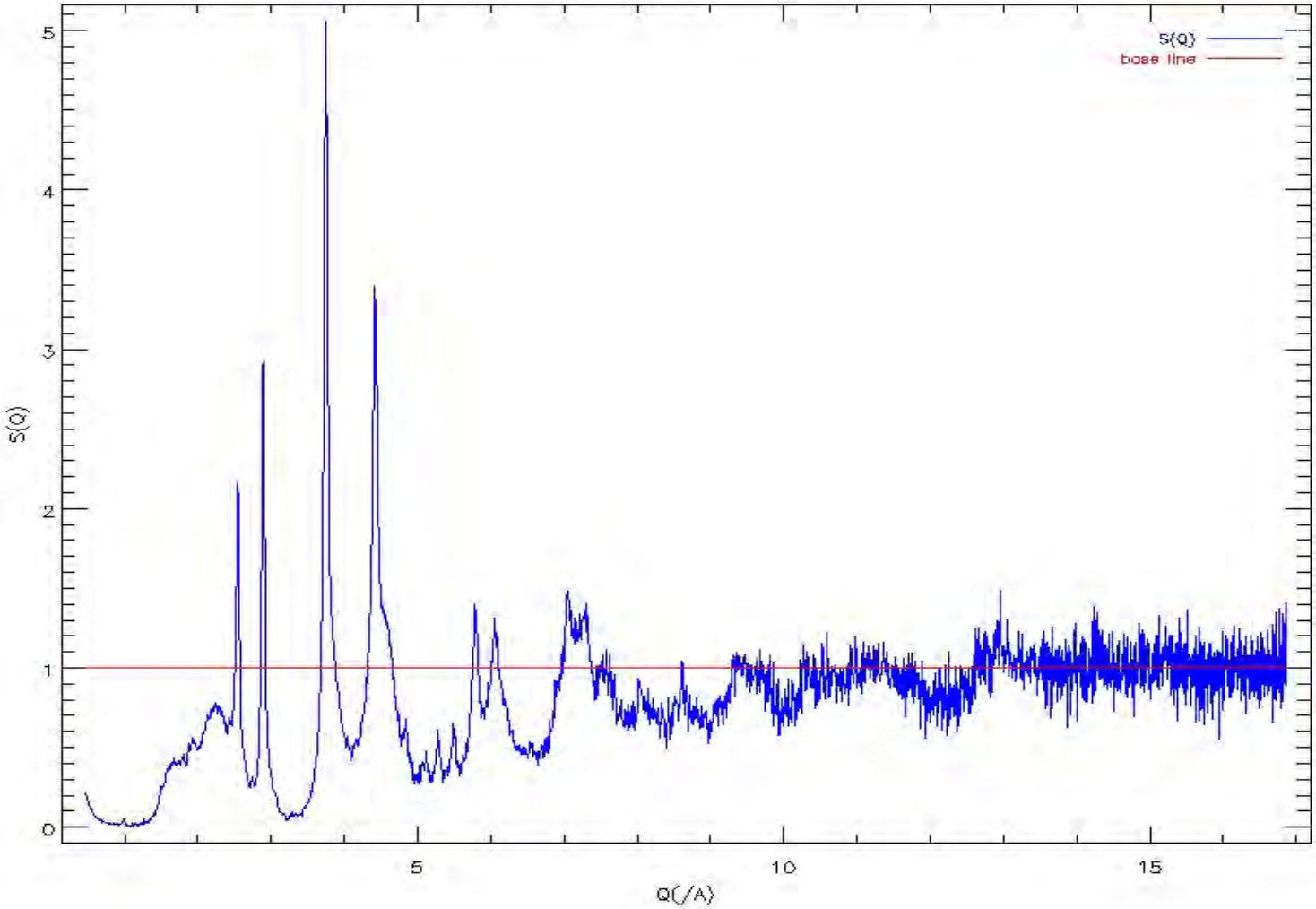

Obtain the experimental PDF (case of B.B. X-rays)

$$G(r) = 4\pi r[\rho(r) - \rho_0] = \frac{2}{\pi}\int_0^{\infty} Q[S(Q) - 1]\sin(Qr)dQ,$$

F(Q)

F(Q)=Q(SQ)-1)

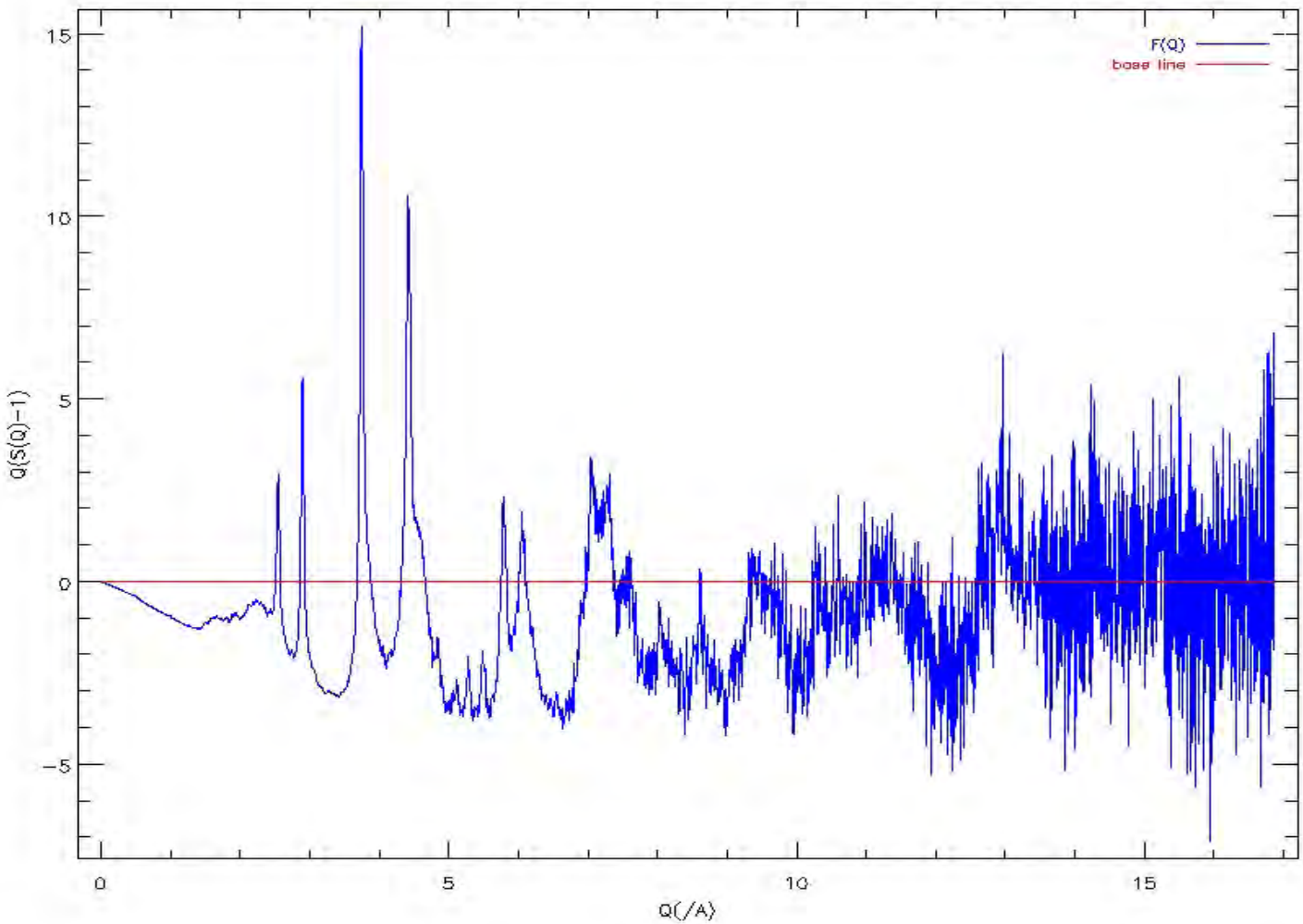

Obtain the experimental PDF (case of B.B. X-rays)

$$G(r) = 4\pi r[\rho(r) - \rho_0] = \frac{2}{\pi}\int_0^{\infty} Q[S(Q) - 1]\sin(Qr)dQ,$$

G(r)

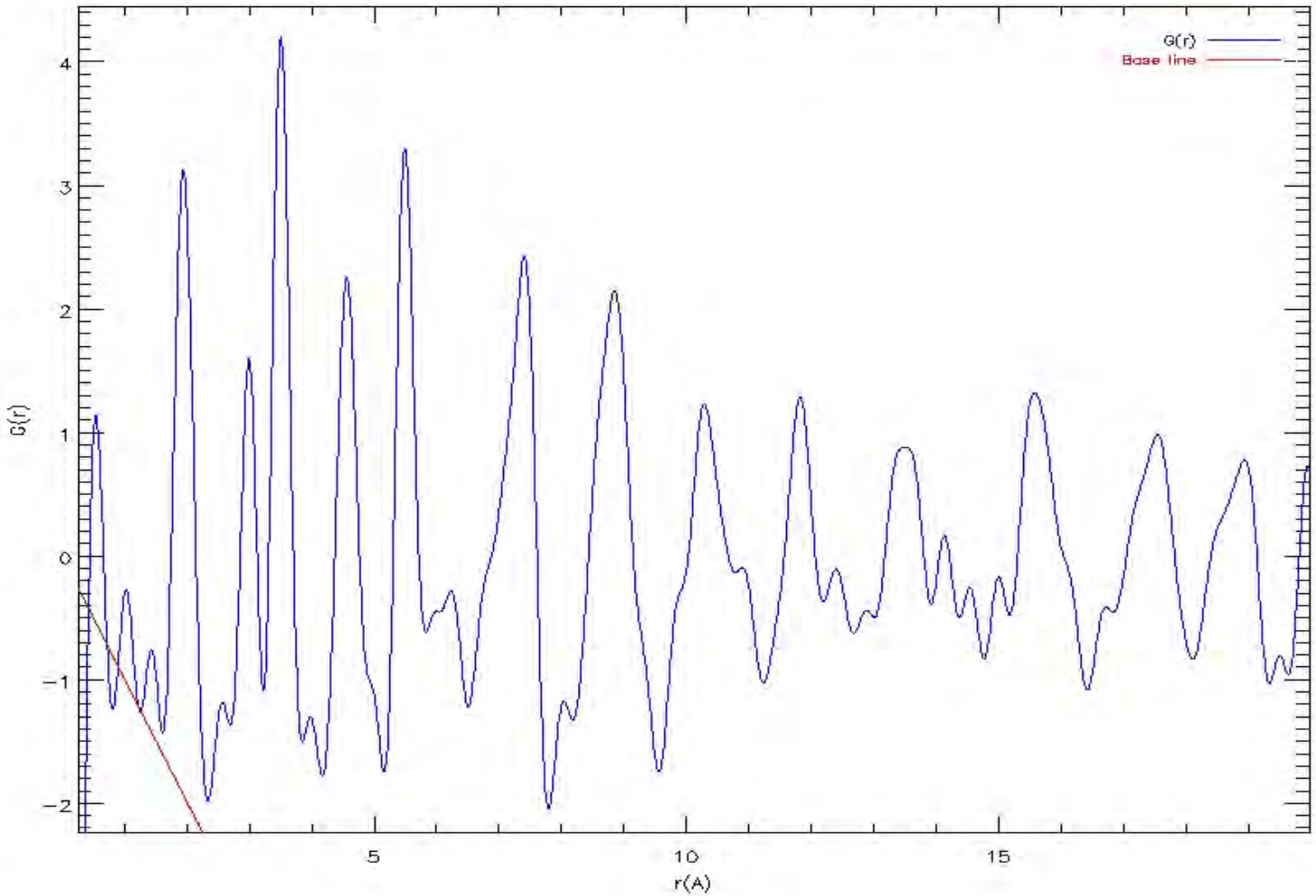

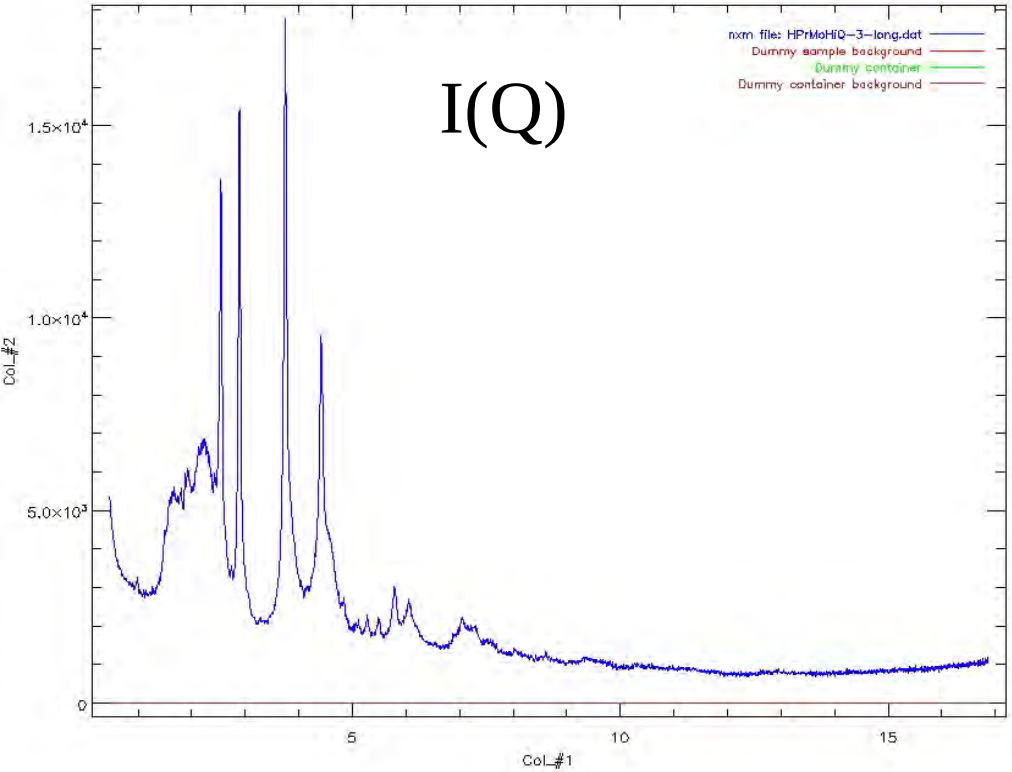

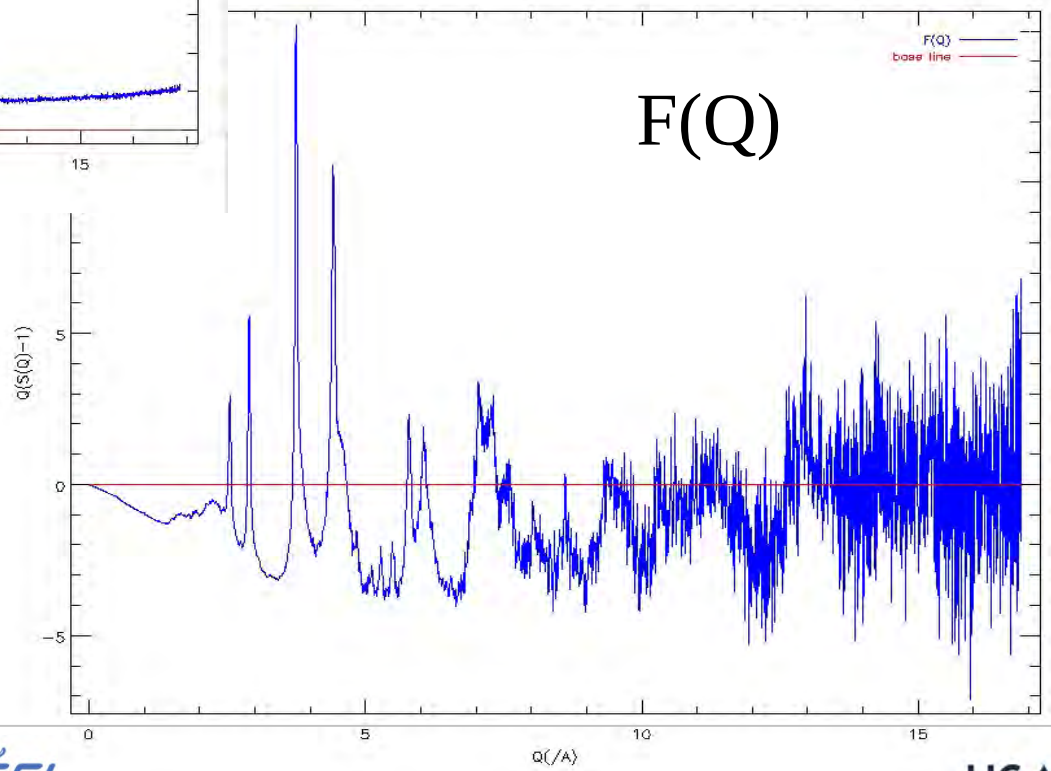

Measure at high Q
Strong stats with high Qs

Obtain the experimental PDF (case of B.B. X-rays)

Damping of F(Q) with the Lorch function

$L=\sin(Q.\pi/Q_{max}) / (Q.\pi/Q_{max})$
& $(Q=0 \text{ for } Q > Q_{max})$
TF de L(Q).F(Q)

⇒ *Reduces noise at large Q*
⇒ *Broadens PDF oscillations*

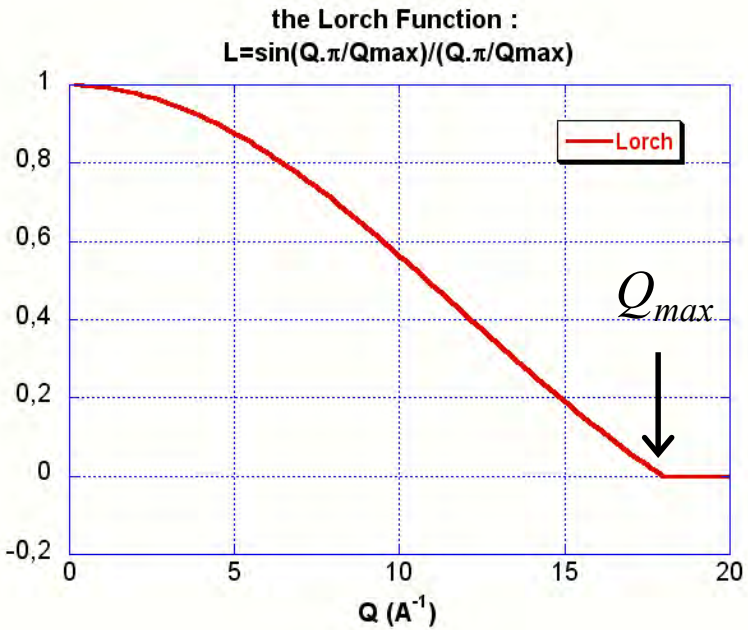

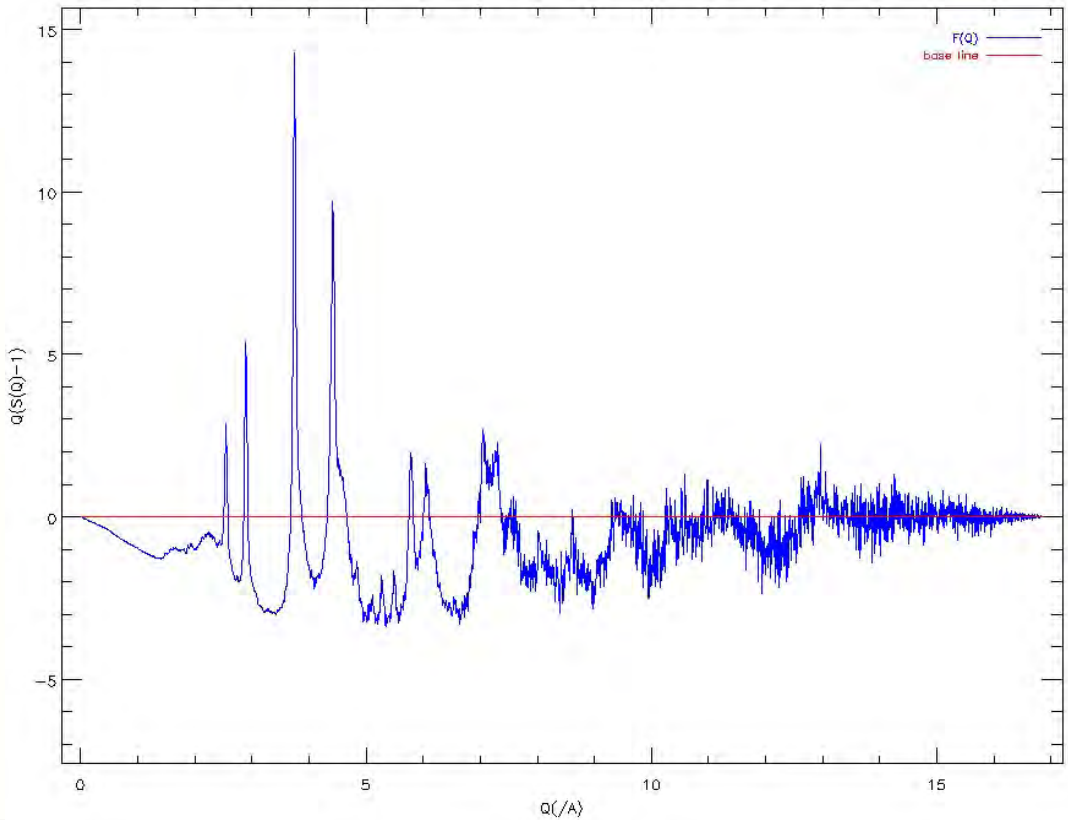

Obtain the experimental PDF (case of B.B. X-rays)

$$G(r) = 4\pi r[\rho(r) - \rho_0] = \frac{2}{\pi}\int_0^{\infty} Q[S(Q) - 1]\sin(Qr)dQ,$$

G(r)

F(Q) damped, Lorch

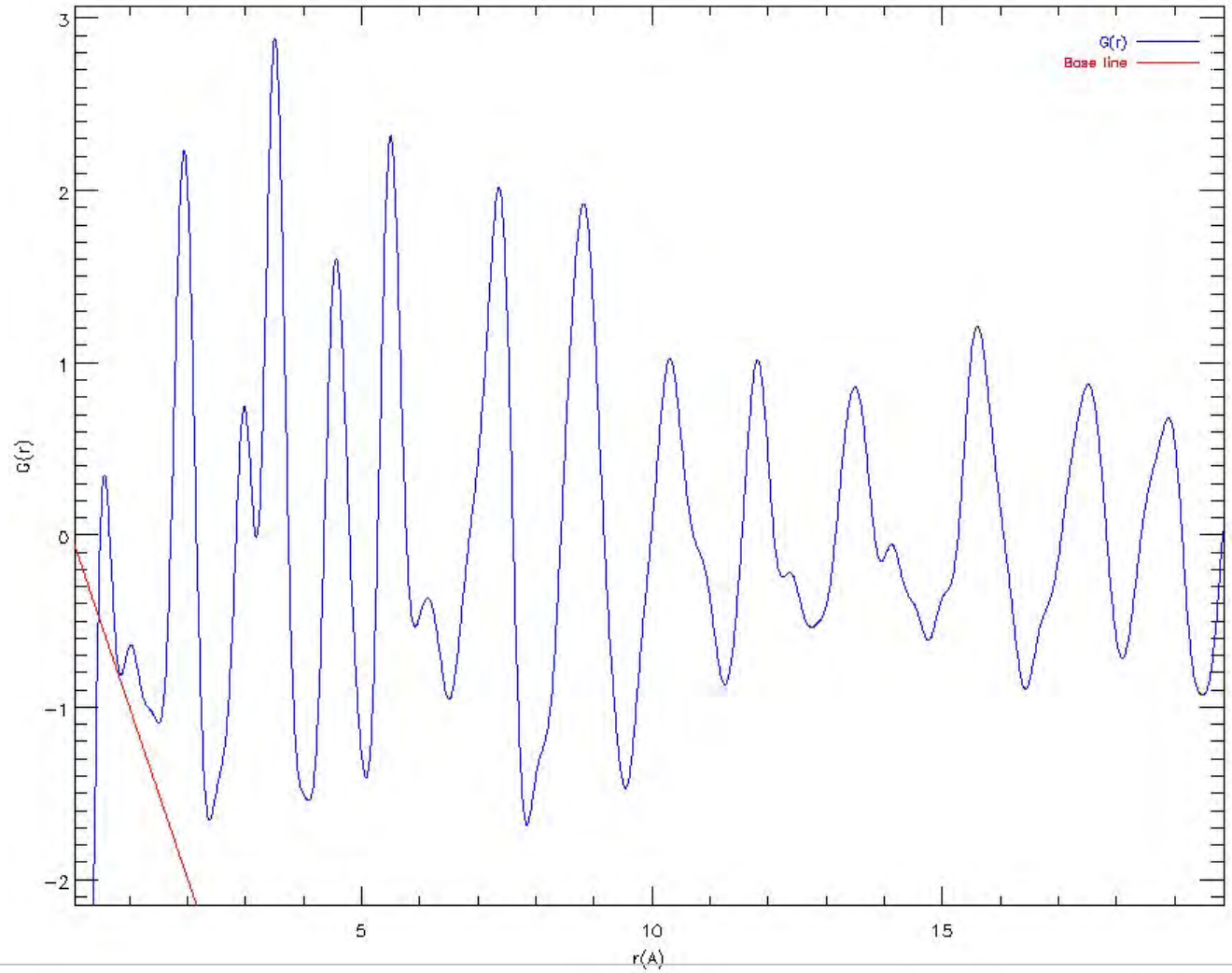

PDFgetX2

Qiu, X. et al. J. Appl. Crystal. (2004)

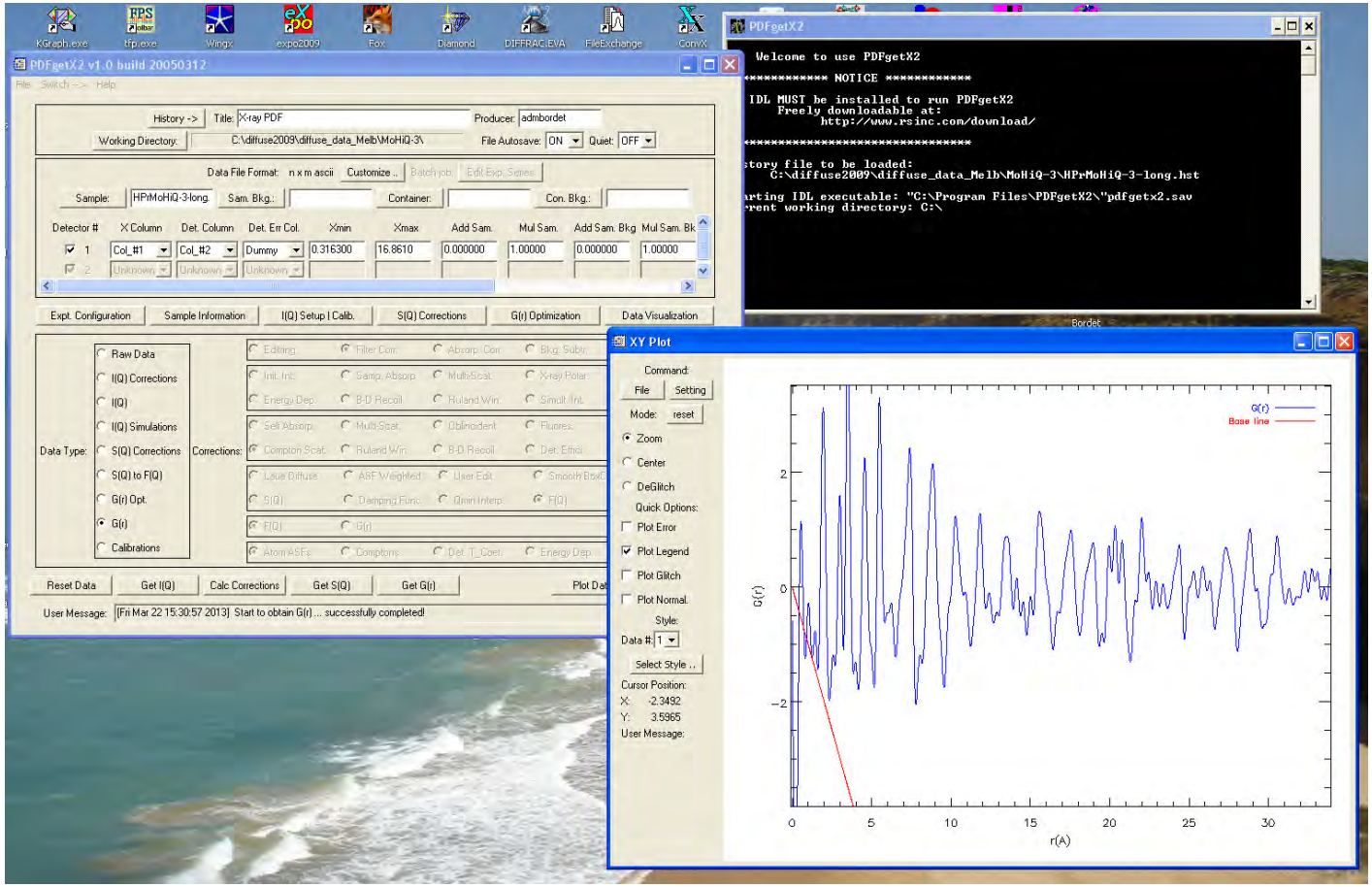

Allows all corrections to be applied successively,
to see their effects and calculate the PDF. (Lorch damping possible).
Rigorous in theory, but can be very long,
Effects of corrections difficult to separate in practice.

The procedure of PDFGetX2 is cumbersome

Many, poorly known correction parameters.

strong correlations between additive+multiplicative corrections...

However, we know that we ***can empirically reduce the set of corrections*** to:

$$I_m(Q) = a(Q)I_c(Q) + b(Q)$$

$$S(Q) - 1 = \frac{I(Q)}{\langle f \rangle^2} - \frac{\langle f^2 \rangle}{\langle f \rangle^2}$$

S(Q)-1 oscillates around 0, used to normalize $I_m(Q)$ after subtraction of the signal from the sample holder

$$S_m(Q) - 1 = S(Q) - 1 + \beta_S(Q)$$

$\beta_S(Q)$ is a slowly variable function of Q

$$F_m(Q) = Q\left[S(Q) - 1 + \beta_S(Q)\right] = F(Q) + Q\beta_S(Q)$$

$$F_c(Q) = F_m(Q) - QP_n(Q)$$

$P_n(Q)$ is a n-order polynomial to be refined between 0 and $Q_{maxinst}$

$$\Delta F(Q) = F_c(Q) - F(Q) = Q\beta_S(Q) - QP_n(Q)$$

$\Delta F(Q)$ Can be approximated by a function oscillating around 0, of half period $Q_{maxinst}/n$

We will have non-physical effects in the FT up to a frequency $r_{poly} = \pi n / Q_{maxinst}$

e.g., for n=8 and $Q_{maxinst}$ = 28 Å^{-1} , r_{poly}=0.9

In practice, $n_r = r_{poly} Q_{maxinst} / \pi$ determines the polynomial degree to be used

=> PDFgetX3 *(P. Juhas et al. ArXiv 2013)*

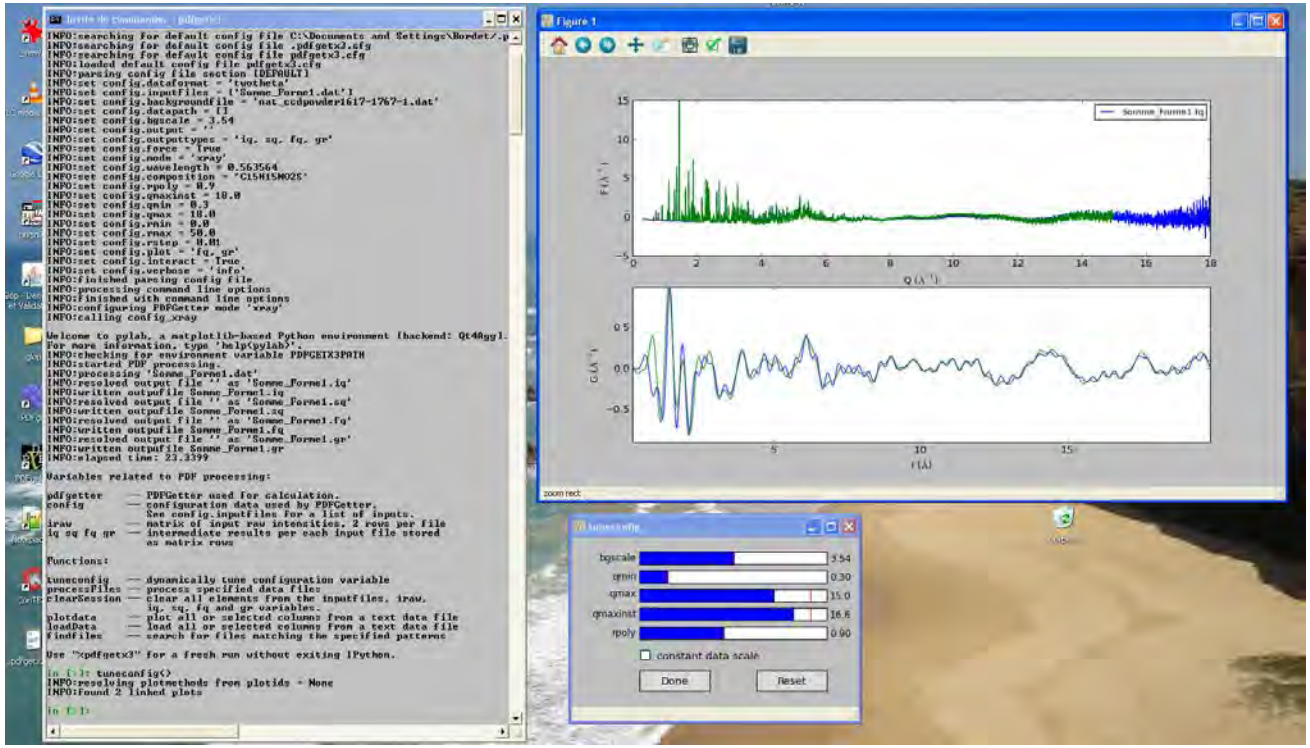

Parameters:

bgscale
Qmin
Qmax
Qmaxinst
Rpoly

Fix the fit range and polynomial degree

Empirical but effective, almost instantaneous correction
Batch processing suitable for in situ/operando measurements
No Lorch damping included

Refine the PDF from a structural model

PDFgui

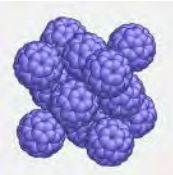

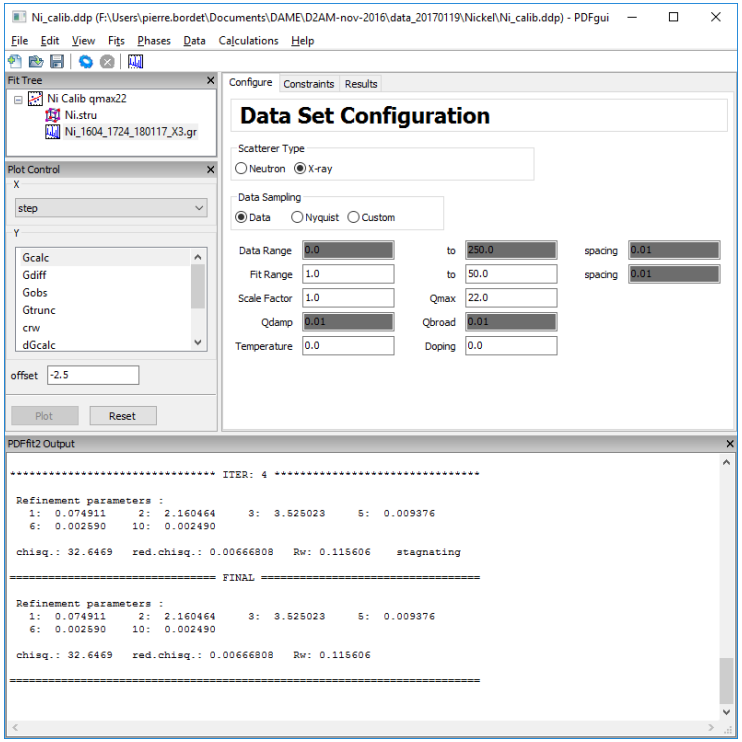

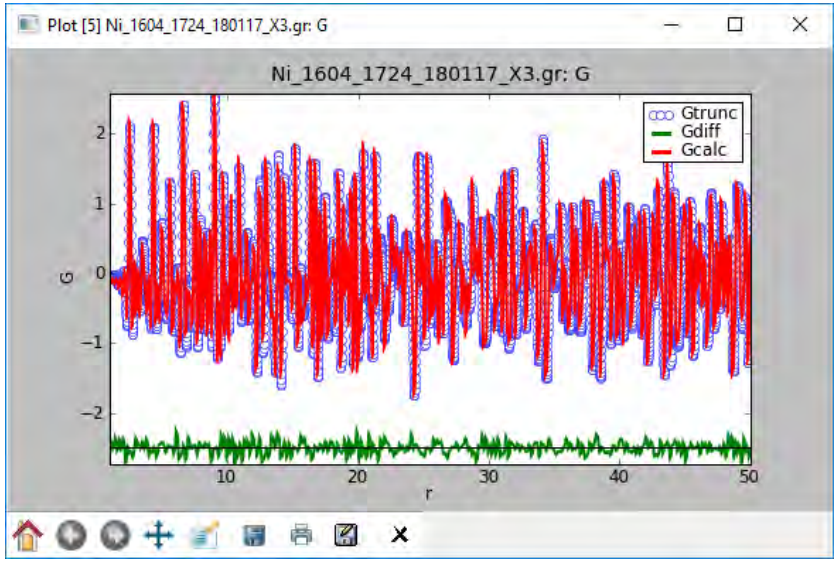

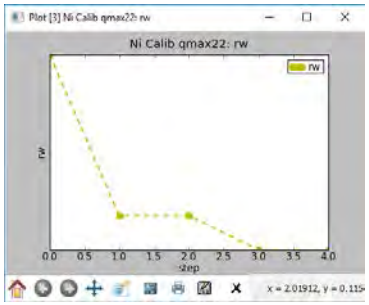

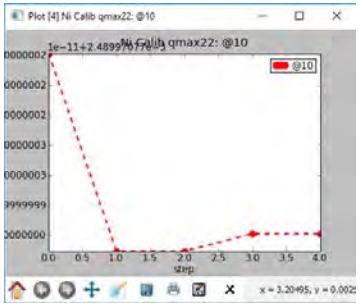

Nice efficient GUI, graphics, etc...
works in P1 + symmetry constraints
Multiple datasets + phases
cyclic refinements (T, distances, etc.)

Farrow et al., J. Phys. Condens. Matter. 19, 335219 (2007)

MolPDF

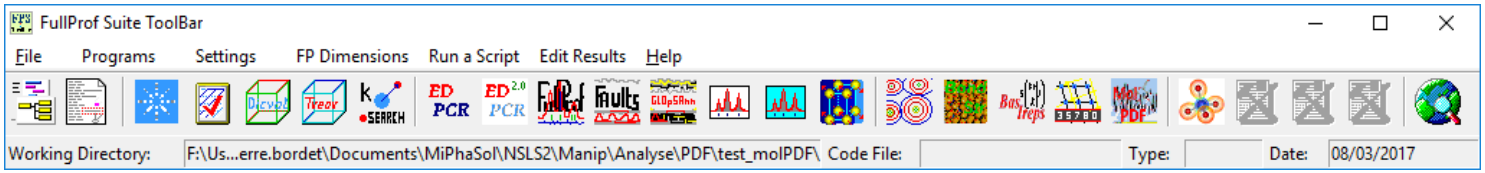

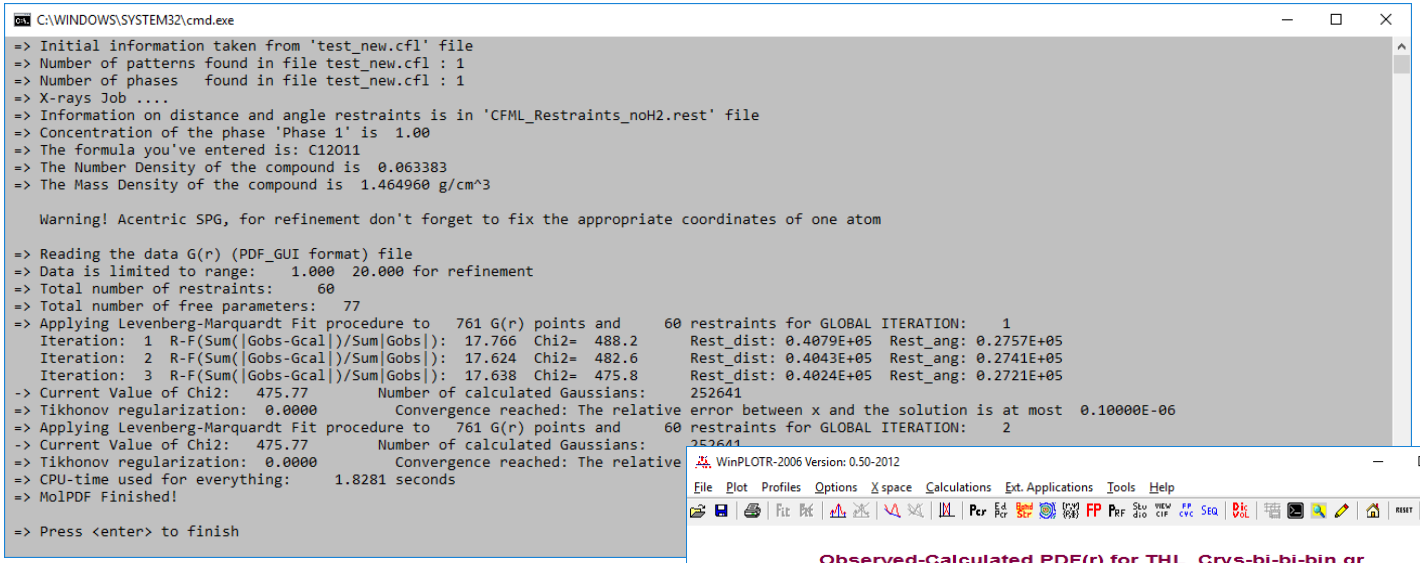

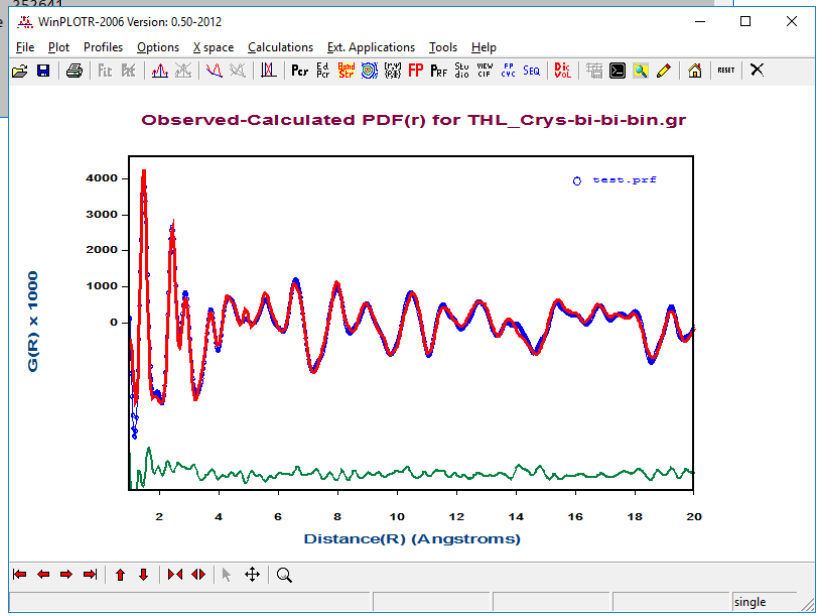

Similar to PDFgui, no GUI, no cyclic refinement with the addition of important specificities for refinement of molecular compounds:

- Distance/angle constraints
- Distinction between intra- and inter-molecular a.d.p.s
- Domain size distribution

J. Rodriguez-Carvajal, EPDIC 2016

TOPAS (or TOPAS Academic)

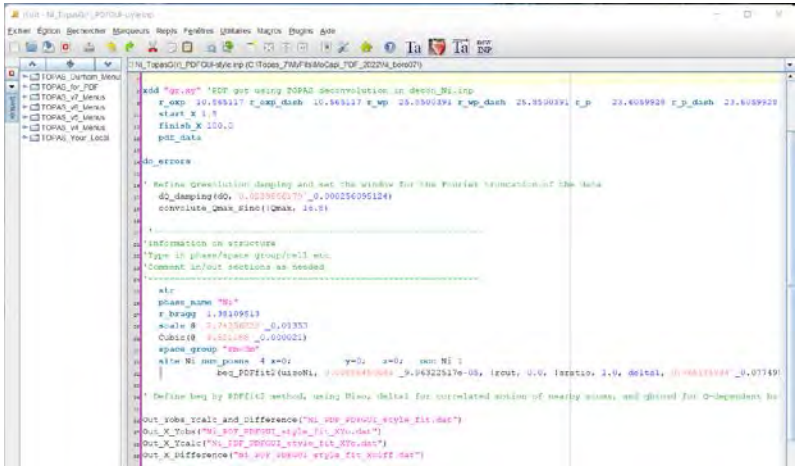

Very fast and very stable
Possible to calculate the PDF after deconvolution
simultaneous PDF + Rietveld
Complex models can be introduced
    (rigid blocks, stacking errors, etc.)
Commercial (Bruker) and expensive
Cheaper TA

Examples

Example : Local structure of nano-crystalline TiO_2

Doped nano-crystalline TiO_2 used in solar cells

Synthesized using soft chemistry

Annealing => anatase

what is the local structure?

X-ray powder diffraction data

Panalytical X'pert diffract.

Mo graded multilayer optics, λ=0.7107Å

Bragg-Brentano geometry

X'celerator detector

Qmax=16.8$Å^{-1}$

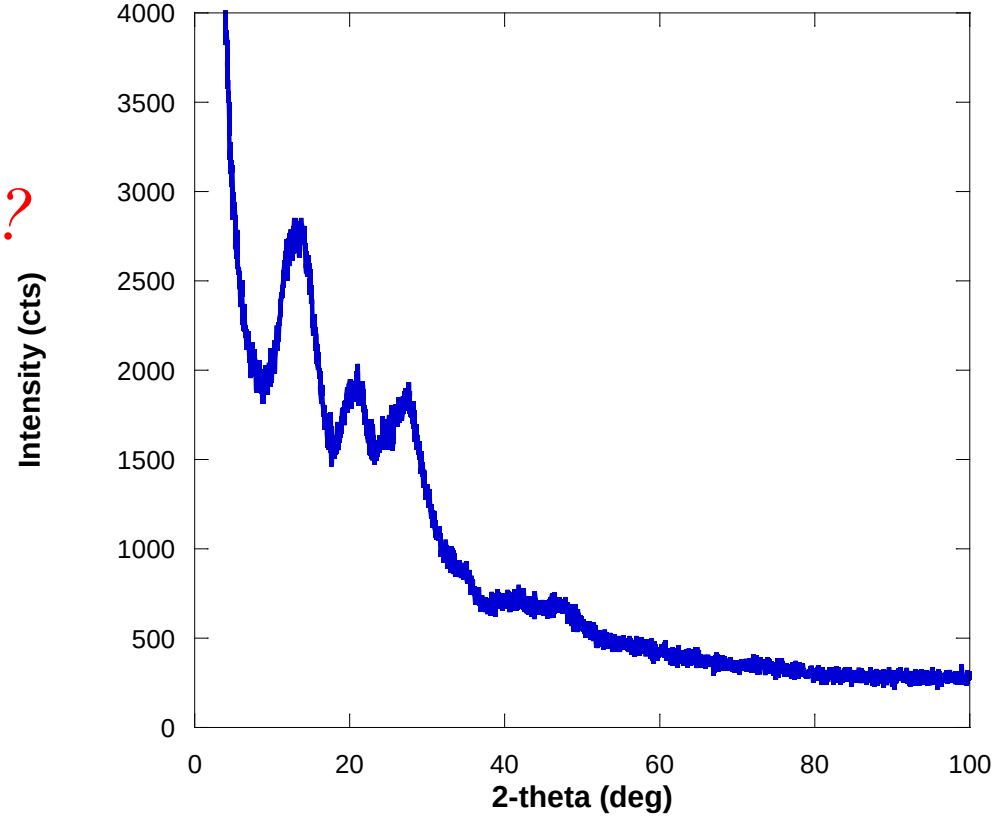

The pdf provides info about the grain size and internal grain structure

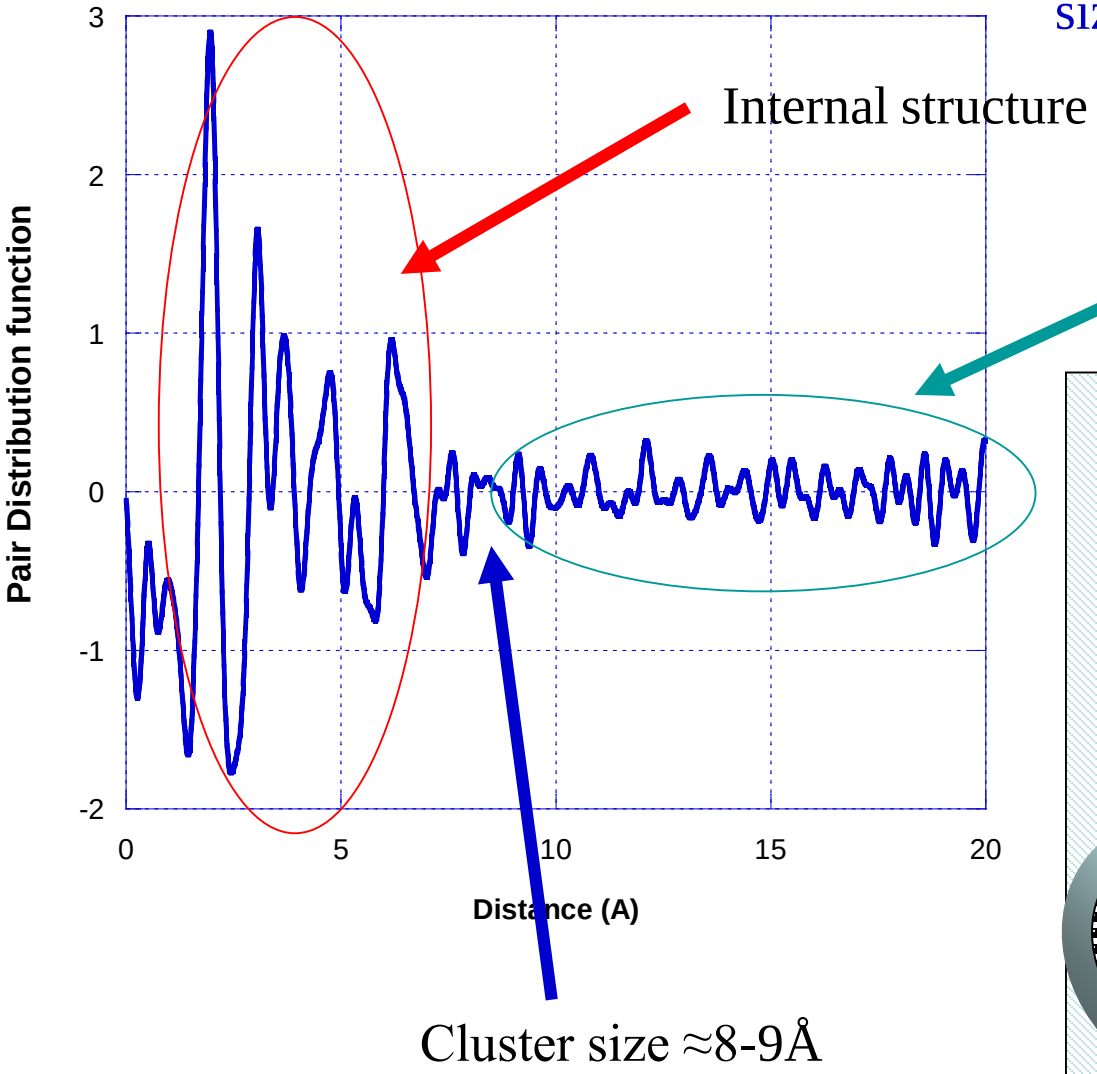

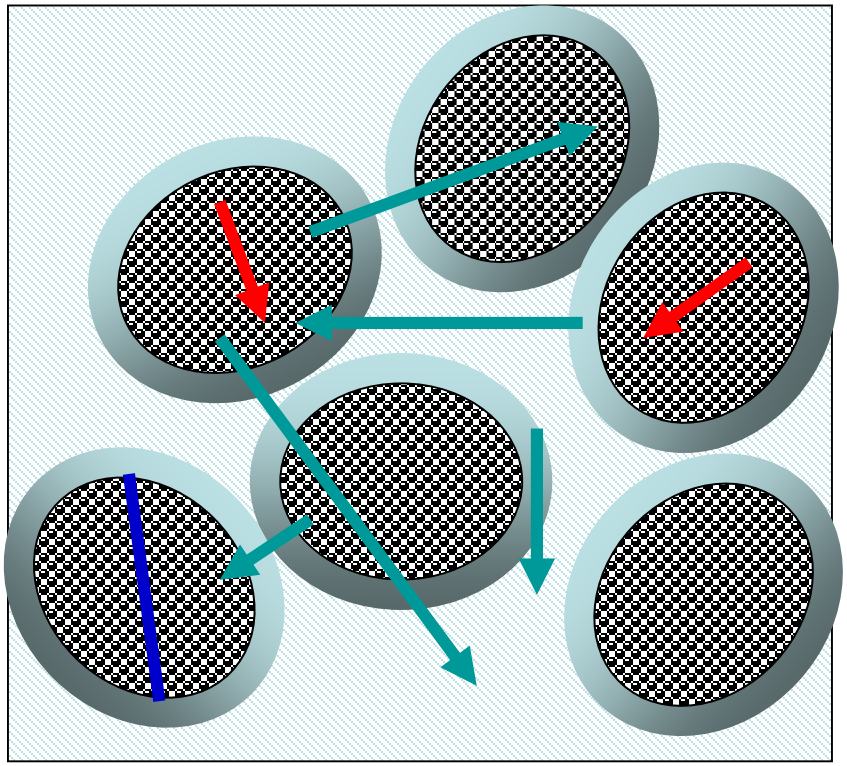

octahedral coordination

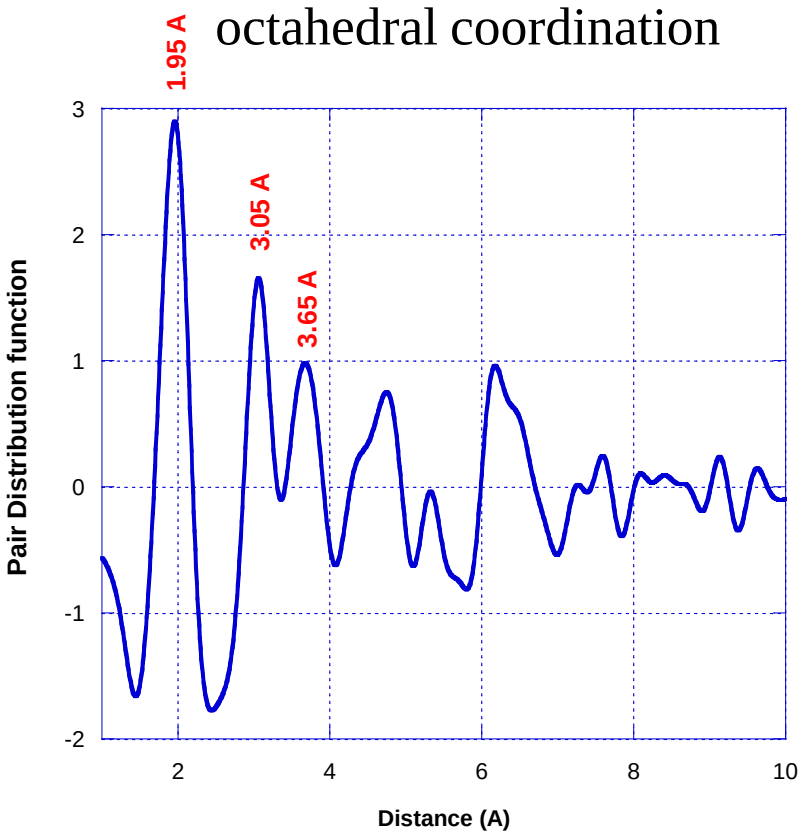

Locally ≠ rutile, anatase

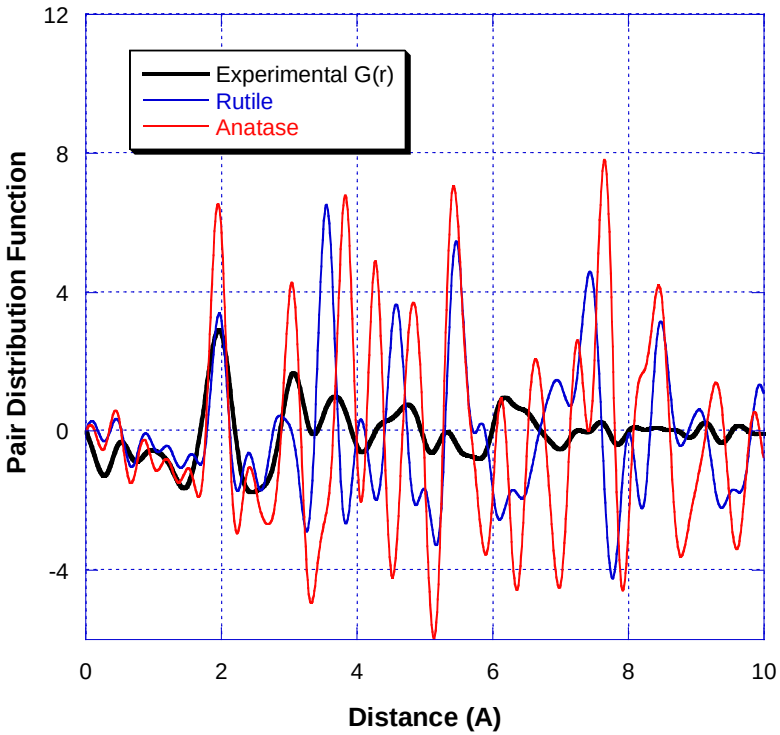

Modelisation of the overall cluster structure

We did not dare to try ab initio structure solution (yet)

Produce a reasonable structural model of the whole nano-particle using

- crystal-chemical knowledge
- quantum modelling
- input from other techniques (e^- microscopy, spectroscopies)

Calculate pdf and compare with experimental pdf

Reject if too bad

Otherwise do direct space refinement

Best model ;
Built from the structure of $H_2Ti_3O_7$

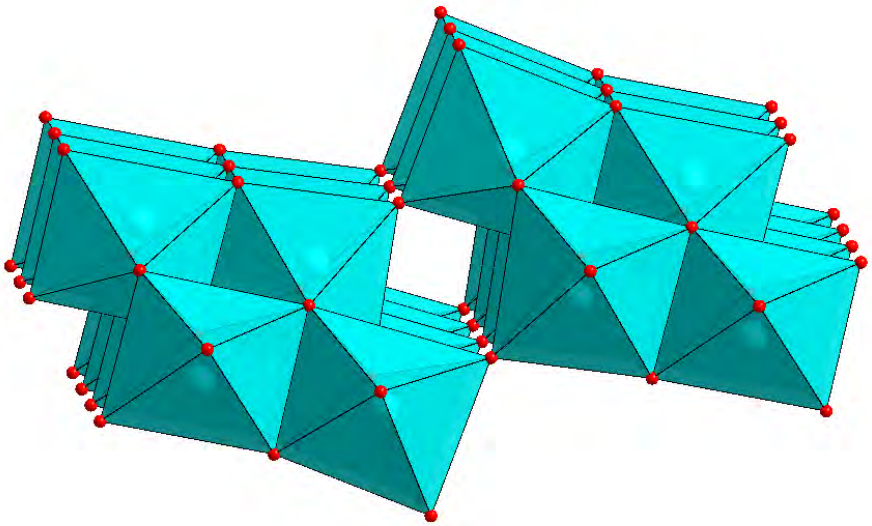

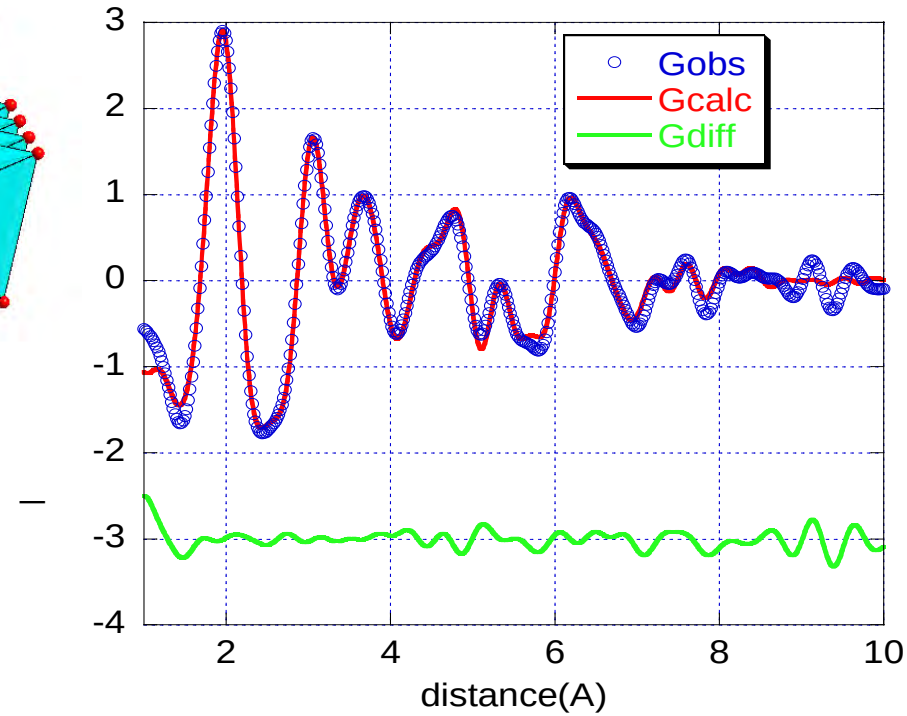

Crystal structure and Spin transition in the compound *[Fe(Htrz)$_2$(trz)](BF$_4$)*

*ICMCB Bordeaux, * LOMA, Univ. Bordeaux ,** Institut Néel Grenoble*

Grosjean et al., Eur. J. Inorg. Chem. **2013**, 796

Polymer material, Fe II complexes, spin transition close to ambient.

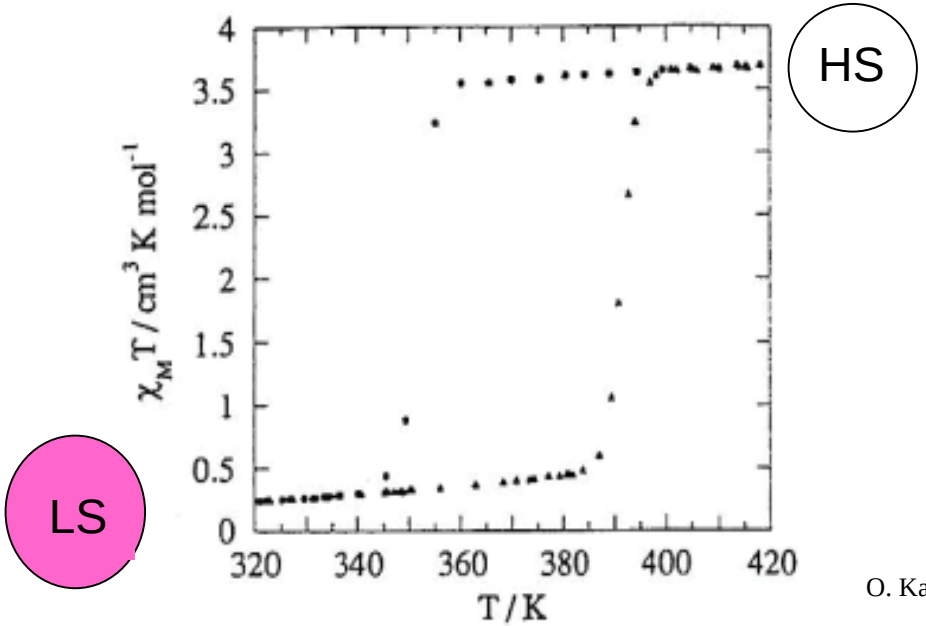

O. Kahn, J. Kröber, C. Jay, *Adv. Mat.* **1992**, *4*, 718

No crystals, poorly crystallized powders => no structure (EXAFS, Raman, etc...)

Urakawa et al. *J. Phys. Chem. C* **2011,** *115,* 1323

Cmcm

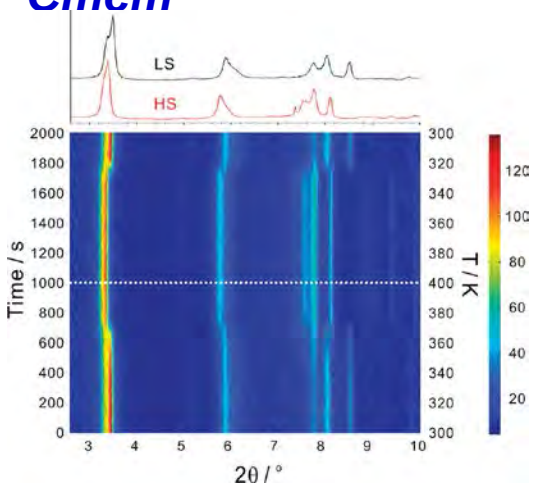

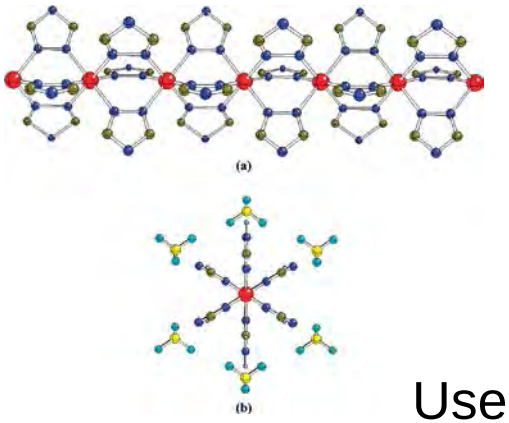

Grosjean et al. *Eur. J. Inorg. Chem.* **2013**, 796

Pnma

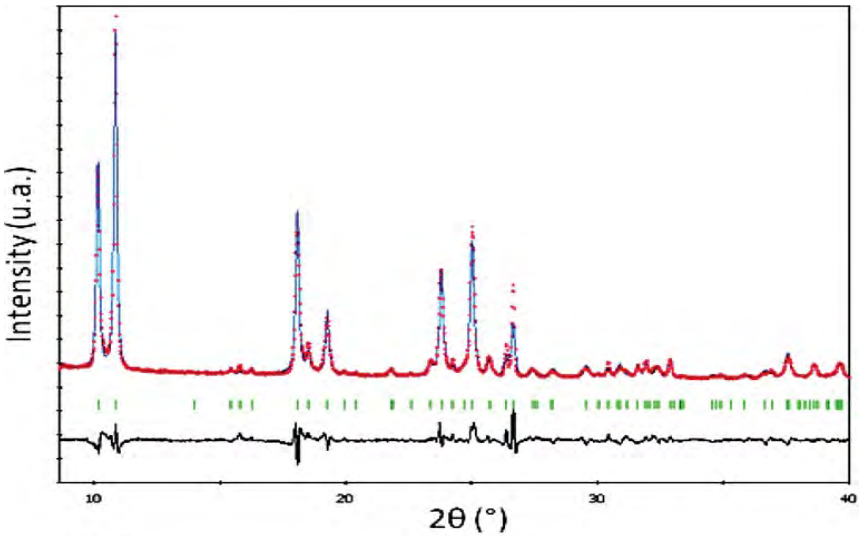

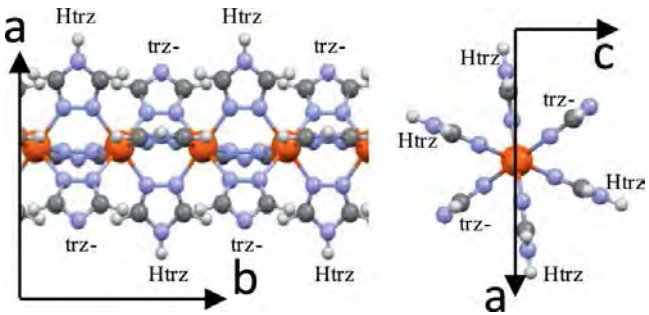

Use PDF to

*confirm structure

*impact of decreasing the size of coherent domains

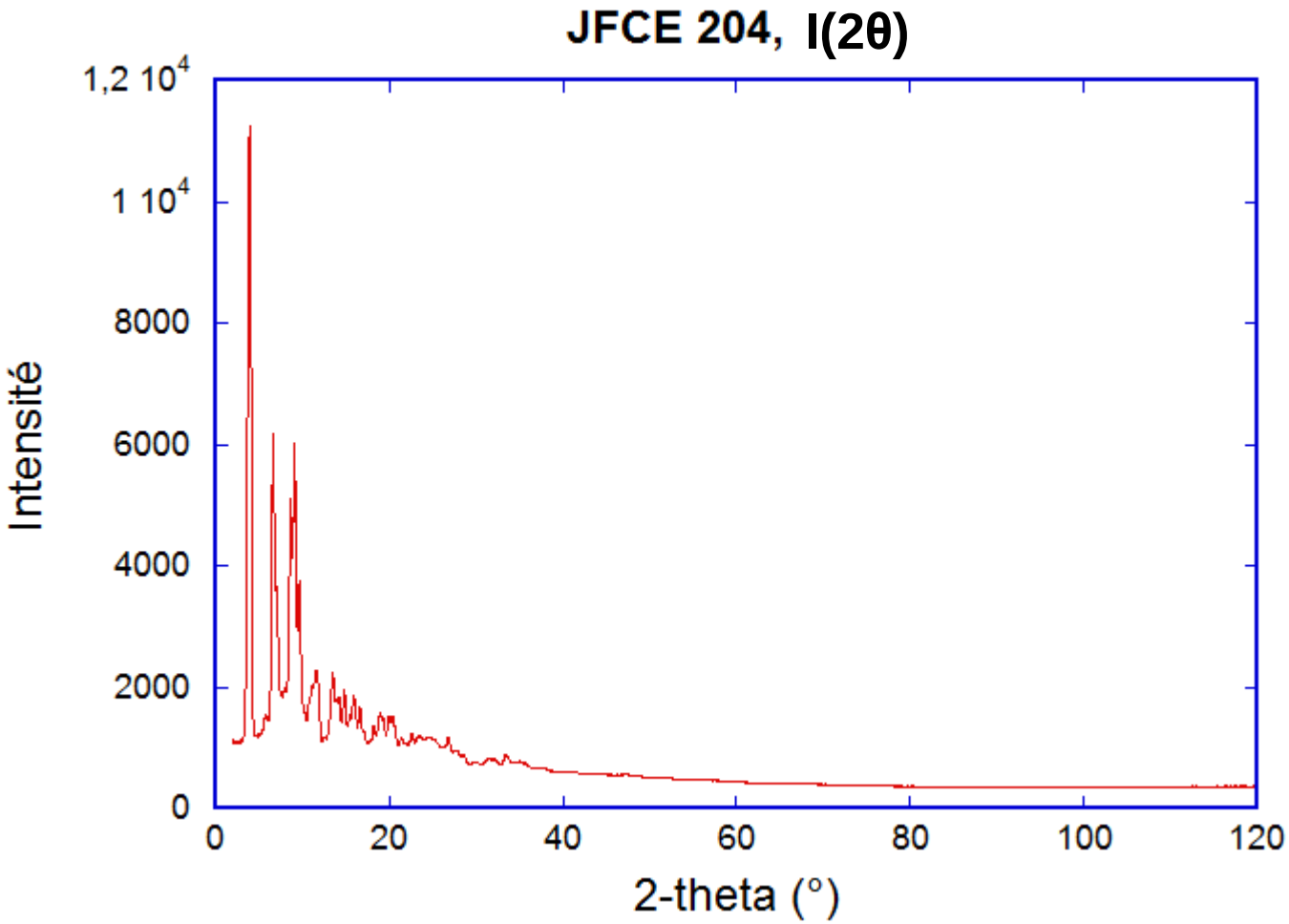
JFCE 204, I(2θ)
1,2 10^4
1 10^4
8000
6000
4000
2000
0
Intensité
0
20
40
60
80
100
120
2-theta (°)

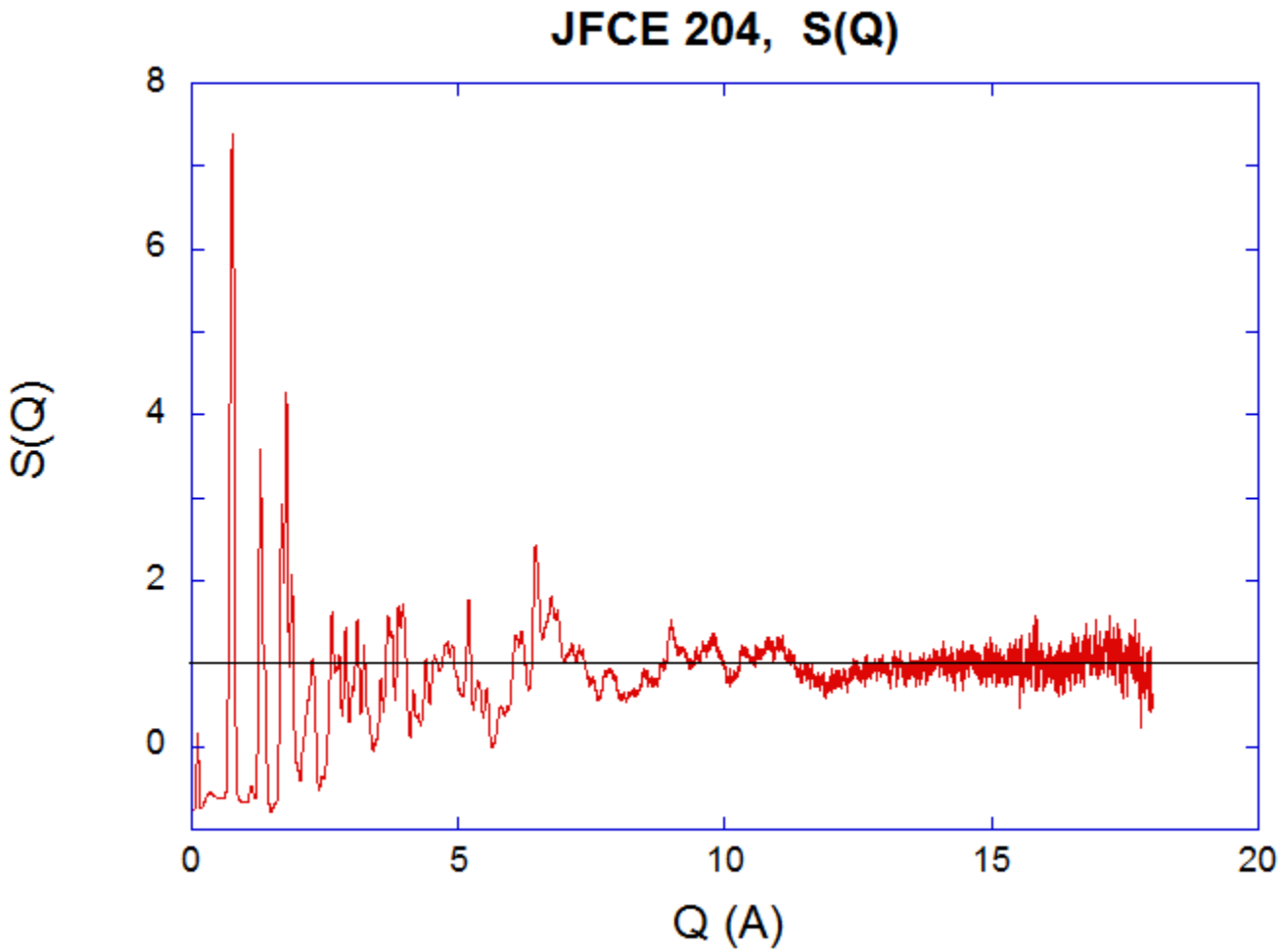
JFCE 204, S(Q)
S(Q)
8
6
4
2
0
0
5
10
15
20
Q (A)

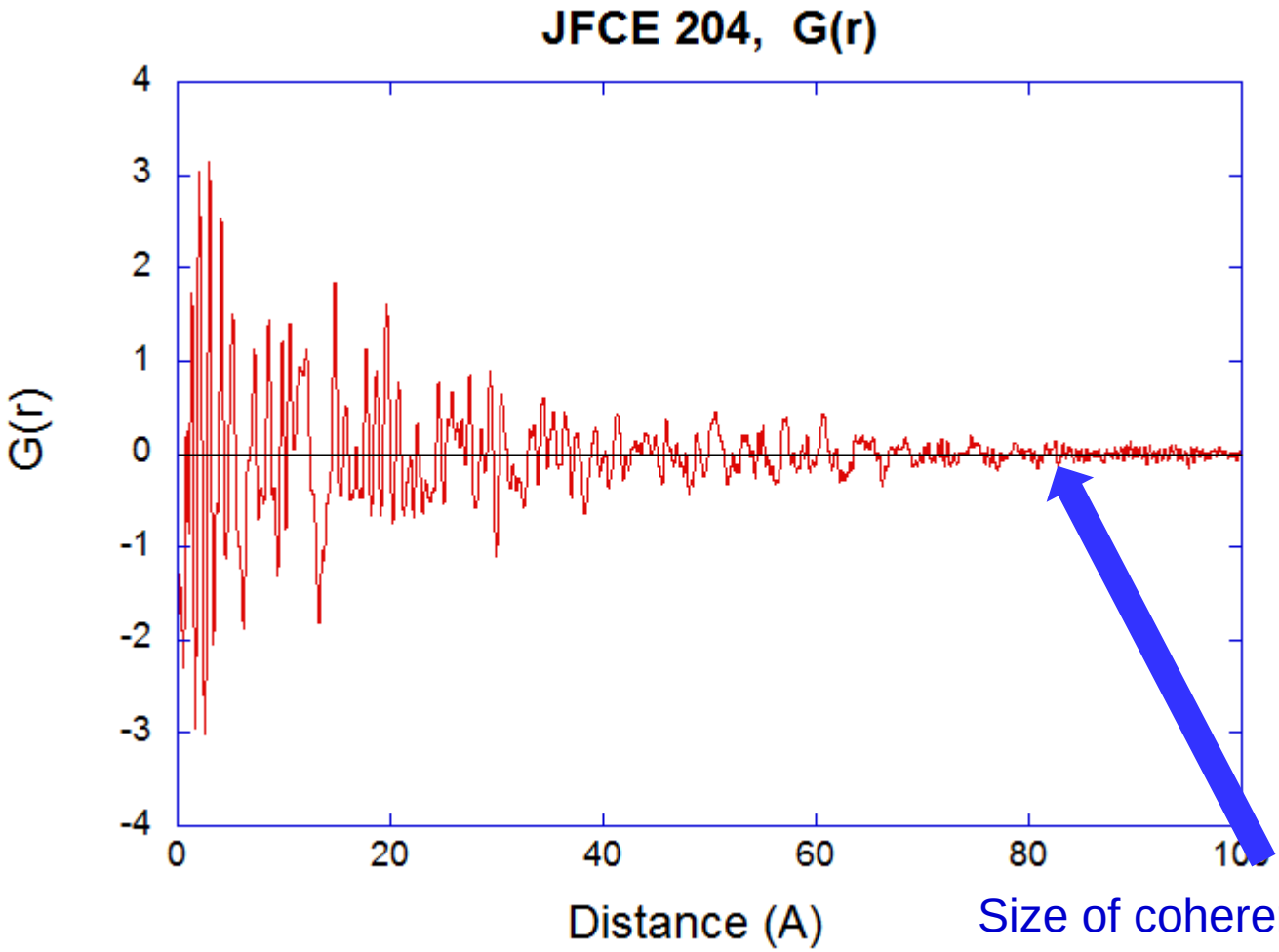

Size of coherent domains
< 10 nm

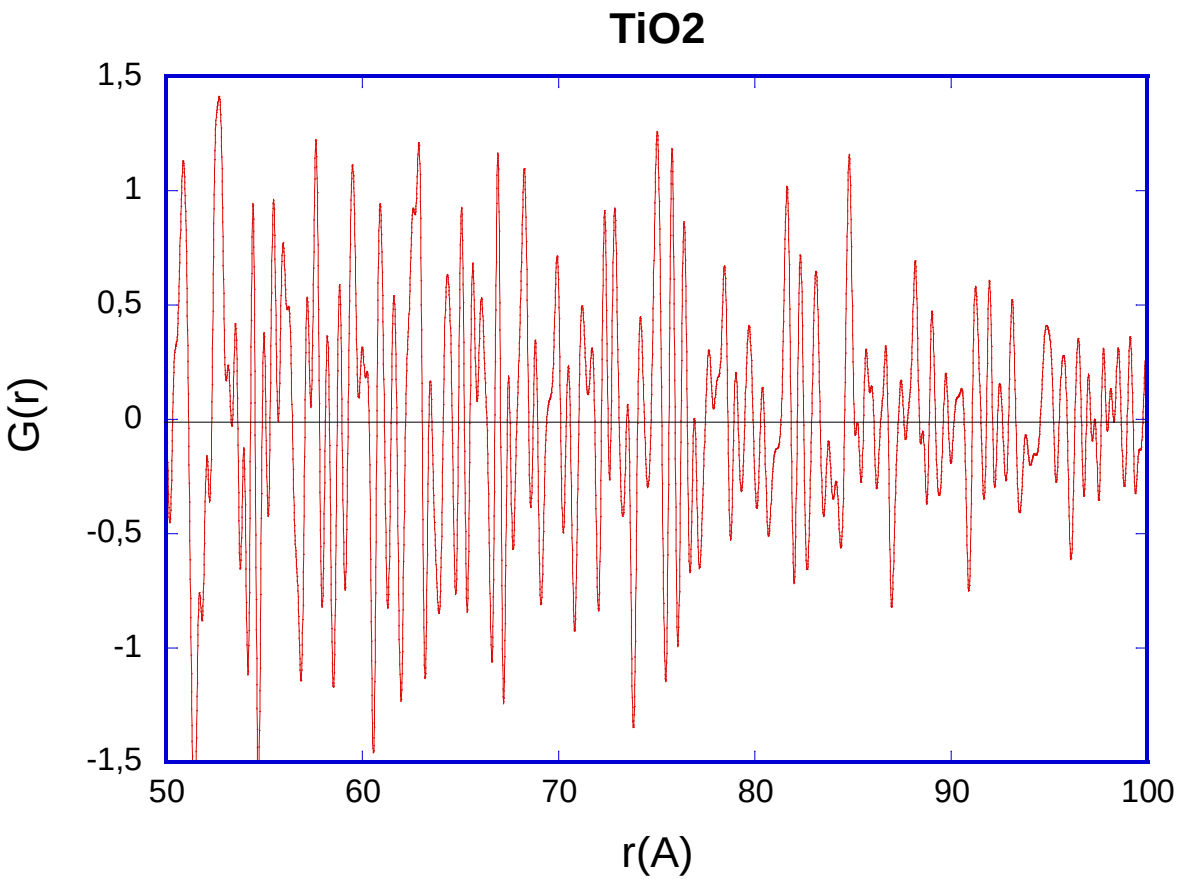
TiO2
1,5
1
0,5
0
-0,5
-1
-1,5
G(r)
50
60
70
80
90
100
r(A)

JFCE204 (50nm) ***Pnma***, Positions = Rietveld, fixed

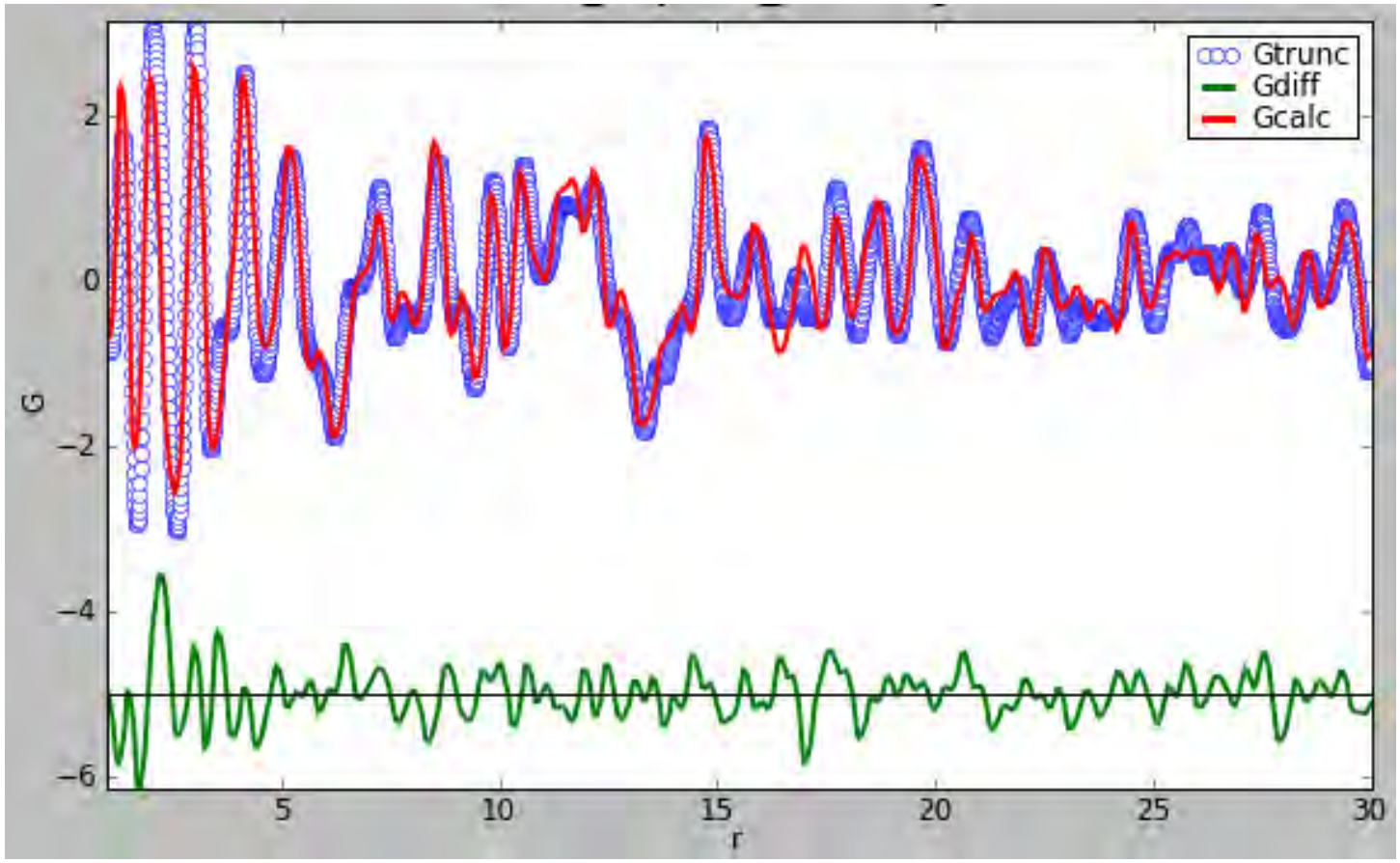

Refined: scale

δ (correlations)

d nanoparticles ~7 nm a, b, c

Uiso (Fe; C,N,H; B,F)

JFCE204 (50nm), Cmcm, Positions = cif, fixées

Urakawa et al. *J. Phys. Chem. C* **2011,** *115,* 1323

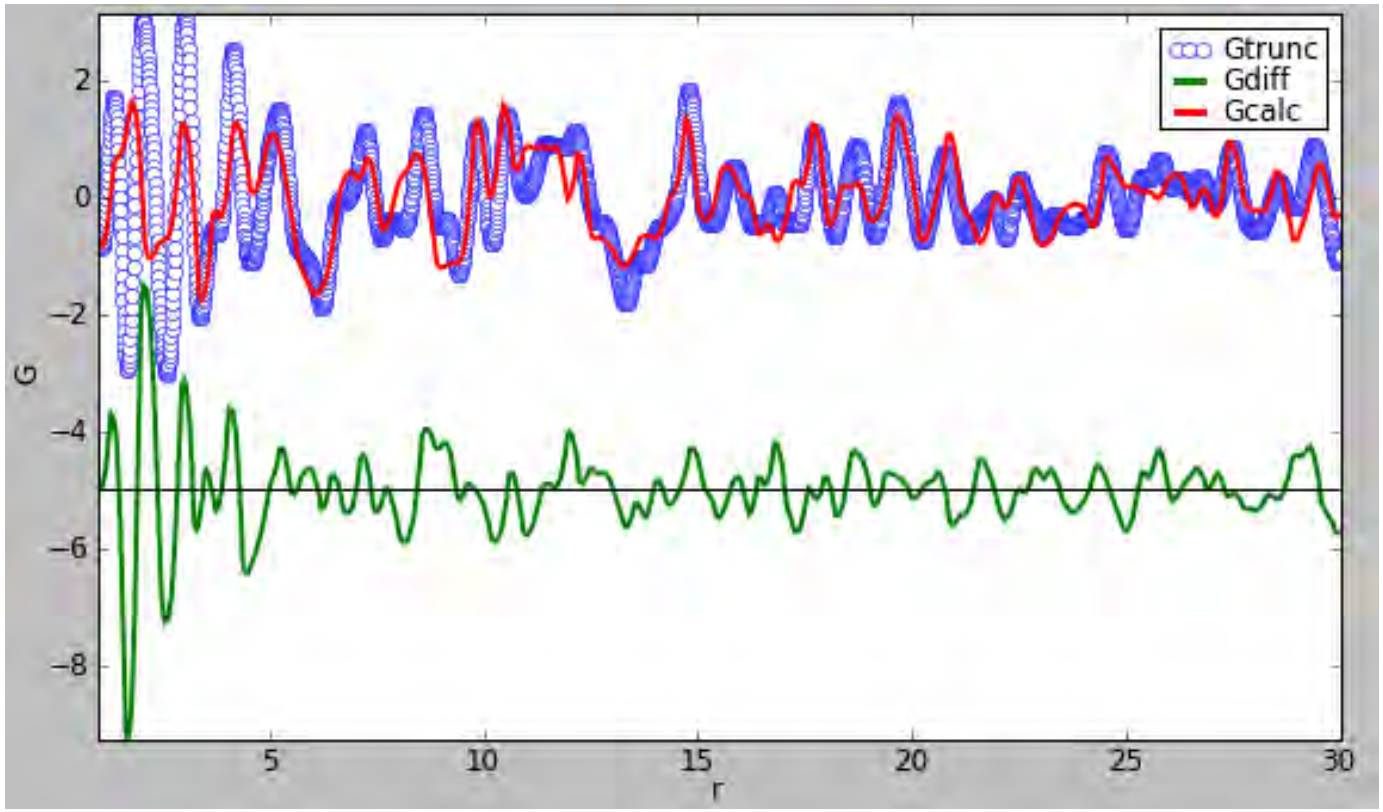

Affinés : échelle
δ (corrélations)
d nanoparticules
a, b, c
Uiso (Fe; C,N,H; B,F)

Cmcm

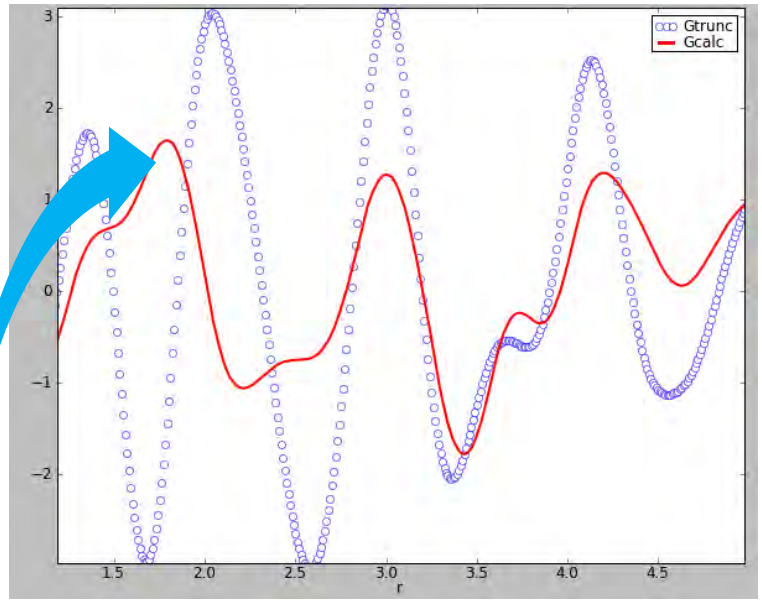

Pnma

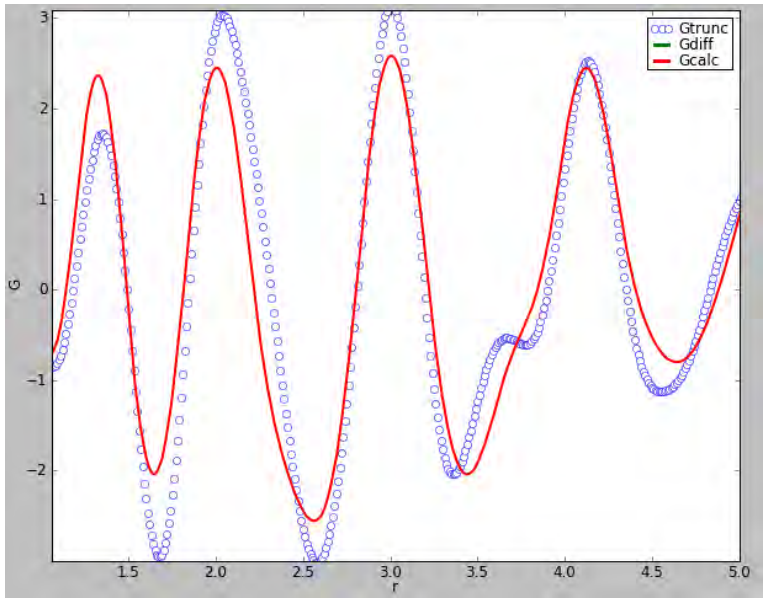

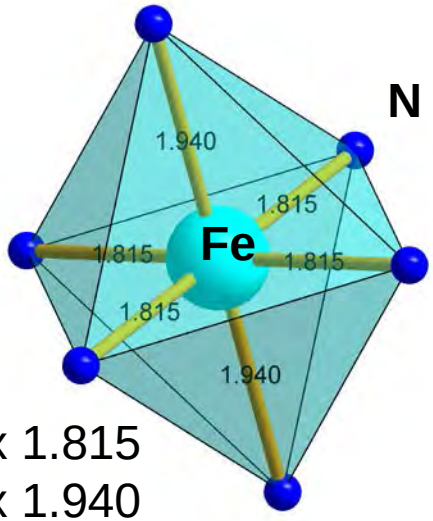

Fe-N : 4 x 1.815
2 x 1.940

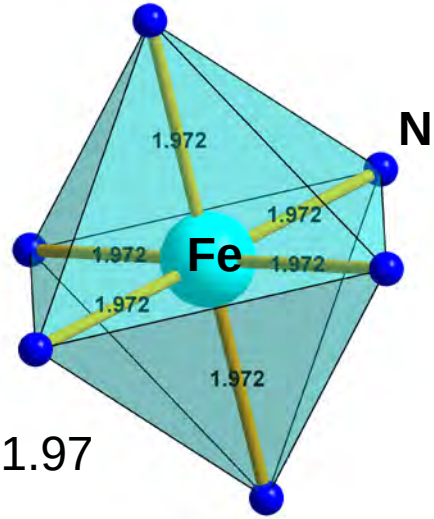

Fe-N : 6 x 1.97

The Pnma structure is the right one!

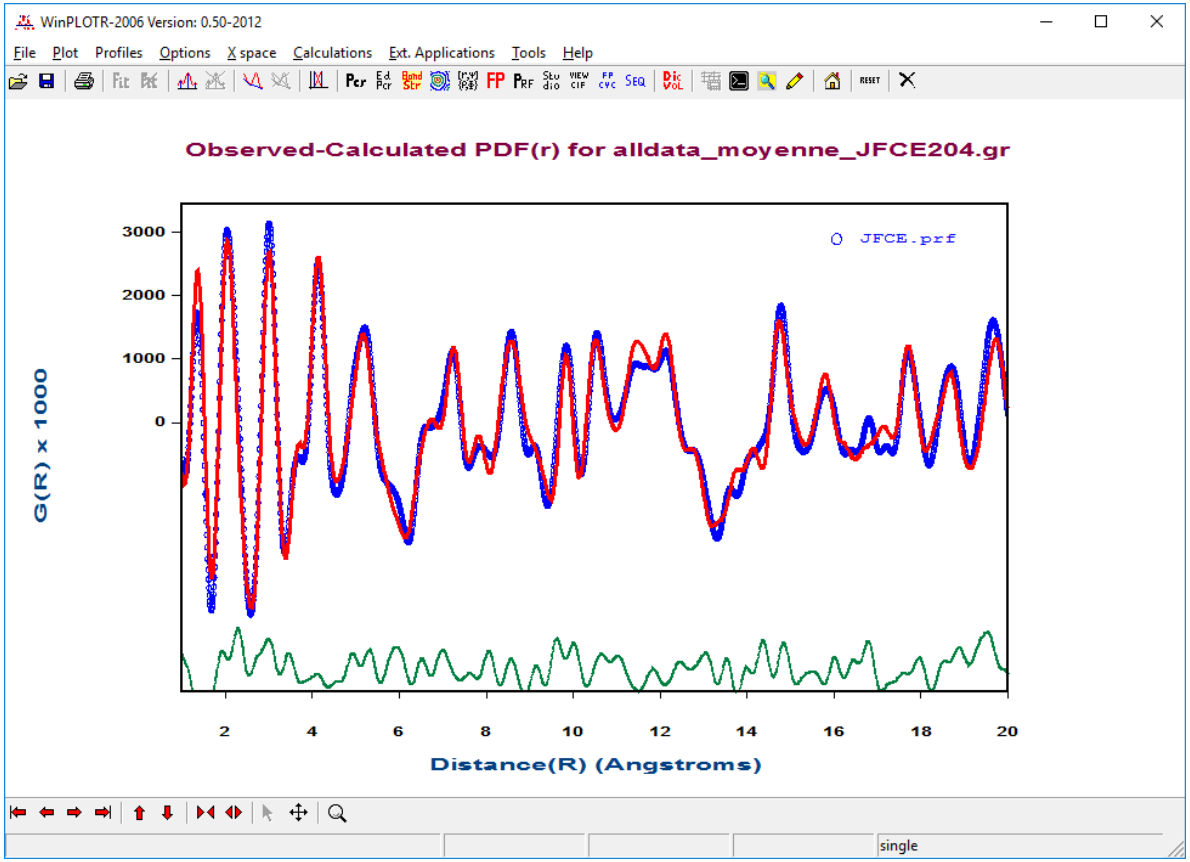

PDF investigation of the local structure of $Li_{4-x}Mn_2O_5$ high capacity cathode

Coll. V. Pralong, M. Freire, CRISMAT, Caen, France

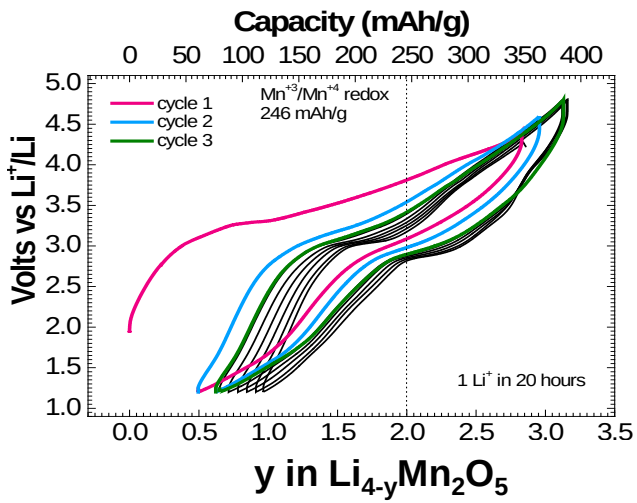

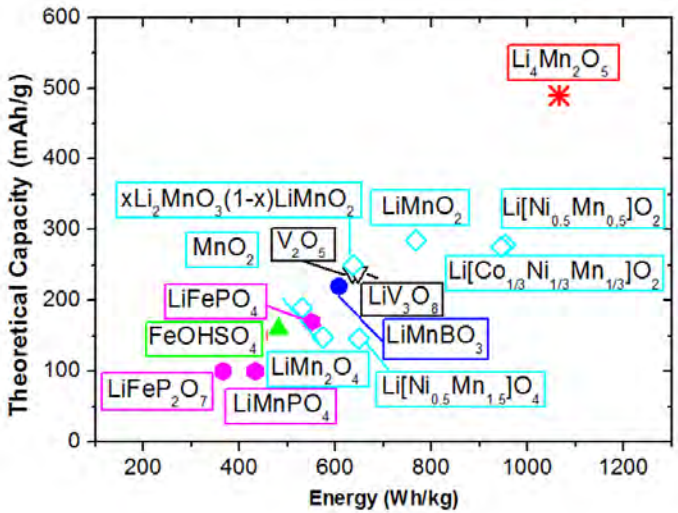

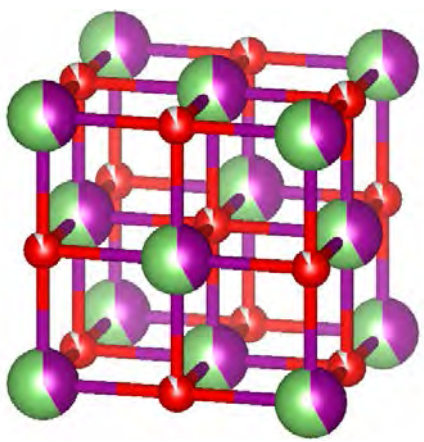

Made by mechanical alloying
Disordered MnO-type structure (Fm-3m)
Li/Mn substitution on cation site
1/6th oxygen vacancies on anion site

⇒ Mn valence vs Li content
⇒ Local structure vs Li content
⇒ Li conduction pathways ?

M. Freire et al. *Nature Materials* ***15***, *173-177 (2016)*

Neutron and x-ray PDF data

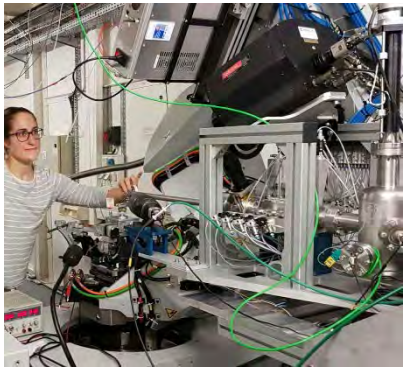

- 2D pixel detector, 1 image/° up to 120°
- Fast Azimuthal Integration with pyFAI
- High resolution: $\Delta Q/Q \sim 10^{-3} - 10^{-4}$
- $\lambda = 0.5$ Å 25 keV, Qmax = 25 $Å^{-1}$

pyFAI *J. Kieffer et al. JAC48 (2), 510 (2015)*

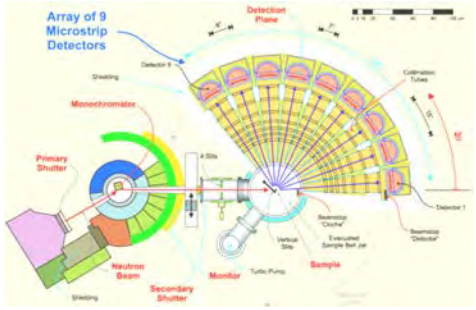

- 9x multidtector
- λ = 0,5 Å,
- Qmax = 25 $Å^{-1}$

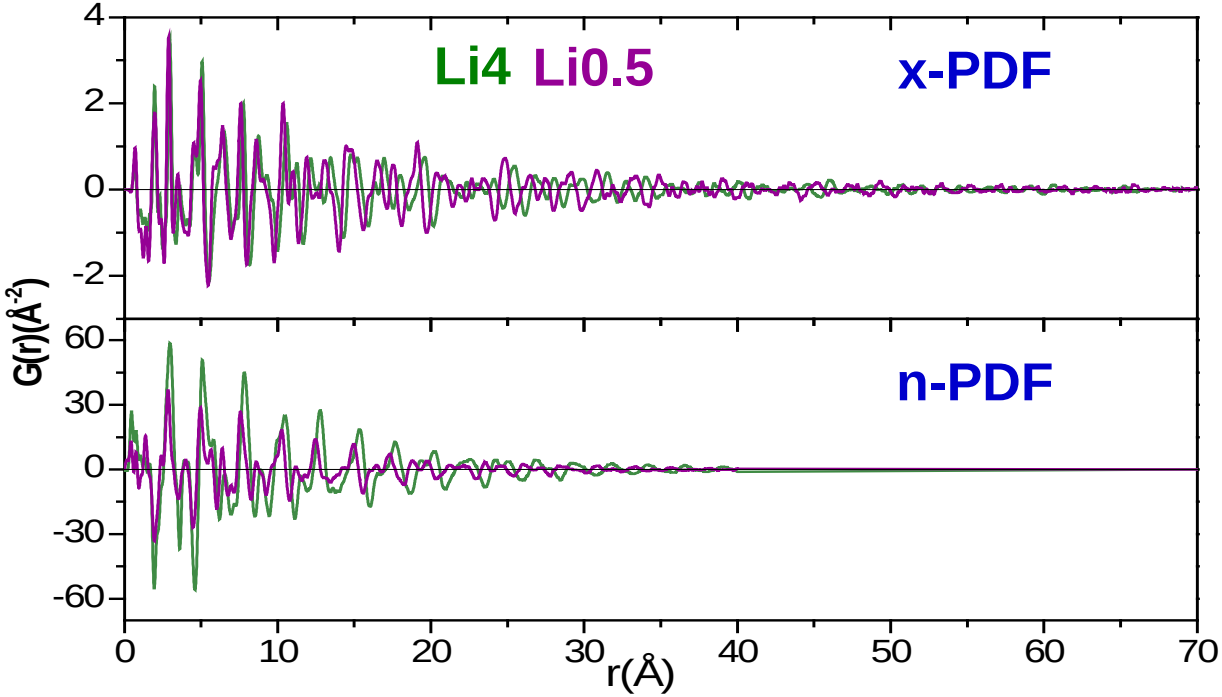

x-PDF Real Space Rietveld refinements

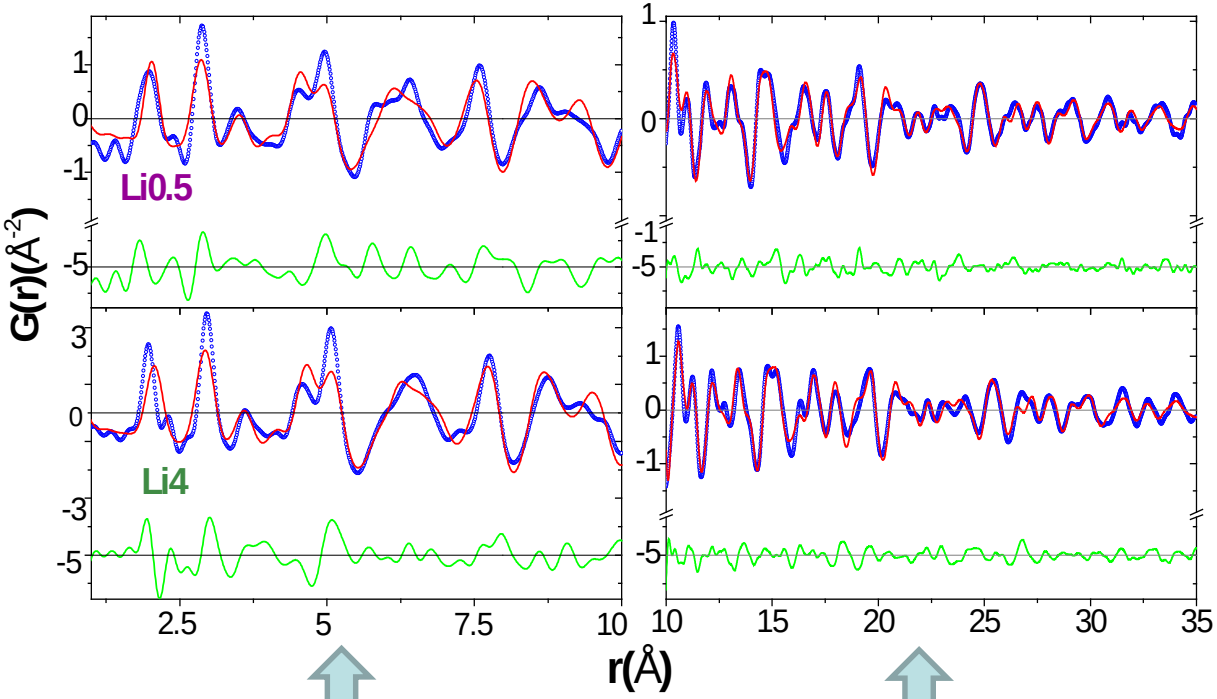

Local structure distortions not described by the average structure model refined at large r

Confirms average MnO-type structure Agrees with structure and coherence length found by Rietveld

Difficult to refine the local distortion with the « real space Rietveld » method:

- correlation between parameters
- mixed occupancies

PDFgui: *C.L. Farrow et al. J. Phys.: Condens. Matter 19 (2007) 335219*

Structure investigation of $Li_4Mn_2O_5$ using RMC modelling

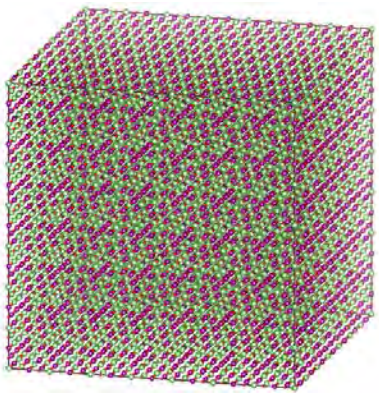

Starting 14ax14ax14a box

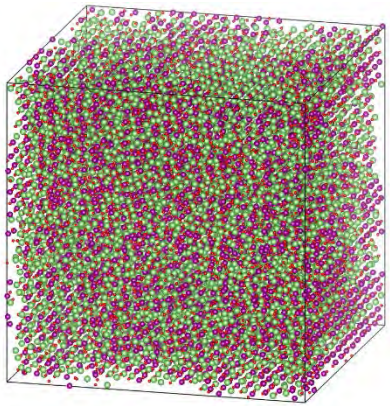

14ax14ax14a box after RMC

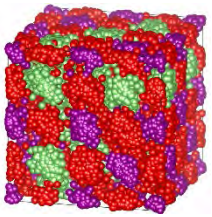

"Compressed" in a 2ax2ax2a Supercell

Reverse Monte Carlo (Large Box modelling) using RMCProfile (Matt Tucker, SNS)

- Large number of atoms (15000-20000) allowed to move around.
- Exploratory unbiased fitting. Good at finding distorted solutions.
- **BUT**, requires an intelligent set of constraints.

Starting model

in a 14x14x14 MnO-type cell,
≈200 kÅ^3, ≈21000 atoms,

- Mn in octahedral coord.
- Li clustered around O vacancies.
- Respected stoichiometry

Combined minimization of
neutron and x-rays S(Q) and PDF
typically 20.10^6 accepted moves/minimization
repeated >x10 for statistics

Constraints:

- Minimal interatomic distances (antibump)
- BVS: Mn^{3+} , Li^{+} , O^{2-}

RMC fits for $\mathbf{Li_4}Mn_2O_5$

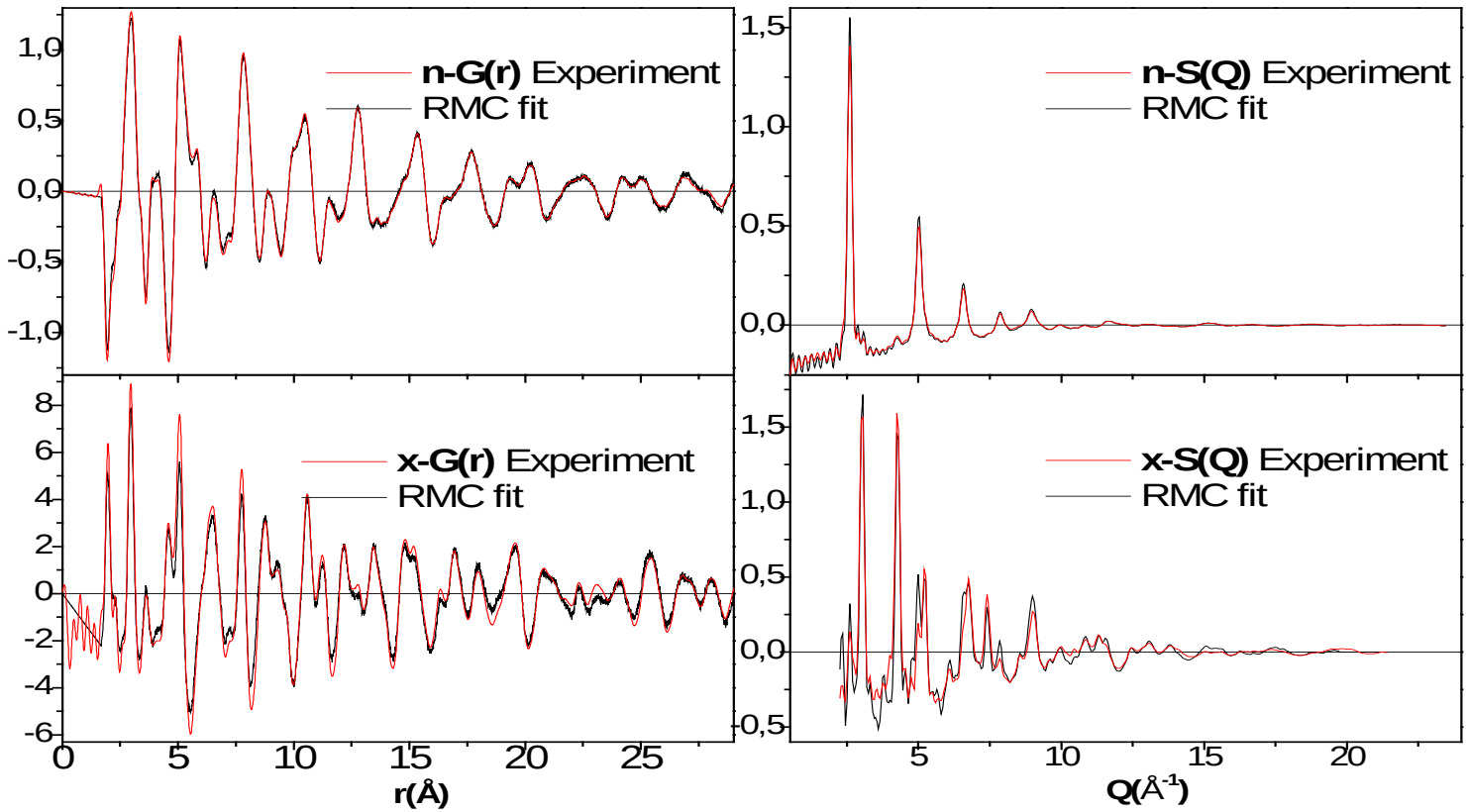

***RMCProfile**: Tucker, M.G. et al. J. Phys.: Condens. Matter 19 (2007) 335218*

RMC refined structural model

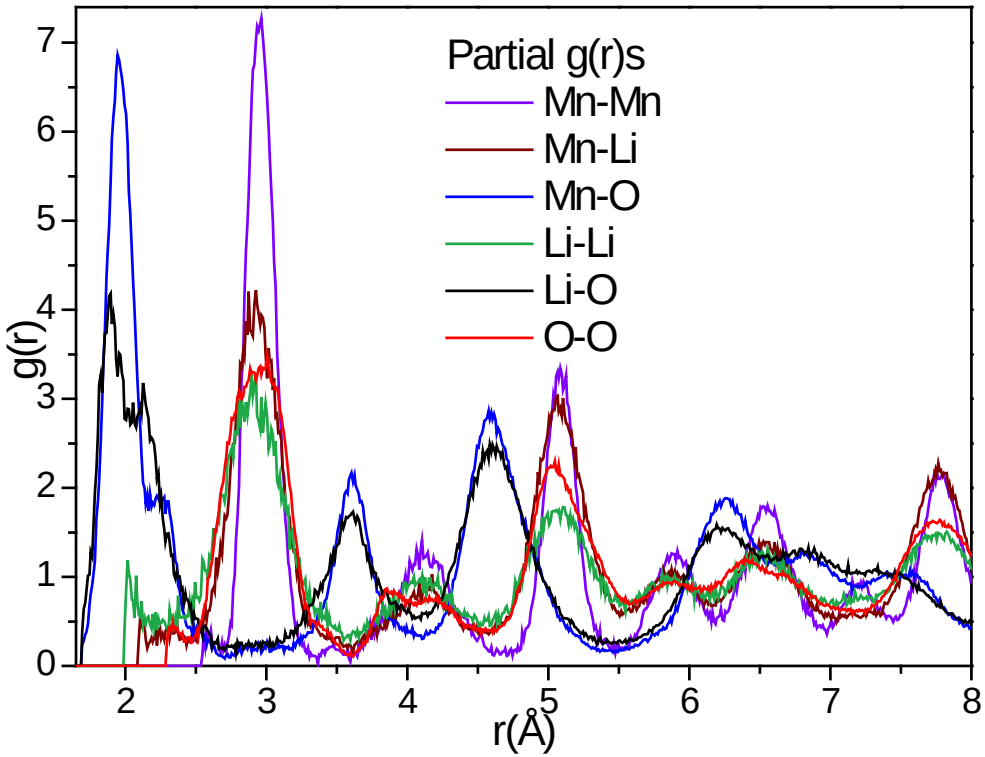

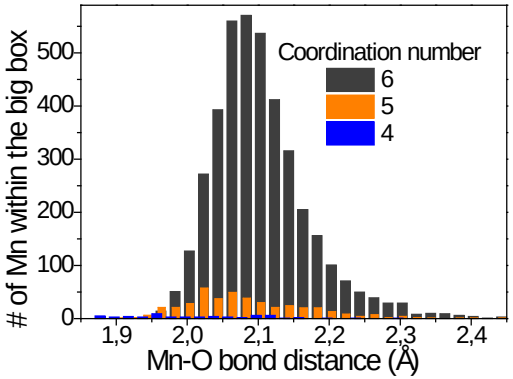

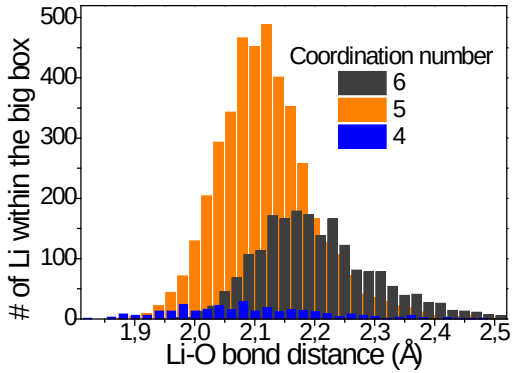

- The narrow Mn –Mn peaks indicate the Mn framework remains cubic and undistorted.
- Both Li and O are displaced with respect their original positions within the rock-salt lattice.

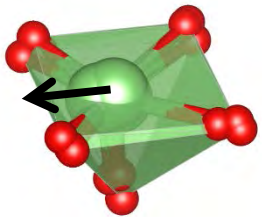

Li-O coordination

2x dLi-O 5CN, short ~ 1.9-2.05 Å
3x dLi-O 5CN, long ~ 2.05-2.3 Å

Li pathways from BVS isosurface maps

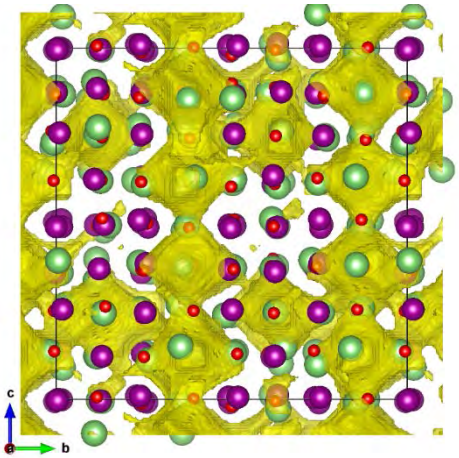

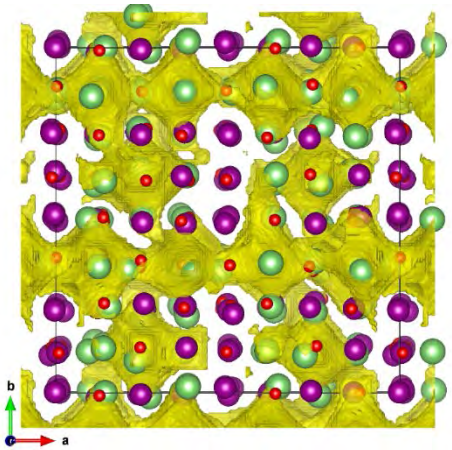

4ax4ax4a box

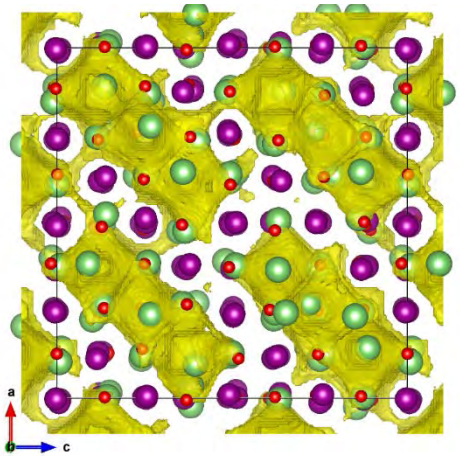

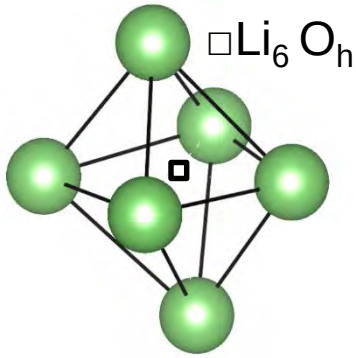

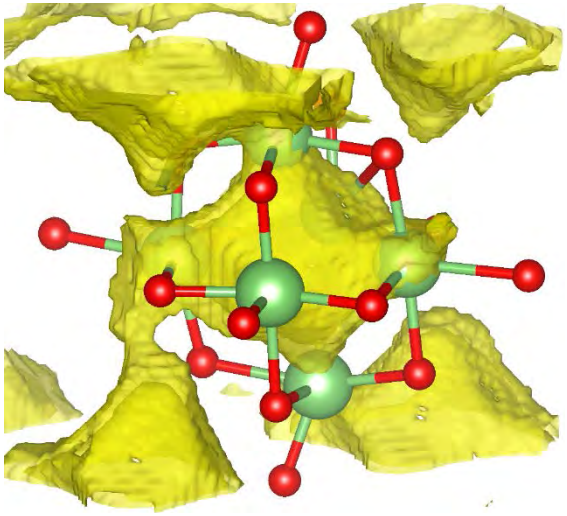

Differential bond valence of lithium in **$Li_4Mn_2O_5$**
(R_{cut} = 6.0 Å, ΔV_{Li} = 0.1 val. un.)

Li can move on the faces of the □Li_6 O_h ocathedra.
The calculated percolation energy is ≈ 1.5eV

Amorphization of β-trehalose by high energy milling

$C_{12}H_{22}O_{11}$

$P2_1$, a=19.97Å, b=8.23Å, c=6.79Å, β=98.12°

Fritsch Pulverisette 7 mill

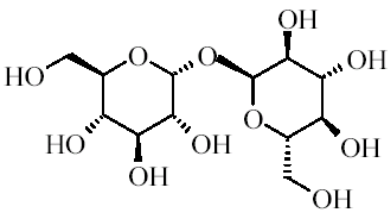

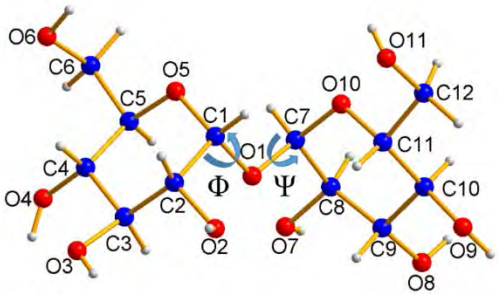

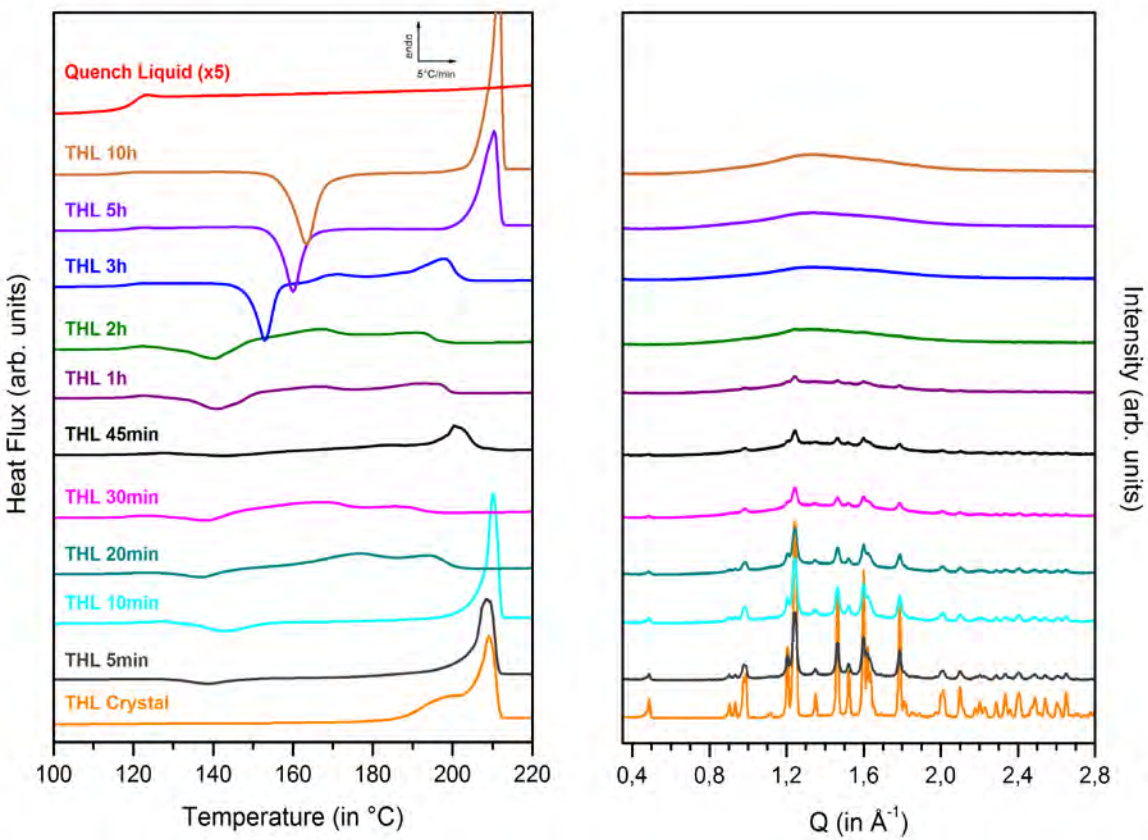

XRPD vs t_{mill}:

Bragg peaks become broader and smaller

Bragg peaks disappear after t_{mill} =2h

A diffuse halo grows

DSC:

Tg and recryst peaks appear

Tg, $T_{recryst}$, T_{melt} change with t_{mill}

$T_{recryst}$, T_{melt} absent in quenched liquid

Study the crystal/amorphous transformation vs t_{mill}

Bordet et al. *Crystal Growth & Design*, **16- 8**, 4547 (2016)

Ex situ high resolution PDF data of samples with increasing t_{mill}

CRISTAL @ SOLEIL, high resolution setup
Multianalyzer 21 chanels , E=22.8keV, λ=0.54Å, Qmax=20.5 $Å^{-1}$, 1 pattern=6h

Trehalose amorphisation = a 2 phase process

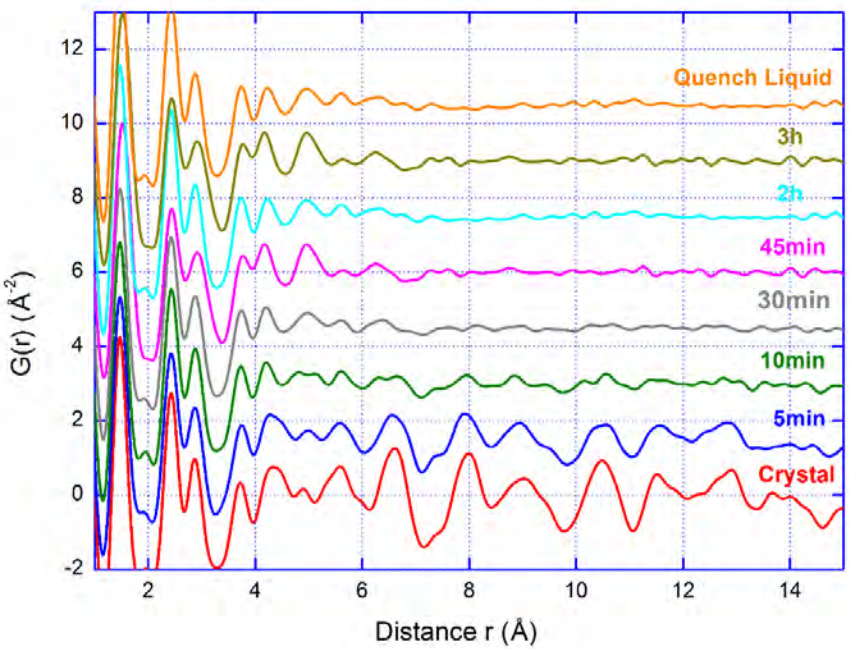

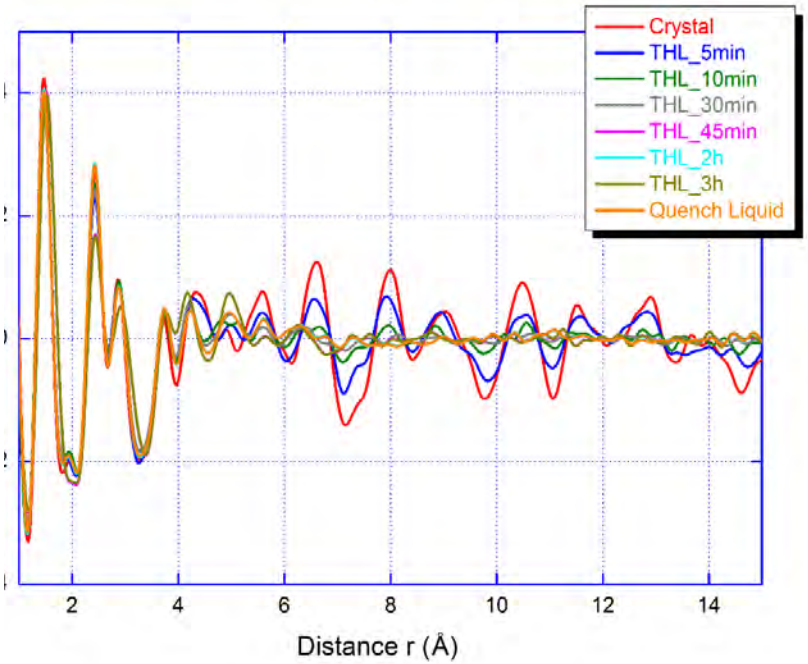

PDF are similar up to ~4Å =>mixing of 2 phases :

1 Short Range Ordered (~amorphous), increases with t_{mill}

1 Long range Ordered (~crystal), decreases with t_{mill}

=> empirical fits of the PDF vs milling time at RT using:

-a weighted sum of the crystal and quenched PDFs

-an enveloppe function to take account of the correlation length of crystalline phase

$$G_{m-calc} = s * \left[s_m * E(D) * G_c + (1 - s_m) * G_q \right]$$

G_q= observed PDF of the quenched sample
G_c= observed PDF of the pristine crystalline material
$E(D)$ = envelope function depending on the structural coherence length
s, s_m = overall scale factor and proportion of the Long Range Ordered phase

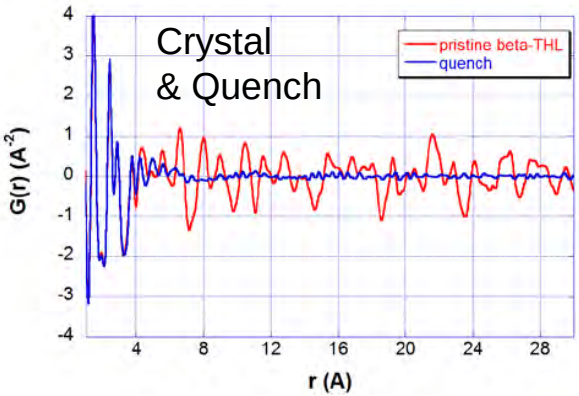

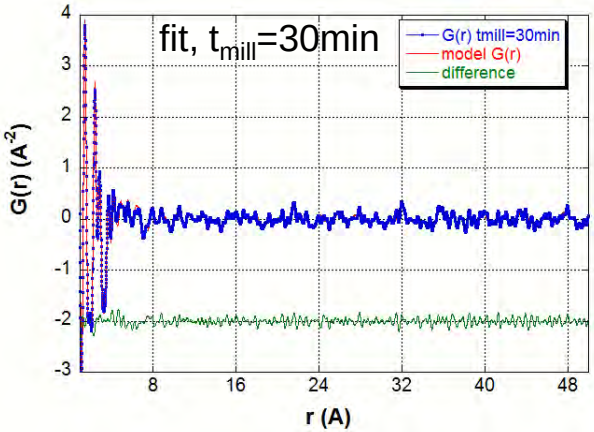

decay of proportion and coherence length of crystalline phase

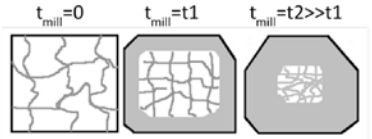

Extraction of amorphous phase PDF

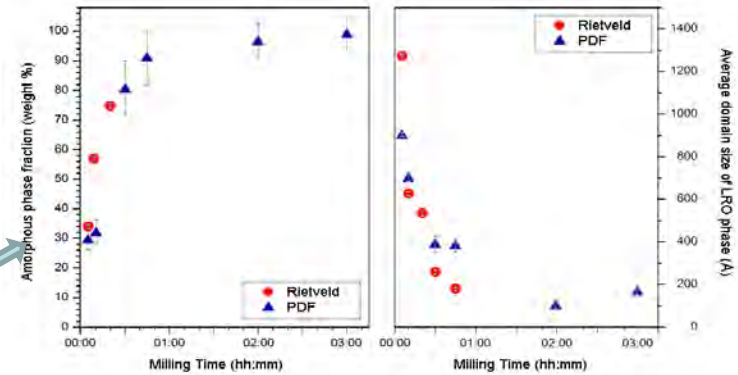

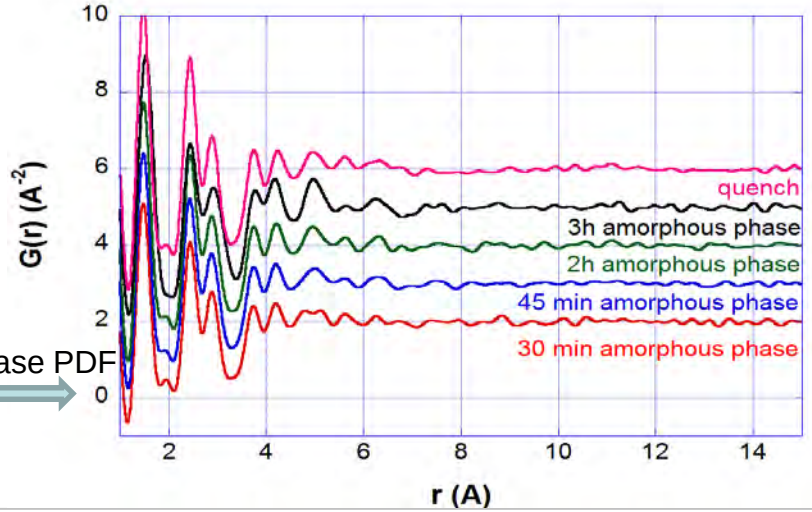

Now, using MolPDF, distances/angles restraints can be applied, allowing the *PDF structure refinement for molecular compounds*.

Sharpening applied to Biso for 2 different sets of distances (inter- vs intra-molecular)

eg: structure refinement of *α-lactose* vs temperature up to melting,

NSLSII, E=67keV, Perkin-Elmer 2D detector

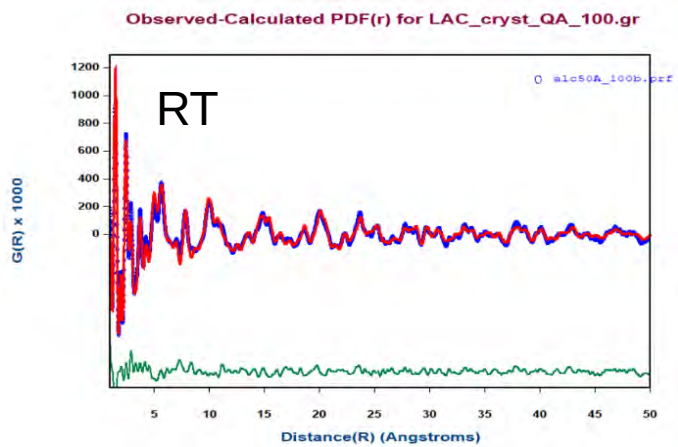

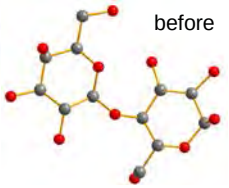

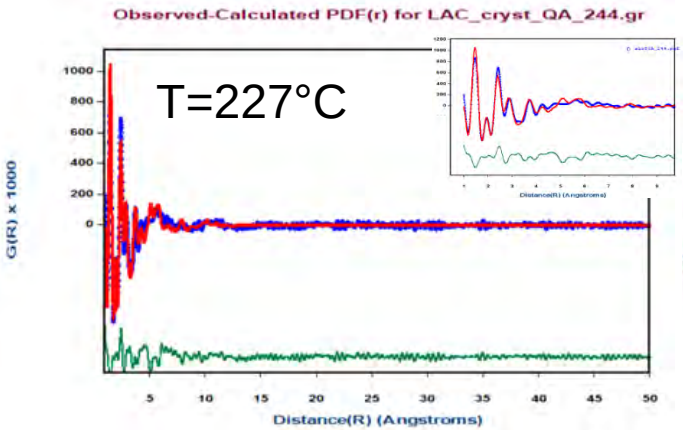

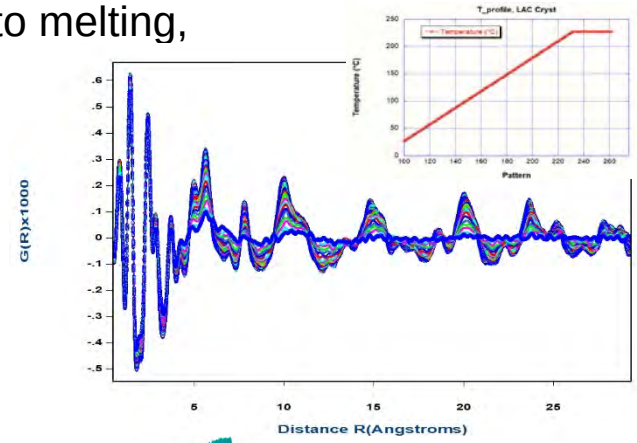

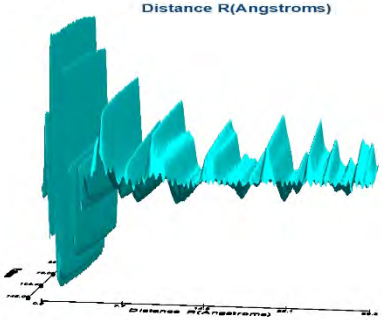

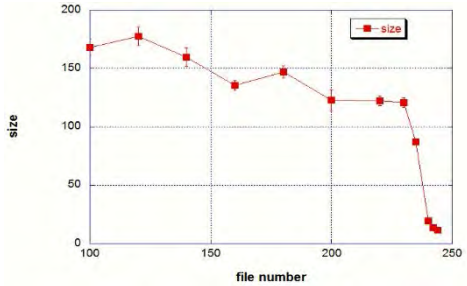

MolPDF, *J Rodriguez-Carvajal, 2017*

Investigation of Pompeii black pigments using PDF

Coll. LAMS, E. VAN ELSLANDE, Ph. WALTER, *CNRS - Sorbonne Université, Paris, France*

Carbon black containers, Pompeii

Pompeii, sectors I and III
P. Baraldi and MC Gamberini (U. Modena and Reggio Emilia)

Archaeological samples

- ✓ 5 black powders, precious, few mg
- ✓ Glass or bronze vessels = inks or cosmetics
- ✓ Roman site of Pompeii
- ✓ Ancient recipes:
  - obtained by burning organic matter ?
  - addition of binders (vegetal oils, gums,…) ?

References

- ✓ 4 modern carbon black pigments,
  purchased from Kremer Pigmente or Ôkhra:
  peach black, lampblack, ivory black and bone black
- ✓ Graphite: 9B pencil core (Faber Castell)
- ✓ Charcoal: homemade

How were the black pigments made ?
For what use (ink, cosmetics…) ?
Container vs content ?

S. Cersoy et *al.*, J. Appl. Cryst. (2016). **49**, 585

XRPD is a non-destructive technique:
the sample is preserved

Optical microscopy

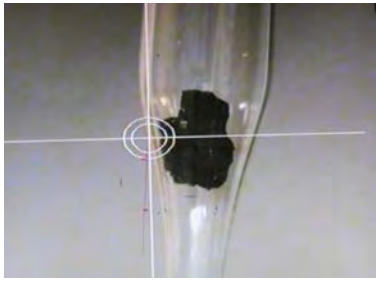

Fragment in boro capillary(Ø = 0.3mm)

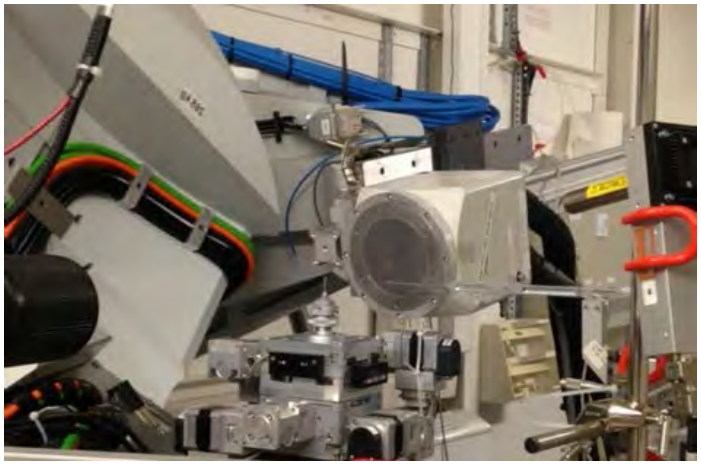

XRPD (BM2-CRG, ESRF, Grenoble, 25 keV)

30 diffraction images up to 2θ=100°,
Integrated, binned and glued to a 1D pattern
Qmax=20Å^{-1}

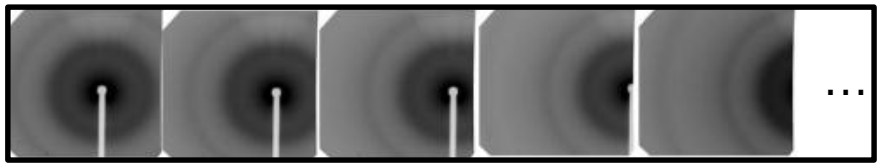

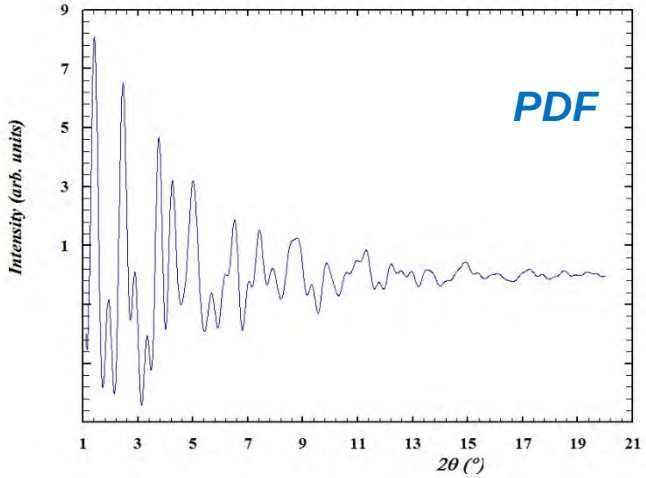

PDFgetX2
Corrections + FT

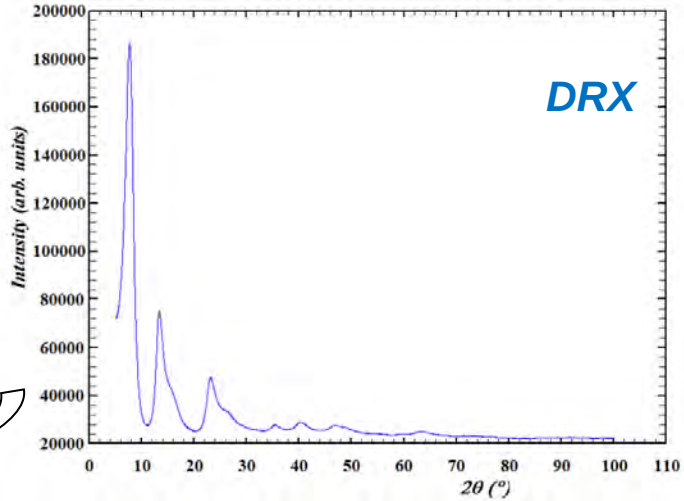

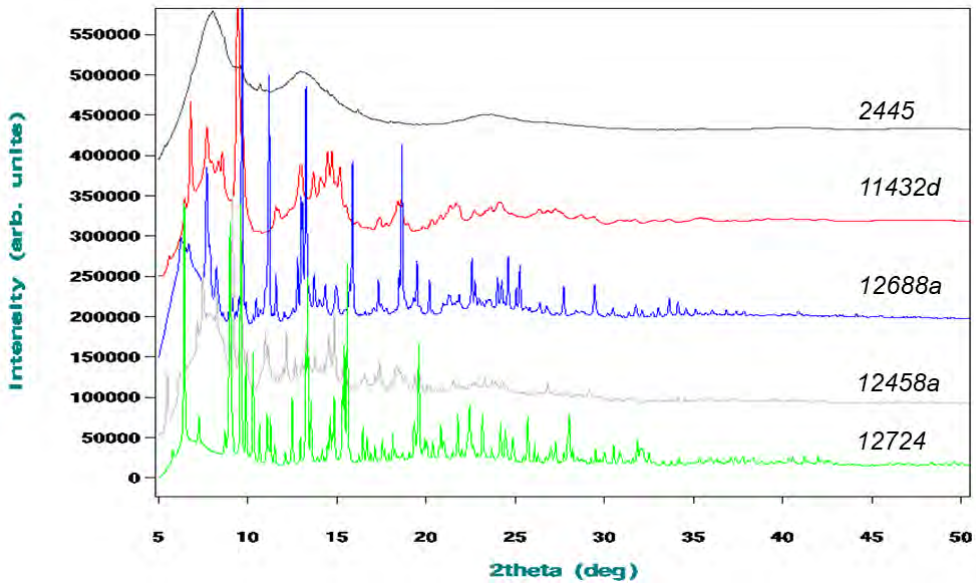

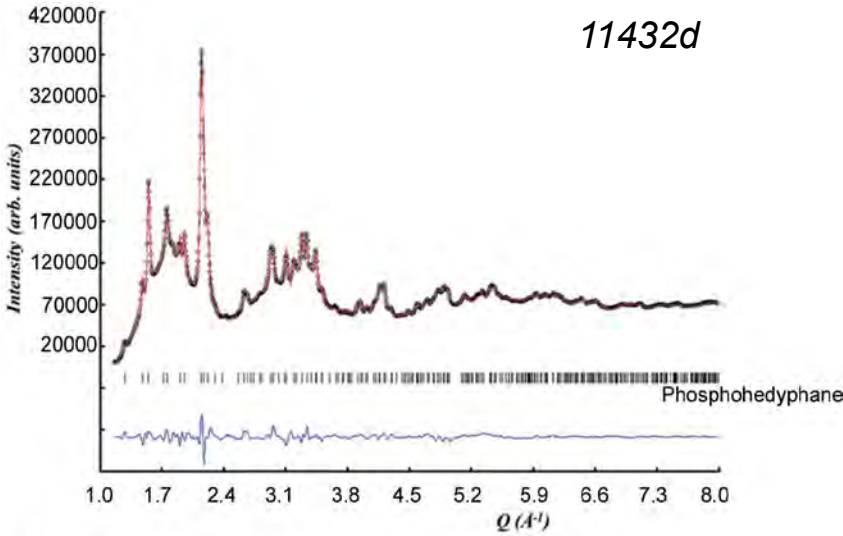

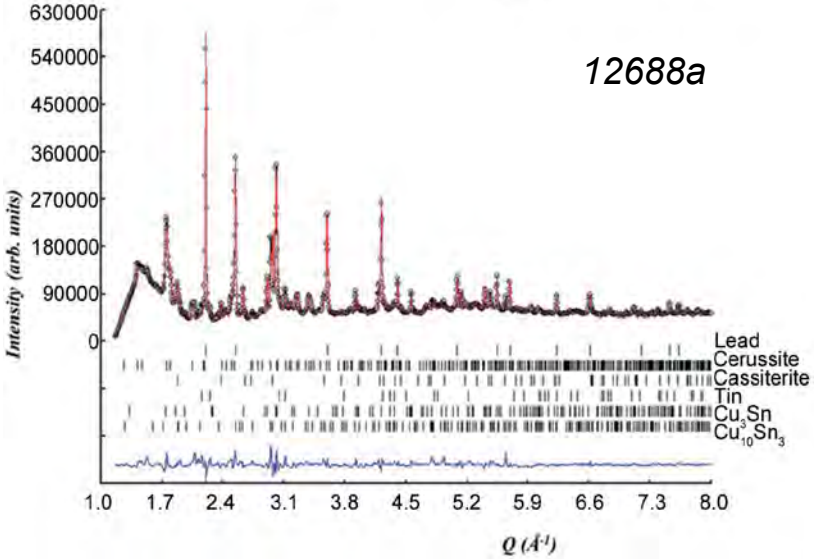

Amorphous + various crystalline phases

Identify and quantify the crystalline phases
ICSD and ***Rietveld*** refinement (Fulprof).
Difficult cases = ***diffraction tomography***.

Amorphous phases:
Only short distance range

Crystalline phases:
Also long distance range

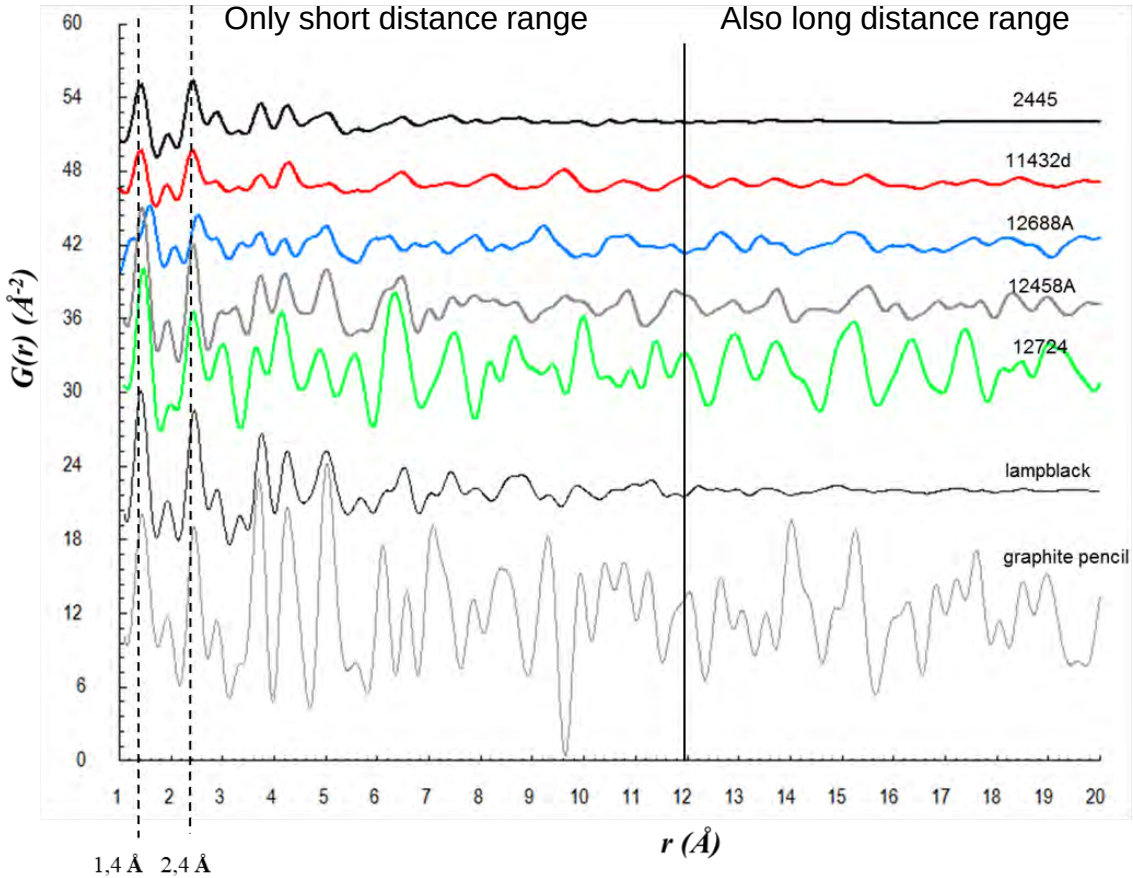

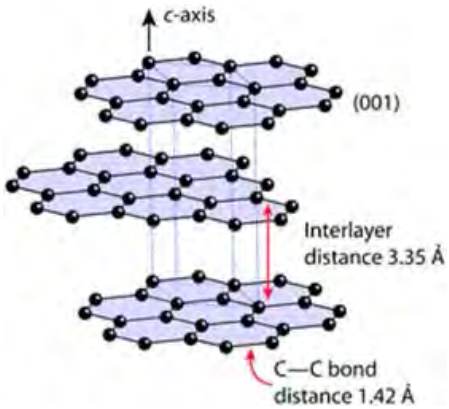

Amorphous phase= « non-graphitic » carbon (Franklin, 1950), but for 12688a ?

=> *extract the PDF of the amorphous phases*

Obtaining the PDFs of the non-crystalline phase(s):

Scale the PDF in the 12-20Å range with crystalline phases from Rietveld
Subtract from the observed PDF to get the PDF of the amorphous phase: $G_{amorphous}$

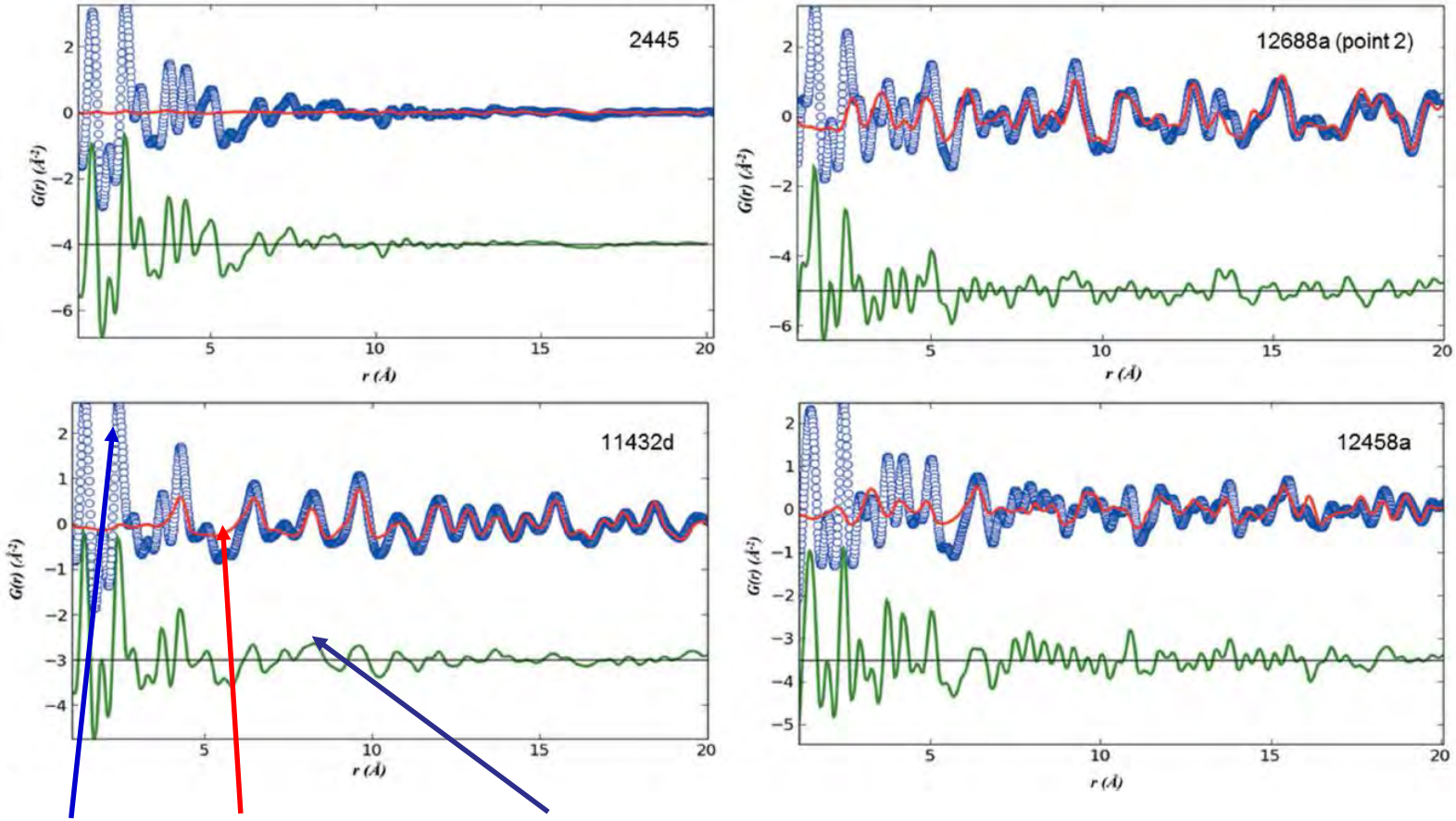

Experimental PDF: G_{obs}

Simulated PDF: $G_{crystal}$ using crystalline phases from Rietveld, Scaled in 12-20Å

Difference PDF: $G_{amorphous}$ = non crystalline contribution

Identification of the amorphous phase

Correlation analysis between $G_{amorphous}$ and $G_{reference}$, PDFs of the reference black pigments: using Pearson correlation coefficients.

$$R(X,Y) = \frac{1}{n-1}\sum_{i=1}^{n}\left(\frac{X_i - \overline{X}}{\sigma_X}\right)\left(\frac{Y_i - \overline{Y}}{\sigma_Y}\right)$$

$R = 1$: *Exact correlation*

$R > 0.8$: *strong correlation*

	Bone black	Ivory black	Peach black	Lampblack	Charred wood	Graphite pencil
2445	0.269	0.291	0.937	0.914	**0.940**	0.548
11432d	0.312	0.317	0.899	0.850	**0.921**	0.484
12688a	0.242	0.270	0.541	0.556	0.556	0.327
	0.210	0.236	0.452	0.466	0.350	0.314
12458a	0.328	0.318	**0.899**	0.894	0.854	0.599

- ✓ Amorphous phase = carbon black, probably charred wood
- ✓ 12688a = lipids (C - C =1,54 Å) ?

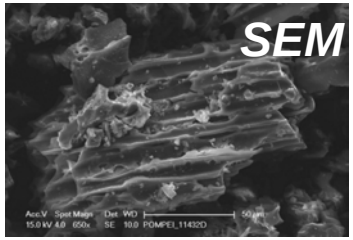

T. Dykhne et al., Pharm Res (2011) 28, 1041

Identifying $G_{amorphous}$ with the corresponding $G_{reference}$, one can quantify the proportion *x* of amorphous phase:

$$G_{total} = s.[x.G_{reference} + (1-x).G_{crystal}]$$

x is obtained by least-squares fit of G_{total} vs G_{obs}

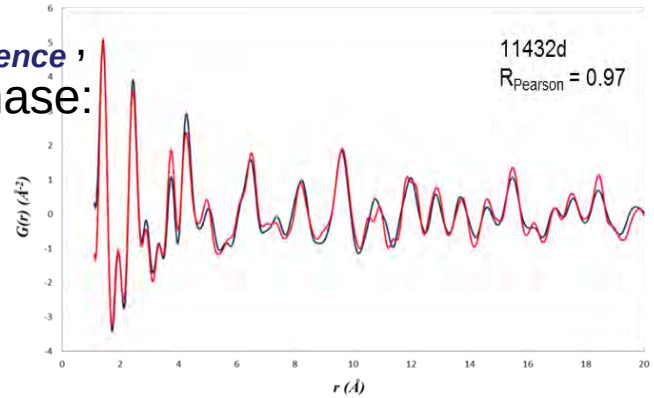

	Amorphous content	Crystalline content										
Sample	Charred vegetable material	Whitlockite ($Ca_9(Fe,Mg)(PO_3OH)(PO_4)_6$	Phospho-hedyphane $Ca_2Pb_3(PO_4)_3Cl$	Lead	Cassiterite	Tin	Tin Bronze (Cu_3Sn)	Tin Bronze ($Cu_{10}Sn_3$)	Cerussite	Gypsum	Calcite	Malachite
2445	100	< 1										
11432d	37		63									
12688a#	Lipids? (unquantified)			33.57 (0.64)	14.67 (0,68)	4.36 (0.59)	46.06 (1.43)	1.34 (0.05)				
				34.30 (0.28)	10,81 (0,29)	2.30 (0.27)	28.97 (0.38)	1.15 (0.02)	22.48 (0.26)			
12458a†	63										18.5	18.5
12724	< 1									92.72 (6.26)	5.26 (0.83)	2.60 (0.46)
	< 1									74.4 (1.93)	25.6 (1.65)	

Charred vegetal + unexpected mineral phases

Metallic phases (degradation of the bronze container) + lipids ?

Charred vegetals + usual mineral phases

Acknowledgements

Maria Diaz-Lopez
Pauline Martinetto
Nils Blanc (CRG-D2AM, ESRF)
Nathalie Boudet (CRG-D2AM, ESRF)
Sophie Cersoy (now at MHN, Paris)
Claire V. Colin
Jean-Louis Hazemann
Yves Joly
Olivier Leynaud
Vivian Nassif (CRG-D1b, ILL)
Olivier Proux (CRG-FAME, ESRF)

Jean-François Willart
Emelyne Dudognon
Marc Descamps

Melanie Freire
Valerie Pralong

Philippe Walter
Elsa Van Elslande

Andy Fitch
Gavin Vaughan
Jakub Drnek
Andrea Bernasconi
Jon Wright

Erik ElKaïm

Eric Dooryhee
Sanjit Ghose
Milinda Abeykoon

Henry Fischer (D4c, ILL)
Juan Rodriguez-Carvajal
Aleksei Bytchkov

DAME
MiPhaSol